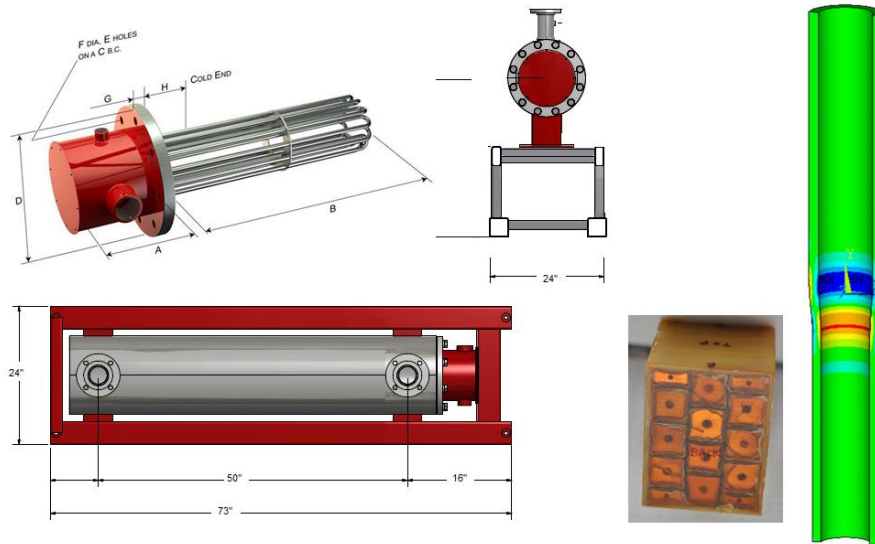


NSTX Upgrade

OH Cooldown System and Preheater

NSTXU-CALC-133-17-0 March 4, 2015



	Section	Preparer	Checker
All Sections	Executive Summary and All Except Below:	P. Titus	P. Heitzenroeder
Wave Stress	8.0	P. Titus	H. Zhang
FCOOL Runs and Wave Stress	9.0	Han Zhang	Art Brooks
ACOOOL Linear Ramp	10	Art Brooks	P. Titus
OH Base Stress	11.0	Andrei Khodak	P. Titus
OH Base Stress	11.2	P. Titus, A. Brooks	Andrei Khodak
System Design and Pipe Flow	12.0	N. Atnafu	Art Brooks
Controls	12.5	Xin Zhou	
CTD Test Results	13.0	P. Titus	P. Heitzenroeder

PPPL Calculation Form

Calculation # NSTXU-CALC-133-17-0 Revision # 00 _____ WP #, 2027 (ENG-032)

Purpose of Calculation: (Define why the calculation is being performed.)

The purpose of this calculation is to provide guidance on initial design and qualification of the final OH Cooldown System. This includes the coil winding pack thermal stresses for the original cooldown temperature sequence – which was essentially a thermal shock, and for a new ramped thermal profile that mitigates the consequence of extreme thermal gradients. The proposed system is also described in detail, and necessary systems calculations such as flow rates and pressure drops are included. Control logic is described and input to the NSTX Failure Modes and Effects (FMEA) is presented. Testing of the winding pack array has been performed to qualify an acceptable level of cyclic tensile strain.

References (List any source of design information including computer program titles and revision levels.)

These are included in the body of the calculation, in section 6.2

Assumptions (Identify all assumptions made as part of this calculation.)

No significant assumptions have been made. Some assumptions are discussed in the body of the calculation

Calculation (Calculation is either documented here or attached)

Thermal stress calculations are included in the body of the calculation

Pipe flow, and systems calculations are included in the body of the calculation

Conclusion (Specify whether or not the purpose of the calculation was accomplished.)

Tensile strains in the insulation system due to OH cooldown have been quantified and electrically qualified by tests at CTD [25]. While the tests show no cyclic degradation of the electrical performance, they do show a progressive reduction in modulus that indicates changes in the inter-laminar bonds of the impregnated Kapton-glass insulation system. A proposed OH Pre-heater and OH cooling system provides an inlet temperature profile for the OH cooling water that produces thermal strains no worse than those experienced successfully in the original NSTX OH coil. CTD test results show that that the insulation system can survive the higher tensile strains expected in NSTXU without the preheater. The need for the preheater is now determined by the desire to mitigate the long term effects of the cooldown mechanical strains, and to support mitigation of tensile strains resulting from the interaction of the OH and TF coil resulting from the failure to remove aquapour. For both of these missions the need for the preheater is not urgent but will be commissioned as soon as resources allow. Ultimately the desired temperature will be 110 to 120 degrees C. CTD creep tests support the higher temperature allowable, but this will be evaluated in another calculation as it impacts the precompression system and other performance characteristics. The instant water heater unit will have the capability to go up to 110C. At this time the system is designed to provide a maximum of 100 C inlet temperature.

Cognizant Engineer's printed name, signature, and date

Neway Atnafu _____

I have reviewed this calculation and, to my professional satisfaction, it is properly performed and correct.

There are multiple authors and checkers for this calculation. A sign-off block is included on the cover sheet

2.0 Table of Contents

Title Page	1.0
ENG-33 Forms	
Table Of Contents	2.0
Revision Status Table	3.0
Executive Summary	4.0
Input to Digital Coil Protection System	5.0
Design Input,	
Criteria	6.1
References	6.2
Photos and Drawing Excerpts	6.3
Photos and Drawing Excerpts	6.4
Materials and Allowables	6.5
CTD 425 Allowables	6.5.1
Tension without Kapton	6.5.1.1
Water Supply Hoses	6.5.2
 Models	 7.0
Equivalent OH Modulus	7.1
FEA Simulated Equivalent OH Modulus	7.1.1
Measured Compressive OH Modulus	7.1.2
Measured Tensile OH Modulus	7.1.3
 Stresses Due to the Cooling Wave, Comparison with the original NSTX	 8.0
 FCOOL Runs, Wave Height Stress, Stepped Cooldown (Han Zhang)	 9.0
ACOOL Runs Ramped Cooldown (A Brooks)	10.0
Linear Rampdown from 100C	10.1
Linear Rampdown from 80C	10.2
Linear Rampdown with 10 seconds of initial 12C water	10.3
Effect of Changing inlet Pressure	10.4
 Thermal Stress at the Restrained Base of the OH (A Khodak)	 11.0
 System Flow Diagram, Alternates, Flow Calculations	 12.0
System Alternates	12.1
PIPE FLOW Flow Calculations	12.2
Transit Time Calculations	12.3
Relief Valve Flow Calculations	12.4
Control System Description	12.5
System FMEA	12.6
 Testing, Creep, and Displacement Controlled Tensile Strain	 13.0
Mis-Aligned Array Tensile Strain Test and Simulations	13.1
Test Results	13.1.1
Bonded Simulation	13.1.2
Un-Bonded Simulation	13.1.3
Aligned Array Tensile Strain Test and Simulations	13.2
Test Results	13.2.1
Bonded Simulation	13.2.2
Un-Bonded Simulation	13.2.3
 Creep Stack Test	 13.3

Attachment A Emails

Attachment B ADPL For Inputing FCOOL Output Files to Han's OH FEA

Attachment C Hysol Wet Lay-up Compression Test (By Stephan Jurczynski)

3.0 Revision Status Table

Rev 0	Initial Issue
-------	---------------

4.0 Executive Summary

Introducing cold cooling water into a coil can cause a “thermal shock” or stress due to a sharp initial temperature gradient. NSTX operated successfully without systems to mitigate this effect. Winding pack and build differences between the new coils used in the upgrade and the original coils in NSTX, have raised concerns over insulation tensile strains in both the new TF and the new OH coils. The TF coil thermal shock was improved by introducing the outer leg cooling water into the inlet of the inner legs. In the new NSTX U TF, the cooling tube centered in the blade or Bitter plate conductor cross section produced contractions and tensile stresses around the soldered coolant tube, which was in the center of the radial build of the TF conductor. TF cooling stresses and analyses of feeding the inner leg with outer leg coolant are included in [12]. Cooling progresses differently in the TF and OH coils, because of the very long path length in the OH, cooling progresses up the coil in a “wave” or transition zone from cold to hot.

OH Thermal stresses and cooling wave height effect on OH stresses were identified early in the NSTX-U project by Ali Zolfaghari and MAST Peer reviewers. Ali’s comments in his calculation follow :

“The temperature of the coil reaches close to 100 C in a few seconds but the water entering the coil (from the bottom of the coil) is at 12 degrees C. As the colder water moves through the coil, it creates a temperature gradient in the coil that causes stress in the coil. To study this effect we analyzed the results of cooling in the inner most layer of the OH coil. The highest temperature gradient (as calculated by FCOOL) over the first 4 turns (each turn is 1.378 m) of the coil happens at $t=5.96$ seconds after the start of the shot.”

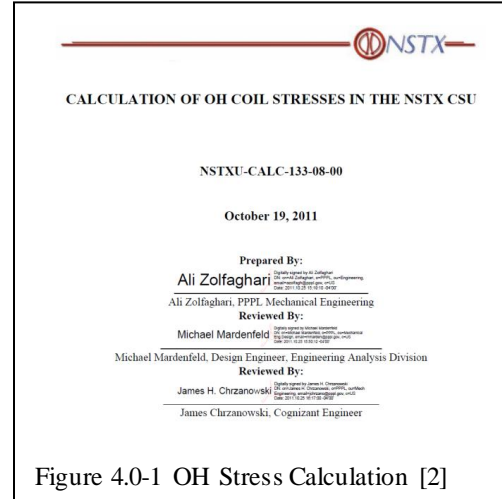


Figure 4.0-1 OH Stress Calculation [2]

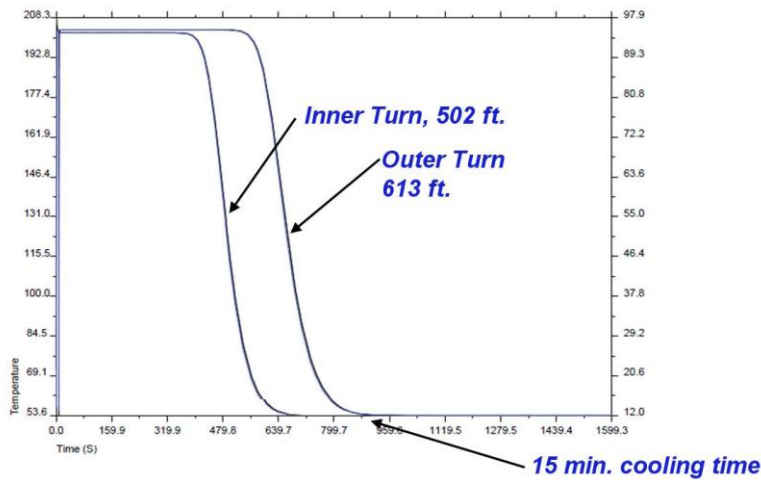


Figure 4.0-2 FCOOL Results from Ali Zolfaghari’s OH cooling calculation [11]

And in another section of the calculation [2]:

“If CTD-425 insulation system is used with primer, the shear stresses are below the static and fatigue limits. The vertical tensile stress limit in some areas exceed the 10 MPa allowable in the insulation. We recommend the use of a more gradual cooling scheme whereby the starting temperature of the coolant is higher than 12 C and gradually reduced as time progresses. This would reduce the temperature gradients at the beginning of the cooling process in the bottom of the coil and therefore reduce the stresses. “

From Ali's Calculation:

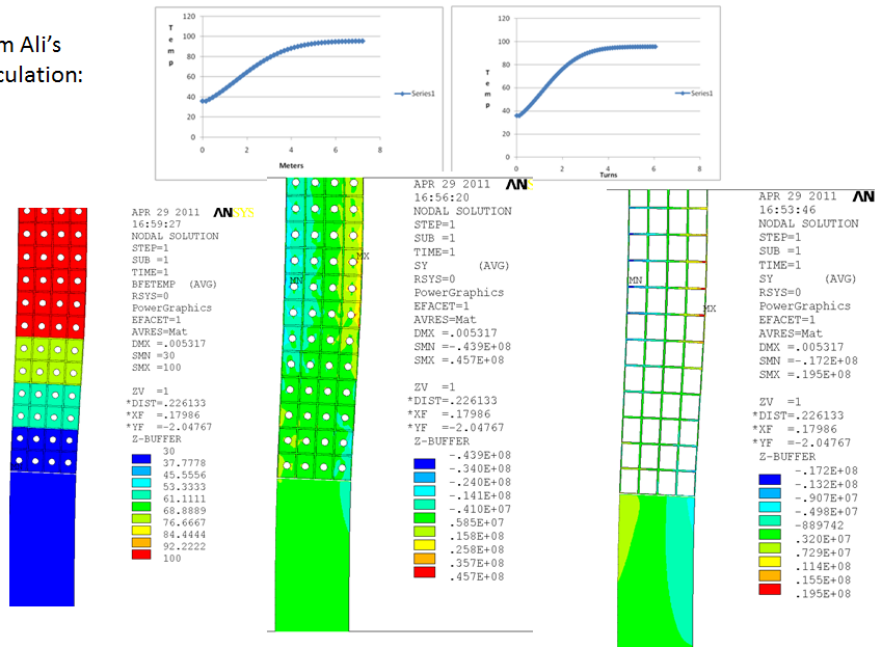


Figure 4.0-3 Vertical Stress in the Coil Due to the Cooling Wave in the Bottom of the Coil [2]

From Ali's Calculation:

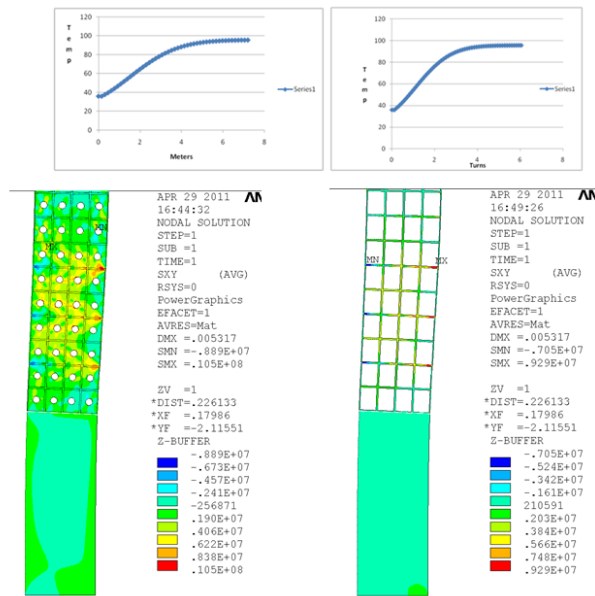


Figure 4.0-4 Shear Stress in the Coil Due to the Cooling Wave in the Bottom of the Coil

Han Zhang more recently simulated the cooling wave thermal strains, and found similar results. These are shown in figure 4.0-5. Her effort centered around finding cooling schemes that might improve the thermal stresses

Han Zhang Results: OH cooling: tension stress from different cooling schemes

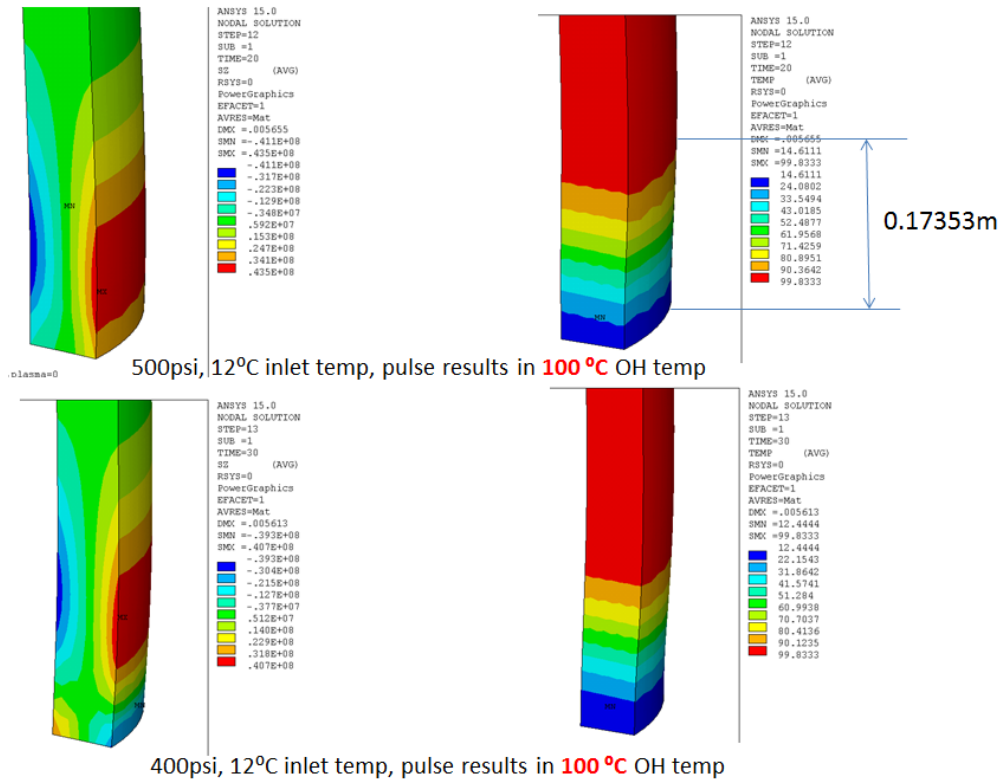


Figure 4.0-5 Axial (Vertical) Tension Stress in the Coil Due to the Cooling Wave in the Bottom of the Coil

Figure 4.0-5 are results from Han Zhang. She took FCOOL temperature results and applied them to her coil model. The ADPL script for this is included in Attachment B at the end of this calculation. She got ~40 MPa, very similar to Ali's results. These are larger than the stresses (26MPa) from estimated wave heights in figure 4.0-5. Han, Ali, and Art Brooks have found the wave height is shortest near the lower base of the coil. The differences in reported stresses are due to the position along the height of the coil that is being analyzed.

The layer to layer stress issue was also identified early and plans for flow metering were included in the requirements for the water system

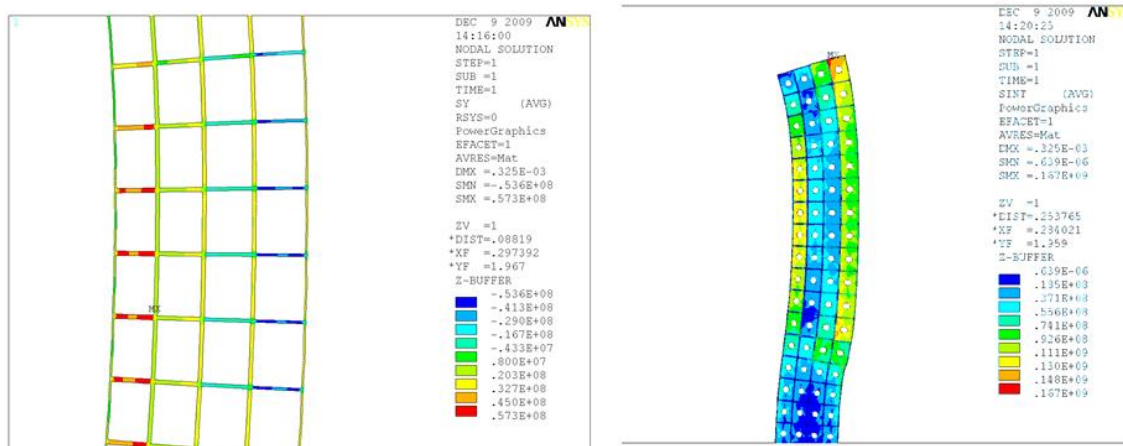


Figure 4.0-6 Vertical Stress in the Coil Due to the Different Cooling Path Lengths in the Coil Layers

Table 4.0-1 Cooldown Axial Tension Results for NSTX-U with 12C inlet water

Analyst	Waveheight	Axial Tension Stress
Han Zhang , Figure 4.0-5	.173 m	43 MPa (Smeared)
Ali Zolfaghari	.4m	25 MPa in the insulation
P. Titus, Figure 4.0-8		25 MPa (Smeared)

The stress results in table 4.0-1 vary. They were calculated independently, but they all point to a stress problem in the OH if the insulation system has a minimal tensile capacity. At the time Ali prepared his calculation, the tensile stress allowable with Kapton was guessed to be ~10 MPa by Dick Reed. Later bond strengths without Kapton were measured by CTD to be ~14 MPa, but with Kapton, the bond strength measured at MIT was nearly zero[6]. This led to the most recent round of CTD tests of the array samples shown in Figure 4.0-9. Without specific allowables from the CTD tests, the Stress limit for the preheater design is taken to be the stress that the original NSTX experienced successfully – see figure 4.0-8

December 4 2014 we had a conference call with MAST regarding this issue. MAST protects their coil against the layer to layer delamination, even though they feel that the delamination would be benign. They have Kapton wrap in their layer to layer interface, not turn to turn. They meter the flow to protect against excessive motion between layers, and expect that the turn to turn to be able to sustain the tensile stresses due to the cooling wave. With the layers poorly bonded, the tensile stresses due to bending of the coil build will be less.

OH Cooling Wave and Gradient in Conductor

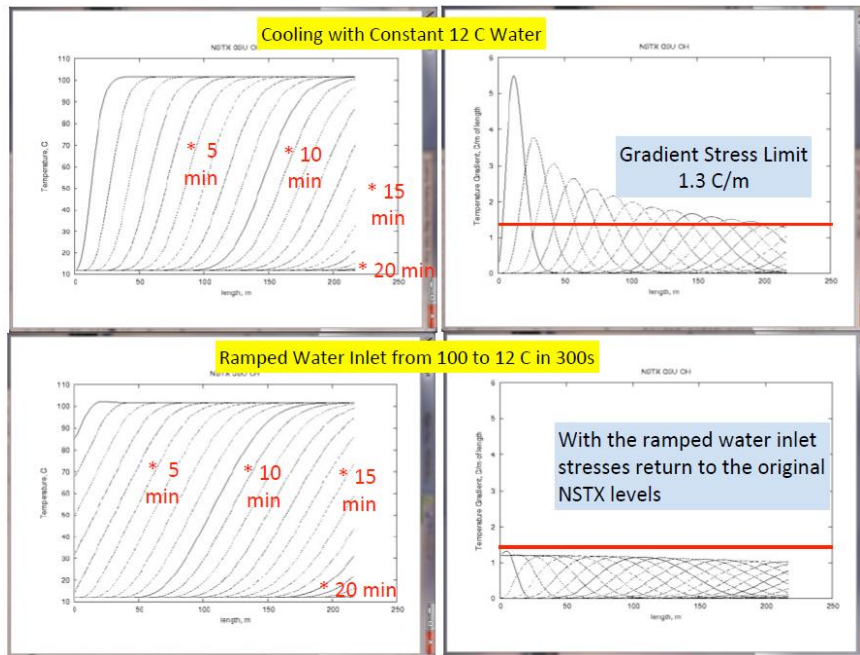


Figure 4.0-7 Comparison of the Temperature Gradient for the 12C inlet and Ramped Inlet Temperature. The gradient stress limit plotted in figure 4.0-4 will be discussed below.

Because details of the water system were deferred until most of the construction was in process, the wave height stress was not addressed until the summer of 2014, partly due to reviews of the “aquacement” issue. Simulations with the aquacement in place showed similar results as Zolfaghari [2]. Also the need for the water system upgrade to solve the wave height issue was not fully understood because it had not been an issue for NSTX.

The cooldown stresses in the upgrade will be much higher than in NSTX. NSTX is not a good basis for qualifying the tensile strains in the Upgrade.

From Ali's NSTXU calc and from Arts NSTX calc, The axial heights of the cooling wave in the two solenoids were estimated to be .27 m in the upgrade and .51m in NSTX - the main reason for this is that the cooling wave along the conductor is comparable for both, but in NSTX it is wrapped around a smaller diameter and thus goes a longer axial distance. for a given displacement the longer wave absorbs the radial strain with less bending stress. Based on a beam analogy the effect goes as L^2 . This makes NSTXU about 3.6 times worse.

The thermal radial growth of the coil is larger for the NSTX U than for NSTX, just because it is larger. The analogous beam stress is linear in displacement. - This is about a factor of 1.7 worse

The thickness of the coil is greater for NSTXU than NSTX - For a given bending displacement a thicker shell will have a bigger bending stress. This makes NSTXU about 1.5 times worse.

The total effect is $3.6 * 1.7 * 1.5 = 9.2$ times worse for NSTXU than for NSTX. NSTX has lower stresses than NSTXU because of geometry. The finite element solution produced a less pronounced effect, but the Upgrade stresses are significantly larger than the stresses in NSTX.

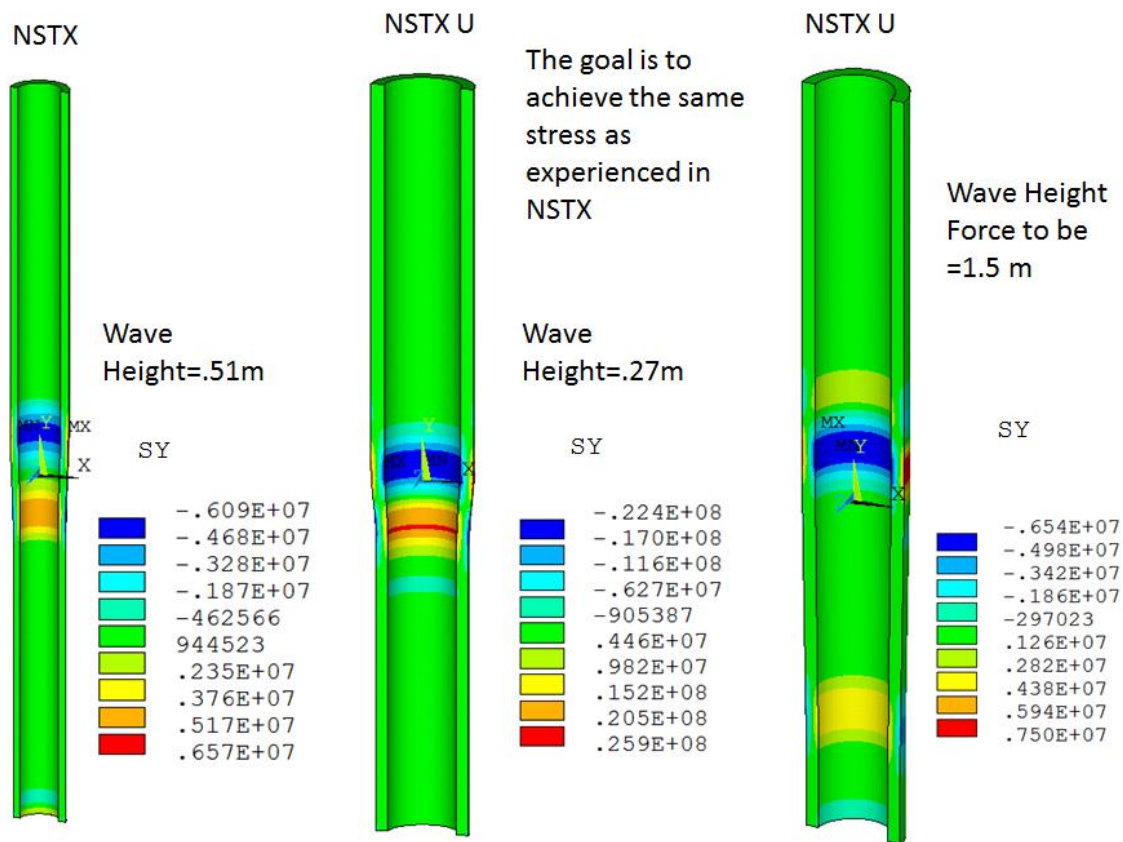


Figure 4.0-8 Axial or Vertical Tension Stress in the OH Coil Due to the Cooling Wave for NSTX, NSTX Upgrade, and NSTX Upgrade with an Arbitrarily chosen 1.5m wave height.

The gradient Stress limit in figure 4.0-4 corresponds to the 1.5m wave height in figure 4.0-5.

The tensile strength of the OH winding pack is uncertain but it is minimal because of the inclusion of interleaved Kapton. Even without Kapton, tensile strength of the epoxy bond to copper is only ~14 MPa with an allowable of about half of this. See Figure 6.4.1-1, Ref [8]. Kapton forms parting planes and is intended to provide electrical integrity even if there are "small" amounts of cracks

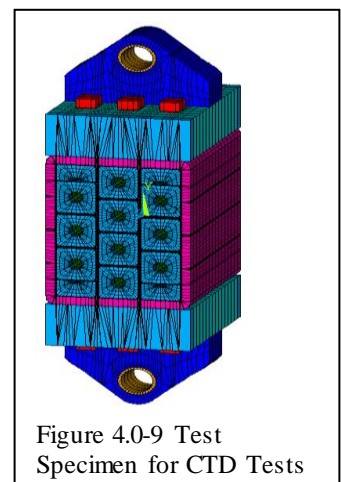


Figure 4.0-9 Test Specimen for CTD Tests

OH Cooldown System

and delaminations that impose strains on the Kapton. The definition of “small” in this instance requires judgement and testing. Testing was attempted for ITER insulation and substantial static load damage could be accepted while retaining electrical function. Fatigue loading was not evaluated in this test [6]. For really small potential delamination and cracking, in the W7X trim coils, a judgmental argument was developed for the W7X trim coils in [7]. As of December 2014, the trim coils have been successfully commissioned. To develop an allowed cyclic tensile strain, tests have been performed by CTD to test strain controlled cyclic electrical degradation. Final test results are available as of Feb 19 2015 [25]. The sample diagram used in the Statement of Work is shown in Figure 4.0-5. The outcome of the tests demonstrates acceptable electrical performance for all of tested cyclic strain. Lacking a well developed tensile allowable, the NSTX value of 6.5 MPa was taken as a target value. The CTD samples (aligned and misaligned samples are being tested) survived well electrically. It has been concluded that the preheater is not needed during early operations. The preheater will be retained to improve the life and reliability of the OH coil because there was some indication of progressive mechanical degradation,. It is also useful for operations to mitigate the effects of the aquapour TF-OH interaction.

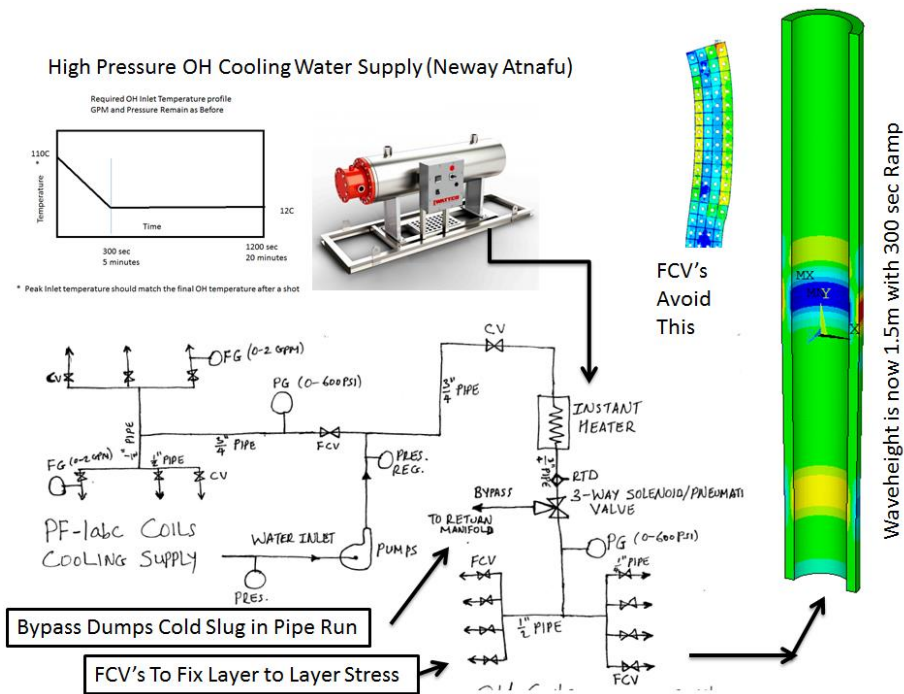


Figure 4.0-10 Early Diagram of the OH Preheater Cooling System

Water Heater Temperature Setting

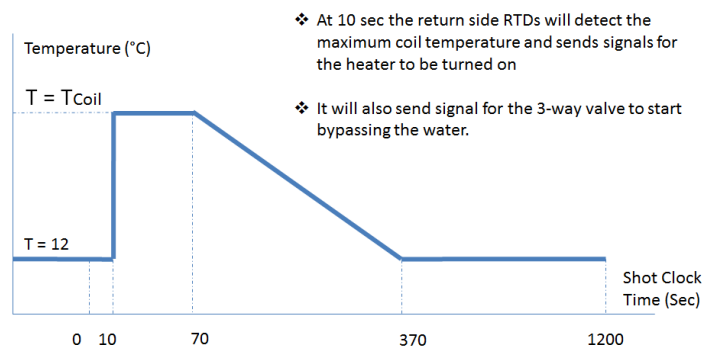
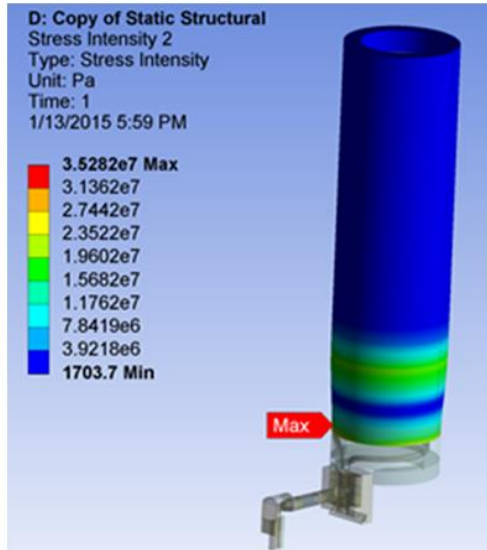


Figure 4.0-11 Target Temperature for the water heater.

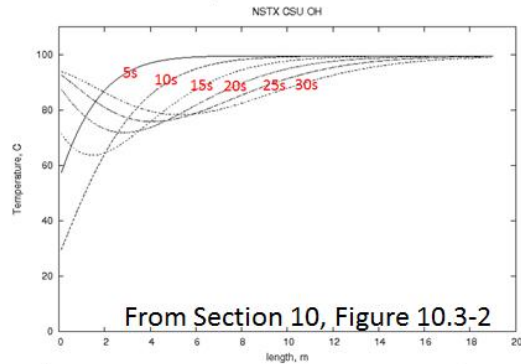
The proposed ramped inlet temperature shown in figure 4.0-11, produces a cooldown time of just 20 minutes. Stefan Gerhardt has expressed an interest in keeping the cooldown time below 20 minutes. The OH cooldown is the longest component that establishes the rep rate, and ideally after the system is configured and run, cooldown times can be improved, at least for OH temperatures less than 100C. The stress in the coil is a function of the temperature gradient, so if the coil starts at , say 50 C, the ramp time of 5 minutes could be halved.

An important consideration in the configuration and design of the preheater system is the transit times of the water flowing in the hoses. Temperature control of the coolant is not possible for some of the hose runs that are between sensors, bypass valves and the OH coil inlet. Time delays are imposed by the lengths of the hose connections from the OH outlet to the RTD's at the top of the machine that provide the target temperature of the OH coil for the preheat system.

End of Pulse OH Temperature, Cold Base Section 11.1, Max Tresca is 35 Mpa. 20 Gpa is used for the Base Pedestal Modulus



Cooling with 12C for 10 sec, stepped up to 100C, ramped down in 300 s



From Section 11.2, Five second time point with 10 seconds of 12C flow

Time, Sec	Sy, MPa
0	24.4
5	49.2
10	34.1
15	33.8
20	48.2

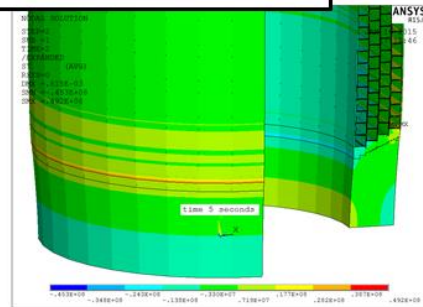


Figure 4.0-12

An inventory of cold water set by the flow velocity and an effective time delay must be accommodated by the coil inlets. This area was the subject of detailed analysis for a worst case situation of a fully hot coil, and 12C inlet temperature. The qualification [14] was challenging and there were a few locations thought to be challenged electrically that had extra Kapton wraps or efforts made to improve bonding. These simulations were revisited in light of the expected best effort temperature delays .

These analyses are included in section 11. Even with the new system, there are local tensile strains that cannot be mitigated by the ramped temperature. The consequences of a 10 second flow of 12C water was simulated by A. Brooks and was evaluated using the [14] model, and another model that treats discrete conductors and layers of insulation and Kapton. The results for the lower base area are small regions which are above the NSTX 6.5 MPa

NSTX
(NATIONAL SPHERICAL TORUS EXPERIMENT)
STRUCTURAL DESIGN CRITERIA
NSTX-CRIT-0001-01
February 2010

Prepared by: Irving Zatz
I. Zatz, MED Engineering
Peter H. Titus
P. Titus, MED Branch Head

Concur: _____
A. Von Halle, Head of NSTX Engineering

Approved by: _____
C. Neumeier, NSTX Project Engineer

Figure 4.0-13

target allowable . The rest of the coil for a 1.5 wave height is near the NSTX target value.

Table 4.0-1 Tensile Strains from Analyses in this Report, and the Test Value

Location	No Preheater Figure or Section	No Preheater	With Preheater Figure	With Preheater
CTD Test SOW	Reference [23]	4.0e-4		
CTD Actual Test	4.0-14	~6.0e-4		
NSTXU Cooling Wave	Figure 8.0-3	2.56e-4	8.0-3	7.5e-5
NSTXU Cooling Wave	9.0-1	4.07e-4	9.0-4	1.3e-4
NSTXU Base	11.8, 11.9			3.37 to 4.1e-4

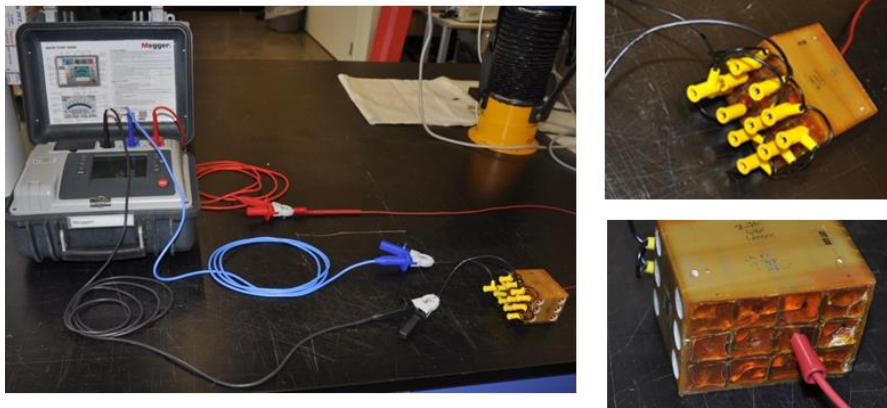


Figure 4.0-14 Electrical Test Setup at CTD Showing the Aligned Array, From [25]

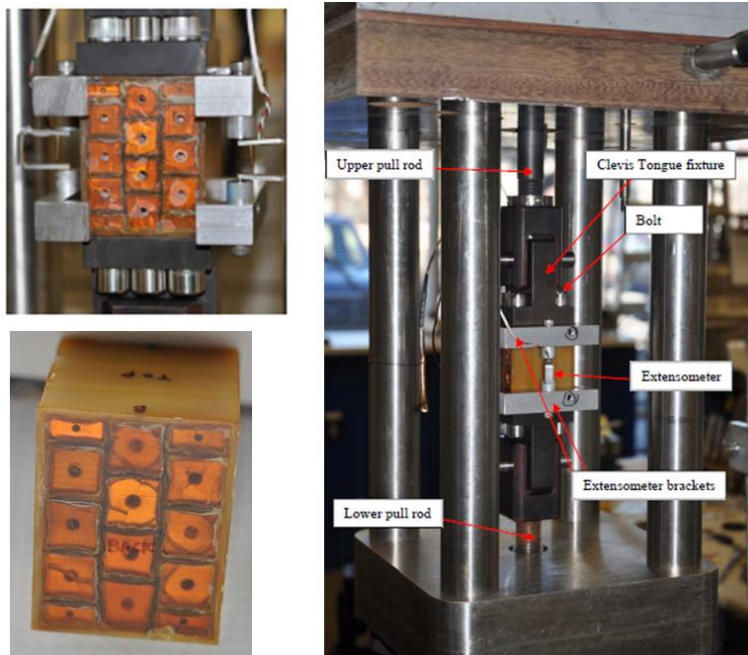


Figure 4.0-15 Array Test Samples and Fixtures from [25]

The CTD aligned conductor tests show a significant accommodation of tensile strains. The tests are displacement or strain controlled, performed at 110 C at a strain rate of 0.4×10^{-3} and a rate of ~10 hz. Table 4.0-1 shows the tensile strains from the simulation in this report along with the CTD test requirement.

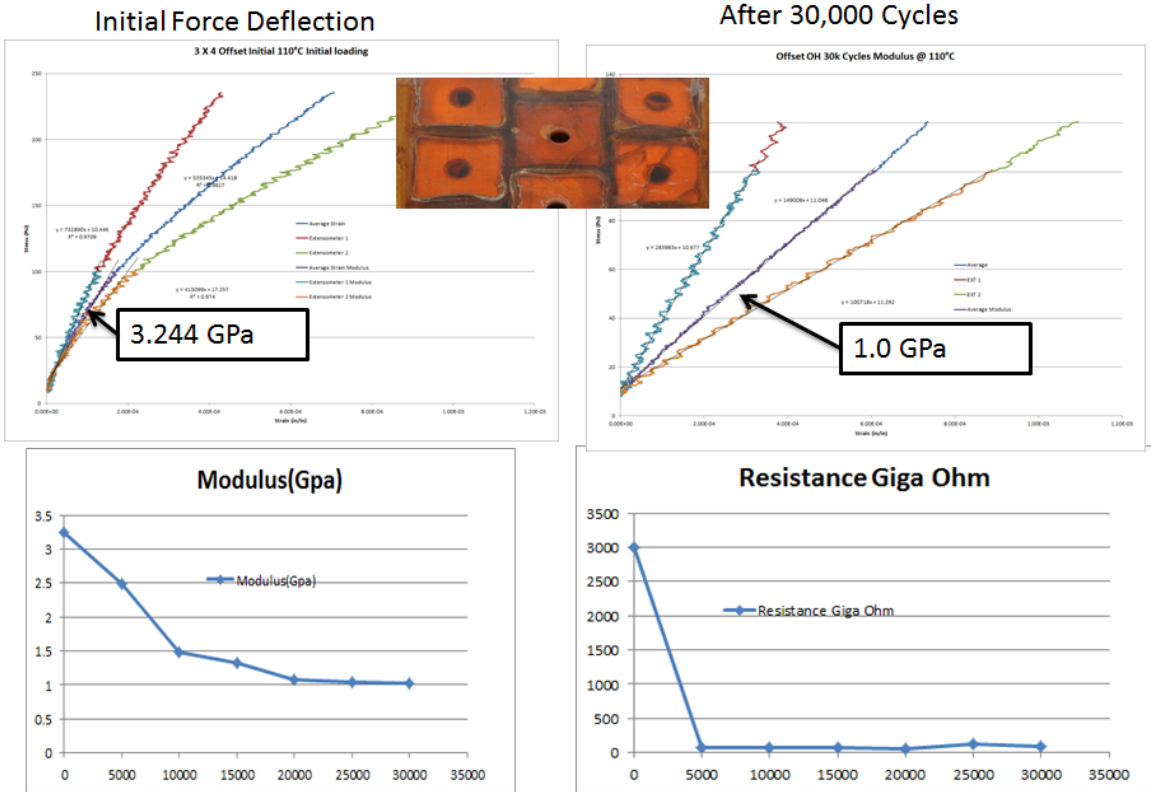


Figure 4.0-16 CTD Tensile Strain Controlled Tests

In the misaligned turn test results provided by CTD, there is evidence of cyclic mechanical degradation. Photos of the samples, Figure 4.0-15, do not show any indication of cracking or delamination, although the photos are of the outer faces of the impregnated samples. These are resin rich areas that often crack just from the cooldown from the cure temperature. There is little difference between the two photos of the same sample before and after cyclic testing. The aligned conductor array looks like whatever mechanical change occurs, and this includes the appearance of cracks in the neat resin, occurs essentially in the first load cycle.

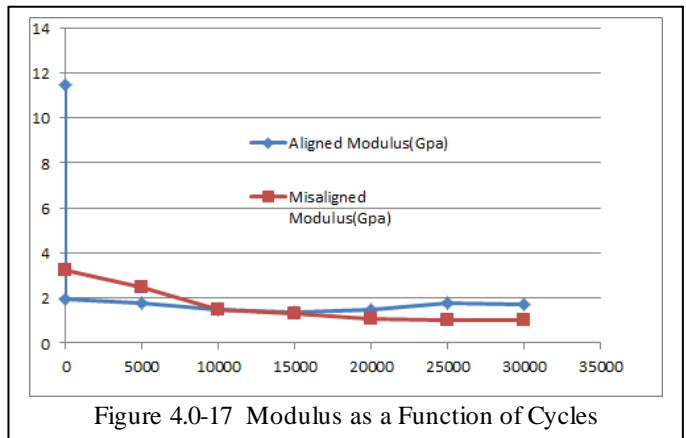


Figure 4.0-17 Modulus as a Function of Cycles



Figure 4.0-15 CTD Tensile Strain Controlled Test, Aligned Sample

Work continues on the OH cooling water preheater system. Results of the CTD insulation array tests have been received and are favorable. Both misaligned and aligned samples have been tested, and no electrical failures have been reported after 30,000 controlled strain cycles. Aligned tests show an initial large drop in the modulus, and the misaligned array shows a more progressive degradation. Either perfectly aligned and maximally misaligned conductor configurations are rare in the coil build. Some average misalignment would characterize the winding pack. Thus some progressive cyclic change in modulus and degree of Kapton adhesion is expected. Based on these results, the preheater system does not have to be fully operational for CD-4. Mechanical behavior of the samples shows some progressive reduction in the moduli of the samples indicating damage to the interlaminar bonds. The conductors are wrapped with Kapton interleaved with glass with the expectation that some mechanical strains would have to be accommodated. Completion and operation of the preheater system is still planned to reduce mechanical strains in the insulation system over time, and to support OH coil temperature adjustments to minimize the OH interaction with the TF due to the Aquapour remaining in the interface gap.

5.0 Digital Coil Protection System.

Cooling wave stress mitigation is not part of the DCPS.

6.0 Design Input

6.1 Criteria

Stress Criteria are found in the NSTX Structural Criteria Document.

2.5.2.1 Mechanical Limits for Insulation Materials

The stress criteria defined herein may be locally exceeded by secondary stresses in an area whose characteristic length along the insulation plane is not more than the insulation thickness and where it can be demonstrated that cracking or surface debonding parallel to the insulation layer and limited to the local length will relieve the stresses without violating the integrity of the structure. In this situation, final verification must be obtained by mechanical/electrical testing of a representative winding pack section.

2.5.1.1.2 Tensile Strain Allowable Normal to Plane

In the direction normal to the adhesive bonds between metal and composite, no primary tensile strain is allowed. Secondary strain will be limited to 1/5 of the ultimate tensile strain. In the absence of specific data, the allowable working tensile strain is 0.02% in the insulation adjacent to the bond.

6.2 References

- [1] NSTX Structural Design Criteria Document, NSTX_DesCrit_IZ_080103.doc, Feb 2010 I. Zatz
- [2] "CALCULATION OF OH COIL STRESSES IN THE NSTX CSU" NSTXU-CALC-133-08-00, October 19, 2011 Prepared By:Ali Zolfaghari and reviewed by M. Mardenfeld
- [3] "OH Coil Thermal/Hydraulic Analysis" Calc No. 13-6 (Original NSTX Calculation) A. Brooks, 4/8/97
- [4] ITER material properties handbook, ITER document No. G 74 MA 15, file code: ITER-AK02-22401.
- [5] NSTX Upgrade General Requirements Document, NSTX_CSU-RQMTS-GRD Revision 0, C. Neumeyer, March 30, 2009
- [6] "Desktop Vacuum Pressure Impregnation Experiment for ITER Insulation Testing' PSFC/RR-06-1 Mahar S., Titus P., Gung C., Hooker M., Minervini J., Schultz J., Stahle P., Takayasu M. April 2006
- [7] Insulation Local De-bonding and Delamination , W7X Trim Coil Collaboration W7X Trim Coil - CALC 01_ Rev 0 December 1 , 2011, P Titus, Reviewed by M. Mardenfeld
- [8] Final Test Report for Purchase Order PE005392-W Through Thickness Insulation and Copper Tensile Adhesion Tests November 2004 Prepared for PPPL, by Composite Technology Development Inc
- [9] NSTX-U Design Point Spreadsheet http://w3.pppl.gov/~neumeyer/NSTX_CSU/OH_Coil.htm, C. Neumeyer
- [10] Inner PF Coils (1a, 1b & 1c), Center Stack Upgrade NSTXU-CALC-133-01-02 May, 2014 Rev 2 by Len Myatt. Rev 2 by A Zolfaghari and A Brooks
- [11] "OH COIL COOLING IN THE NSTX CSU" NSTX-CALC-133-06-00 October 07, 2011Ali Zolfaghari
- [12] TF Coupled Thermal Electromagnetic Diffusion Analysis (R3v2) NSTXU-CALC-132-05-02, January 2013, Han Zhang,
- [13] Fatigue Testing of CTD-425/S2 Glass with CTD-450 Primer/Copper Sheet Paul Fabian and Mark Haynes, Composite Technology Development, Inc.
- [14] "NSTX Upgrade OH Coaxial Cable and Embedded Leads" NSTXU-CALC-133-07-00 10 October 2011 Prepared By M. Mardenfeld, Checked by Ali Zolfaghari
- [15] Evaluation and Testing of Pure Cyanate Ester Resin at UKAEA. Garry Voss 27 August 2007
- [16] Final Test Report,PPPL Purchase Order PE010637-W Fabrication and Short Beam Shear Testing of Epoxy and Cyanate Ester/Glass Fiber-Copper Laminates April 8, 2011 Prepared for: Princeton Plasma Physics Laboratory Prepared by: Composite Technology Development, Inc.2600 Campus Drive, Suite D Lafayette, CO 80026
- [17] Final Test Report, PPPL Purchase Order PE010925-W Fabrication and Testing of Cyanate Ester - Epoxy /Glass Fiber/Copper Laminates, October 7 2011, Prepared for Princeton Plasma Physics Laboratory Forrestal Campus by Composite Technology Development Inc. 2600 Campus Drive Suite D Lafayette CO 80026

- [18] Performance Evaluation of Cyanate Ester Resin G. Voss¹, P. Fabian², S. Feucht², M. Harte¹ and C. Terry³ IEURATOM/UKAEA Fusion Association, Culham Science Centre, Abingdon, UK. 2Composite Technology Development Inc. Lafayette, Colorado .
- [19] Manufacture and Test of a Prototype Cyanate Ester Coil, Davis, S.R. Voss, G.M. Culham Sci. Centre, EURATOM/CCFE Fusion Assoc., Abingdon, UK Applied Superconductivity, IEEE Transactions Issue Date: June 2010 Volume: 20 Issue:3 On page(s): 1479 – 1483
- [19] Email from James Chrzanowski <jchrzano@pppl.gov> to Jonathan, Stefan, Lawrence, Ronald, Steve, Peter May 6 2014 , providing the total as-wound number of turns in the OH coil
- [20] Email from Mike Mardenfeld Jan 16 2015, describing the manufacturing of the G-10 OH support pedestal
- [21] NSTX Failure Modes and Effects Analysis / NSTX-FMEA-71-10, Revision 10 Dated November 2014 by K. Tresemer, M. Smith, S. Raftopolis, T. Stevenson, W. Blanchard
- [22] Final Report, Qualification of CE Blends for the TF Coil Insulation, Contract ITER/CT/08/10000115, April 19 2010, Harold Weber, Atominstitut, Vienna University of Technology, Austria - Reingard Maix secondary author
- [23] STATEMENT OF WORK FOR NSTX-U OH Coil Insulation Strain-Controlled Tests and Elevated Temperature Creep Tests D-NSTXU-SOW-13-197 REVISION 0 DATED *October 22, 2014*
- [24] email from John Desandro <desandro@pppl.gov> On February 6, 2015 at 6:54:28 PM EST, “Using the black compression ring we tested the hose to 700 psi at room temperature and 500 psi at 120 C. The hose has passed both tests.
- [25] Final Test Report, “PPPL Purchase Order PEO13945-W” “Fabrication and Testing of OH Coil Mockups”, Feb 19 2015, Composite Technology Development Inc.

6.3 Design Data

James Chrzanowski <jchrzano@pppl.gov> May 6 2014 to Jonathan, Stefan, Lawrence, Ronald, Steve, Peter [19] :

Jon


FYI- The new OH Solenoid has a total of 880 turns. This compares to the 884 turns shown in the design point checked tables. Jim

Layer 1~ 224 turns

Layer 2~ 220 turns

Layer 3~ 219 turns

Layer 4~ 217 turns



COMPOSITE TECHNOLOGY DEVELOPMENT, INC.
ENGINEERED MATERIAL SOLUTIONS

Final Test Report
PPPL Purchase Order PE013945-W

Fabrication and Testing of
OH Coil Mockups

Feb. 19, 2015

Prepared for:
Princeton Plasma Physics Laboratory
Forrestal Campus
US Route 1 North @ Sayre Drive
Receiving Area 3
Princeton, NJ 08543

Prepared by:
Composite Technology Development, Inc.
2600 Campus Drive, Suite D
Lafayette, CO 80026

2600 CAMPUS DR., SUITE D • LAFAYETTE, CO 80026 • 303-864-0394 • WWW.CTD-MATERIALS.COM

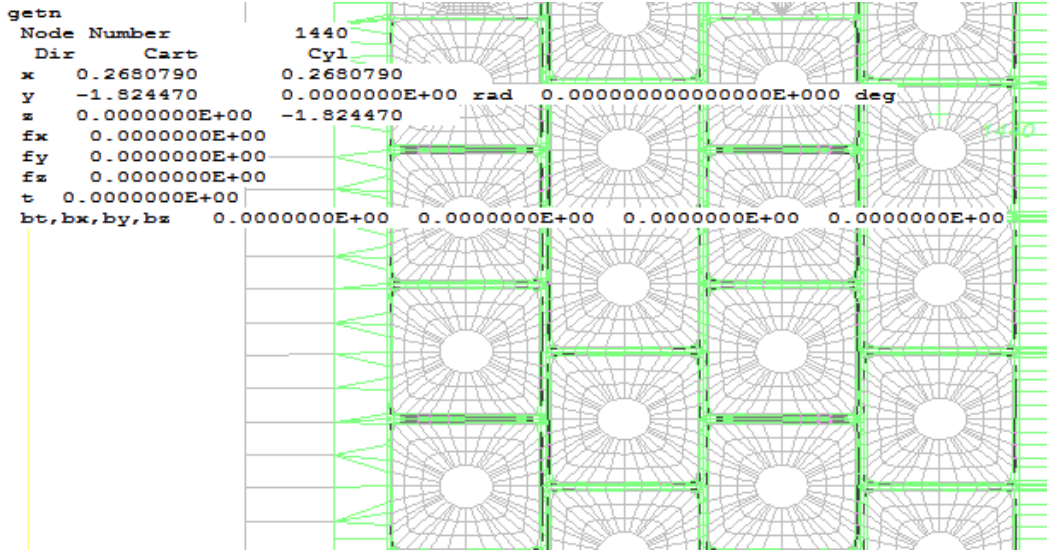


Figure 6.3-1 OH Build and Outer Turn Radius

The longest path is $.268079 \times 2 \times \pi \times 217/2 = 182.756$ meters

6.4 Photos and Drawing Excerpts

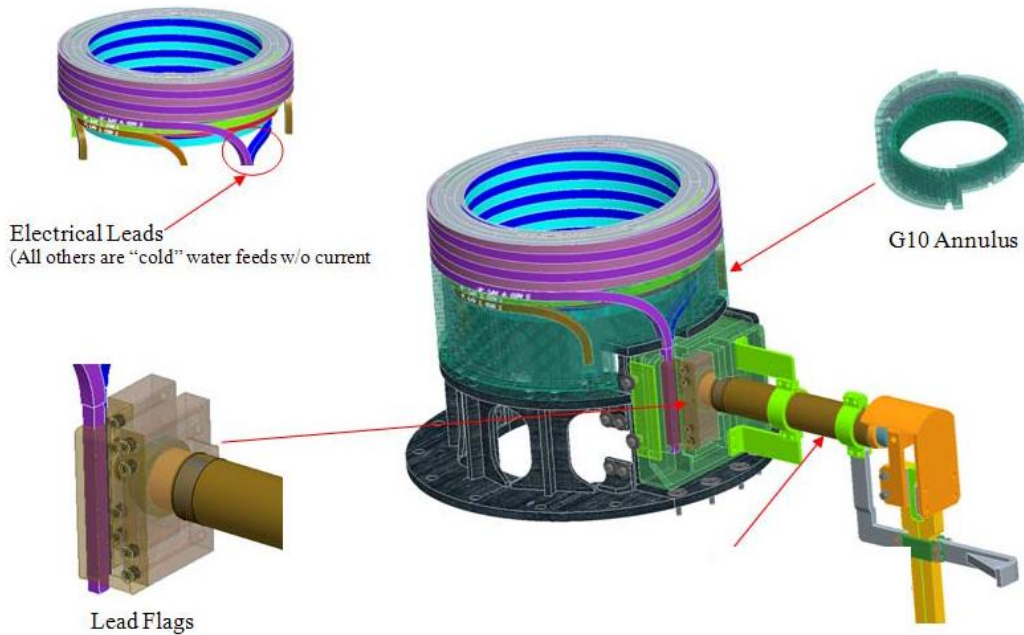


Figure 6.4-1 OH Coax Solid Models from [14] "NSTX Upgrade OH Coaxial Cable and Embedded Leads"

SUNFLO PUMP

- Series P-1000; Model # P1-DQB; S/N 984313839
- Max 810 Ft. Hd; Available 5-15 GPM; Best @ 700 Ft. Hd. & 14 GPM; 3500 RPM
- Requirement: 300 psi dp=693 Ft. Hd. Plus head loss due to piping ~720 Ft. Hd.
- At 720 Ft Hd. The flow is ~10 GPM per pump. Thus, these pumps are OK for NSTX-U.



Figure 6.4-2 High Pressure Pumps Used to Supply Water to the OH, PF1a, b and c Coils

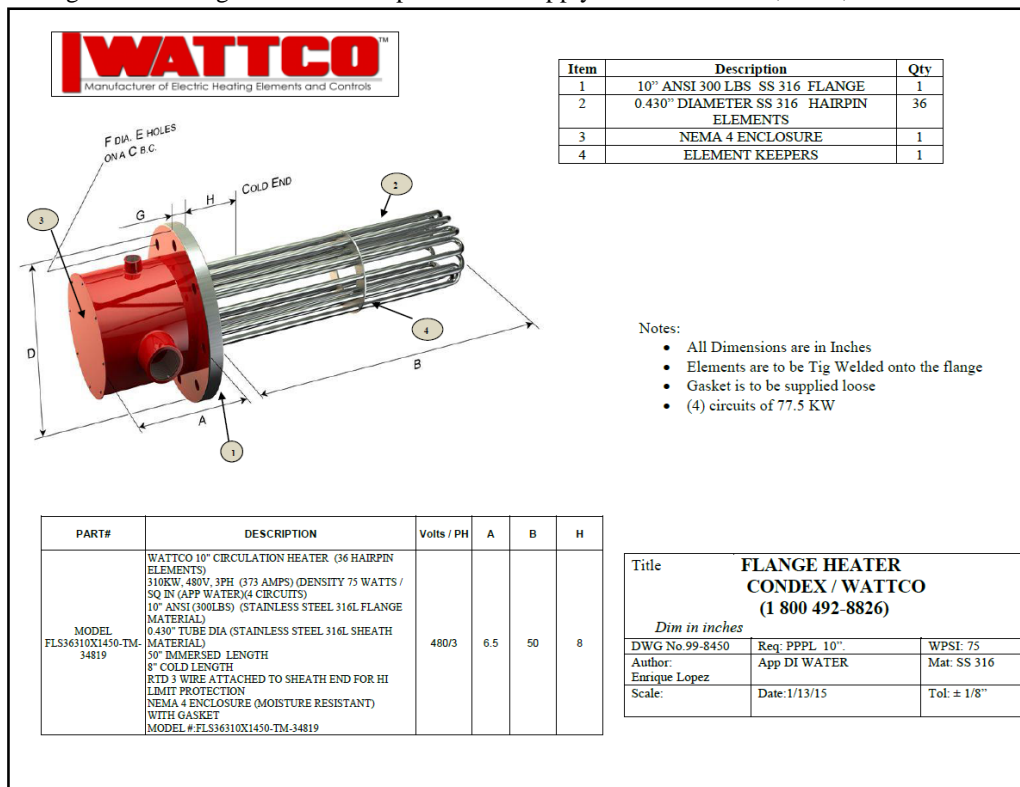
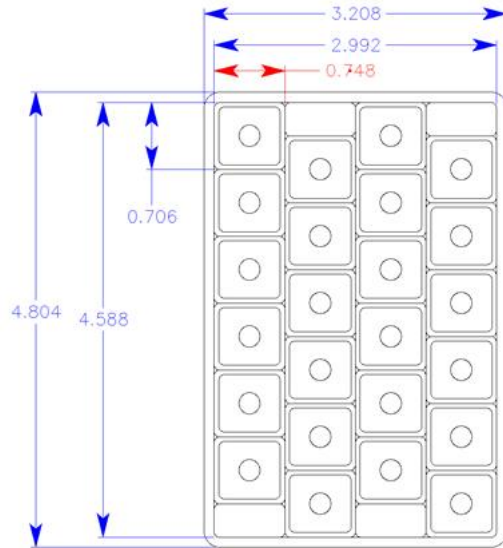


Figure 6.4-3 WATTCO Drawing of the Heater Elements

CTD Misaligned Specimen



Preliminary Sample Dimensions. Note that the sample was reduced in size to a 3 by 4 array to save costs

Figure 6.4-4 CTD Tensile Strain Array Sample

6.5 Materials and Allowables

6.5.1 CTD 425 Properties

6.5.1.1 CTD 425 Tensile Properties

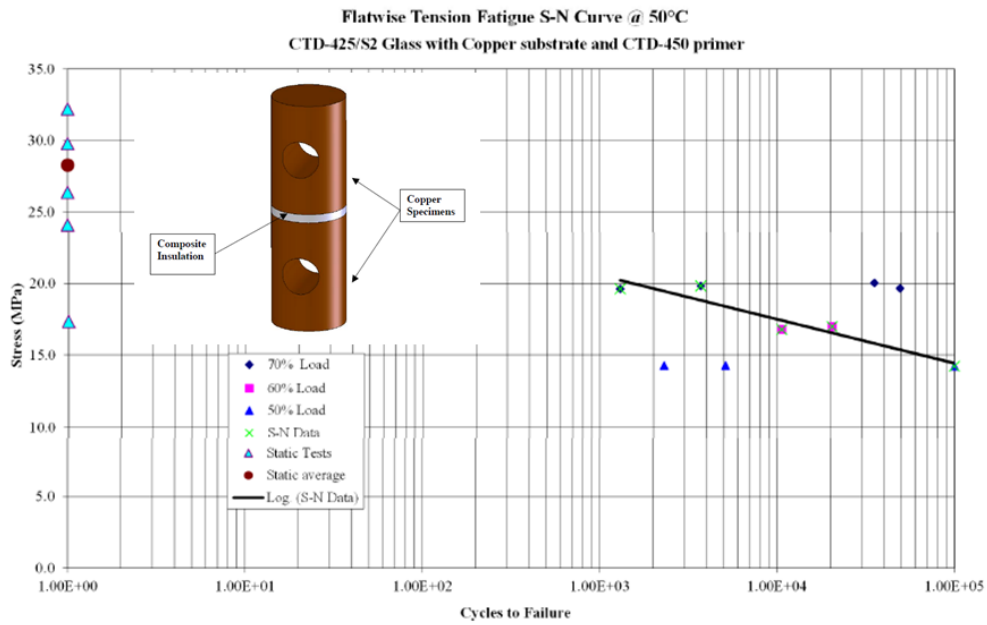


Figure 6.5.1-1 (CTD [8])

TEST RESULTS

Specimen #	Composite Bond Thickness (in)	Diameter (in)	Area (in ²)	Ultimate Load (lbs)	Tensile Strength (MPa)	Failure Mode	Notes
377009-1	0.044	0.497	0.194	906.3	32.2	SG	
377009-6	0.045	0.495	0.192	672.5	24.1	SG	
377009-7	0.043	0.494	0.192	733.1	26.4	SG	
377009-11	0.045	0.495	0.192	831.2	29.8	SG	
377009-13	0.043	0.495	0.192	483.9	17.3	AB	invalid
Average					28.1		
Std. Dev.					3.6		
CV					0.13		

Notes:

The (SA) and (AB) failure modes are not acceptable failure modes and the strength data shall be noted as invalid
 SA- partly through the specimen surface ply or plies and partly through the adhesive
 SG- along a single plane within the gage section of the specimen
 AB- adhesive failure along bond line

6.5.2 Hydraulic Hose

Choice of the hydraulic hose for the cooling system has been a challenge. Prior to the OH preheater upgrade, the high temperature requirement was at the low pressure end of the OH, and the high pressure requirement was at the low temperature end of the OH. With the preheater, the hose must now meet high temperature and high pressure requirements concurrently.

- ¼” Hydraulic Hose (500 psig, 100 C and non-conductive) will be used for OH water supply. Thus, reduces transit time.
- Hi-pot test result proved non-conductivity (1.5 µA at 15 KV).
- Hydrostatic test
-

From email from John Desandro [24] “Using the black compression ring we tested the hose to 700 psi at room temperature and 500 psi at 120 C. The hose has passed both tests.”

As of Feb 6 2015, hoses that meet the electrical, thermal , and pressure requirements have been found.

7.0 Models

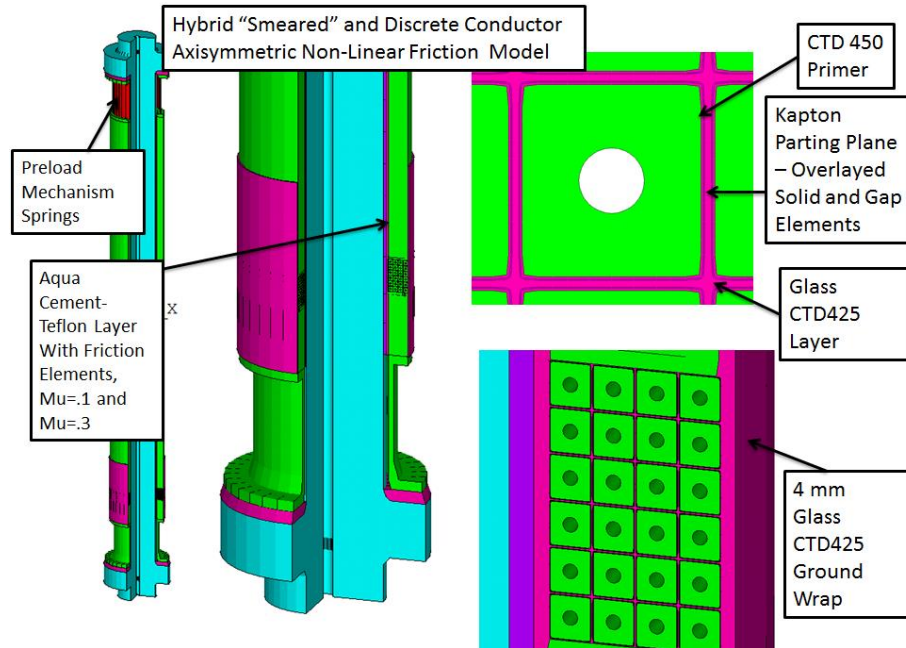


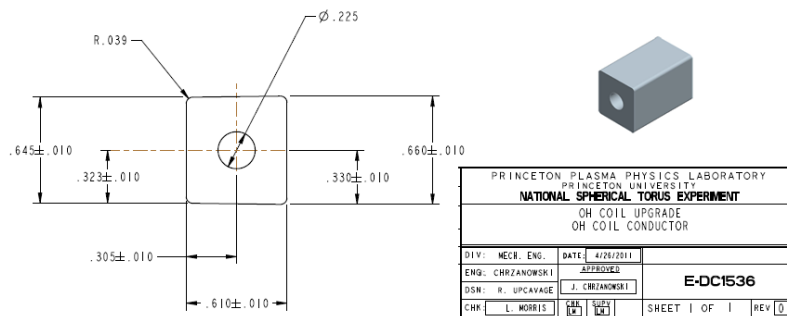
Figure 7.1

The primary model used in this calculation is a 3D, 360 degree model shown in figure 7.1.

7.1 Equivalent OH Modulus

7.1.1 FEA Simulated Equivalent OH Modulus

Aligned and misaligned stack test models were loaded in the coil axial direction with a unit displacement. The resulting stress divided by the strain is the modulus. These models are elastic and the same results would be obtained from tensile and compressive loading. The elastic models will give the same modulus even for the large stress that results from the unit displacement imposed.



Note the Keystoning. – The average coil axial dimension is $(.645+.660)/2 = .6525$ in. = .016573 m. For 222 turns in a layer and a height of the OH of 4.206 meter, the insulation thickness is 2.3729mm or .093422in insulation thickness

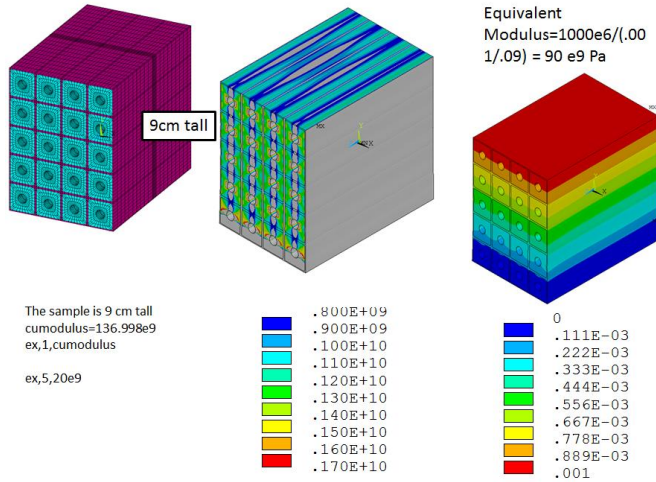


Figure 7.1-2 Unit Array Analysis with Cu modulus = 117 GPa and Insulation Modulus = 20 GPa,

The model in figure 7.1-2 is an early model. For the misaligned case in figure 7.1-3, the conductor build is more accurate, but has a bit more insulation in the vertical load path. Smeared $E=90$ GPa

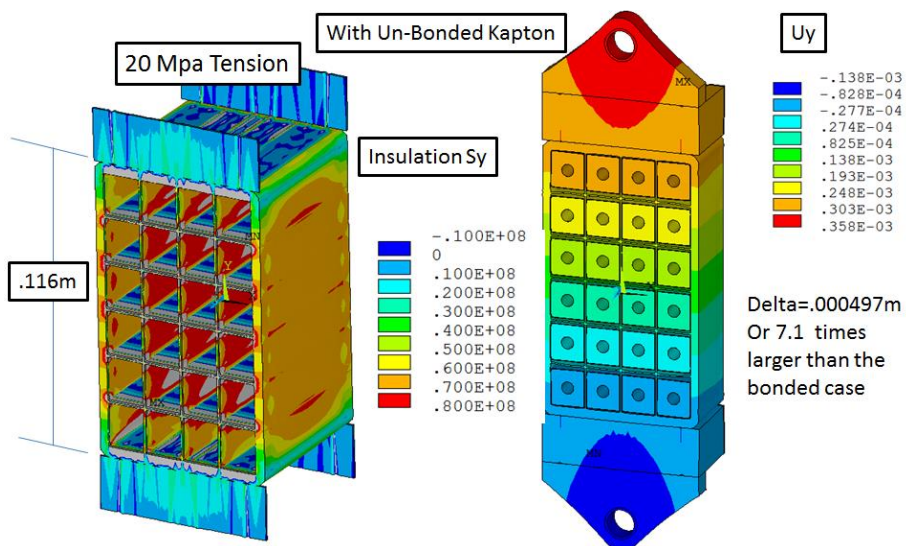


Figure 7.1-3 Unbonded Aligned Simulation, $E=20/.000497=40$ GPa

The model in figure 7.1-2 is an early model. For the misaligned case in figure 7.1-3, the conductor build is more accurate, but has a bit more insulation in the vertical load path.

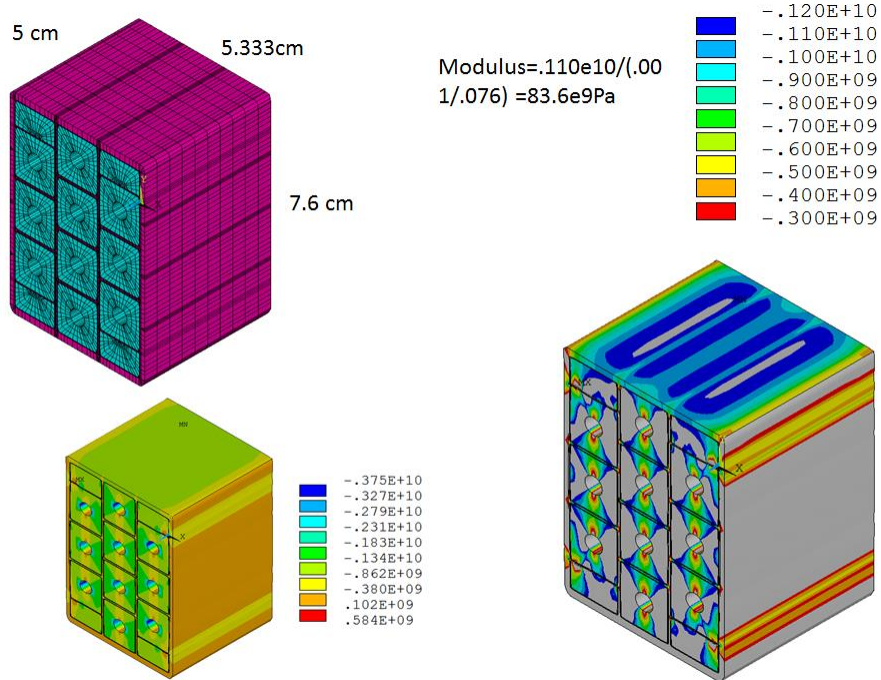


Figure 7.1-3 Misaligned Array Model

The hoop direction modulus can be simply obtained from the packing fraction. From the design point spread sheet [9] this is 0.7012. as $.7012 \times \text{copper modulus}$. Copper's modulus is 17e6psi or 117e9 Pa. Ignoring the insulation, the hoop modulus is $.7012 \times 117 = 82 \text{ GPa}$.

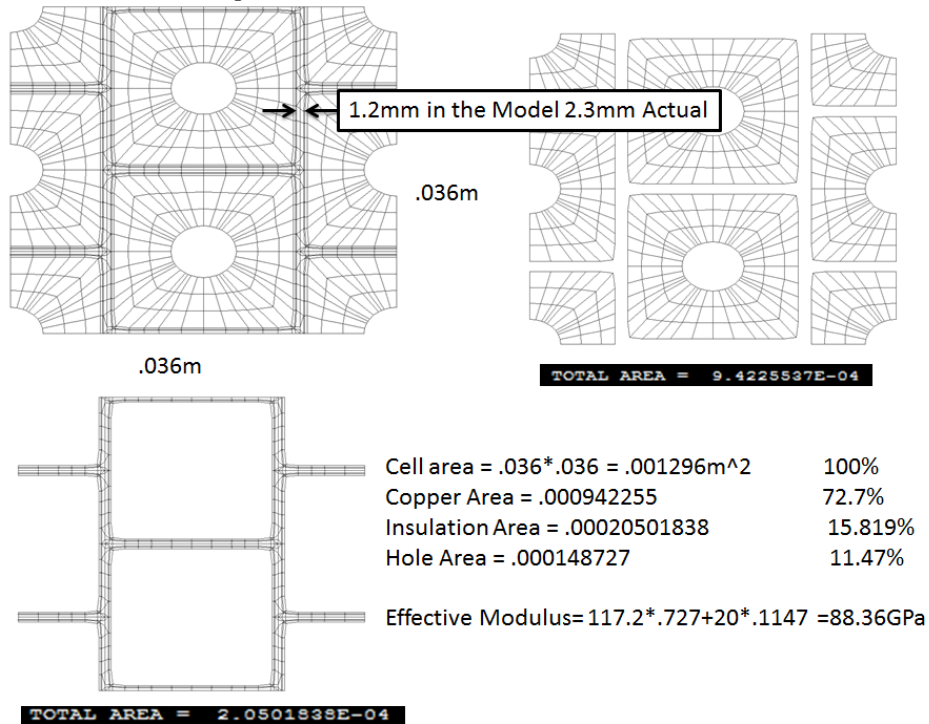


Figure 7.1-4 Hoop Direction Cross Sections and Effective Modulus for a 4 Conductor Cell
 In Figure 7.1-4 the effects of the holes and insulation are included. The hoop modulus is obtained from the mixture rule. The insulation is assumed to have a modulus of 20 GPa and this results in a hoop modulus of 88.36 GPa. Orthotropic properties are difficult to calculate rigorously. Given the similarity in the three directions, an isotropic modulus of 85 GPa is recommended.

	RT	77 K
CTD-425	19.0 ± 1.2	28.0 ± 2.9
Huntsman	16.9 ± 0.6	22.7 ± 2.3

Ref [22]

Radial and Vertical composite moduli of ~85 MPa for the winding pack appears the most reasonable until there are more test results. Models by Zolfaghari, Zhang and Brooks, as well as Titus unit cell analyses, above, show similar behavior above that of the CTD test. There will be a number of opportunities to benchmark the axial modulus of the coil. CTD will provide results for the array samples – both aligned and misaligned, as well as for the creep samples. The best indication of the coil modulus will be from LVDT readings from the OH Belleville preload mechanism.

7.1.2 Measured Compressive Equivalent OH Modulus

CTD is performing electrical tests on samples to address the creep behavior of the CTD425 system under load at the original temperature and a proposed elevated temperature of 120 C. The details of this test are included in section 13.0 as well as here to quantify the modulus for the test. The stresses imposed on the insulation during the cooldown process are displacement controlled, and thus are a function of the modulus of the coil winding pack. Planned tests are displacement controlled with the displacements calculated from the cooldown strains. So the test results should be independent of the modulus of the coil. Analyses of the coil stresses employ a modulus. The uncertainty in the modulus dictated a conservatively stiff modulus for analysis purposes. In this section, a reasonable modulus for analysis will be developed.

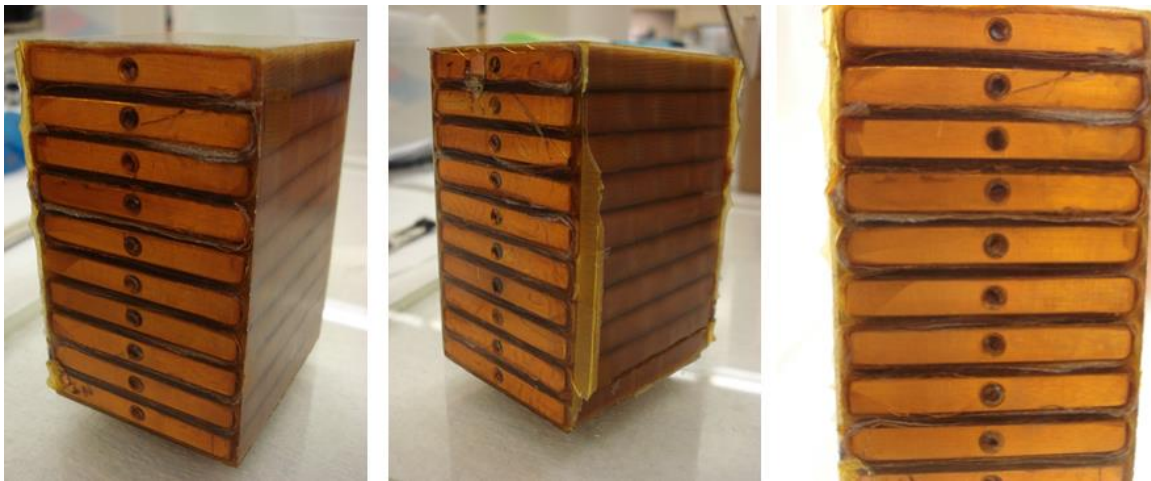


Figure 7.1-1 CTD Creep Stack Test
There are 10 layers of insulation in the test.

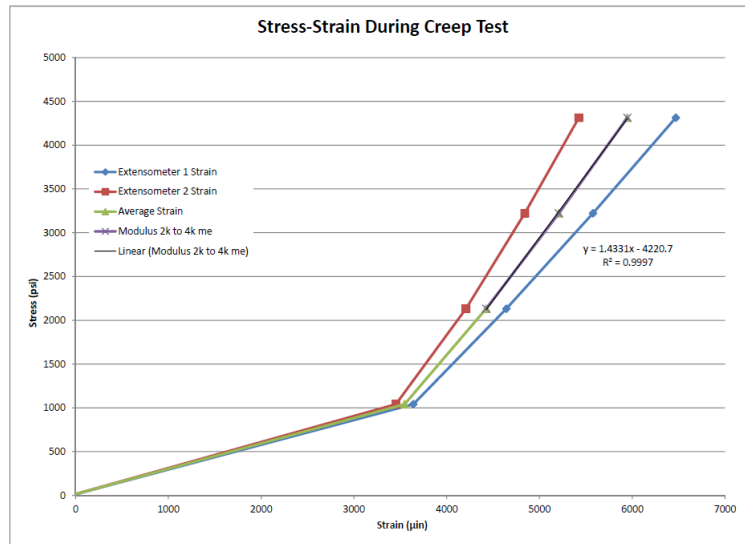
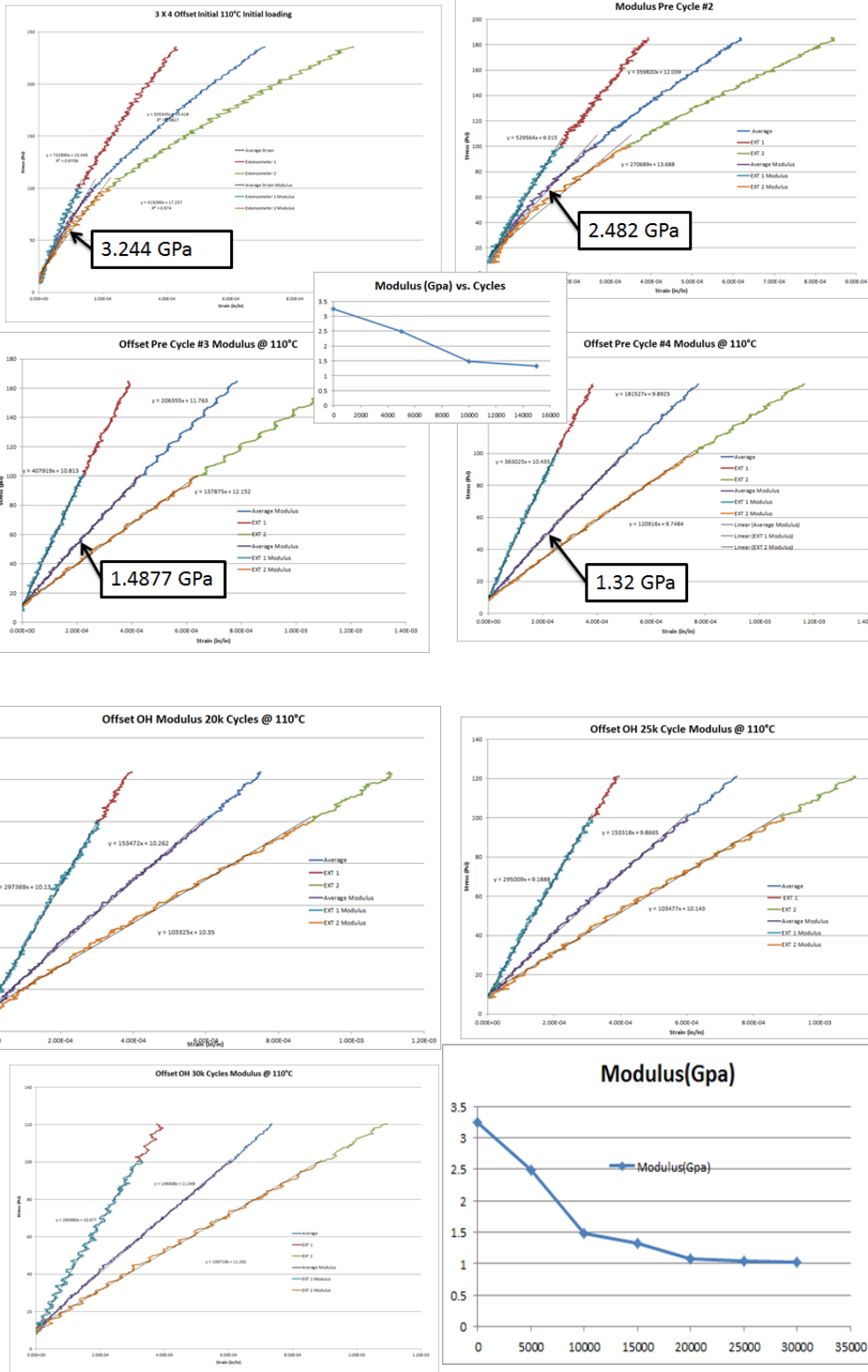


Figure 7.1-2 CTD Load Deflection Curves for the Creep Test

The slope of the curves after “squeezing the air out of the load train” is $(4250-1000)/(6000e-6-3500e-6) = 1.3e6$ psi. This is for 10 insulation layers. The displacement for the 10 layers is .008863 inches. This is calculated from the sample stack height of 3.545 inches and a strain range (.006-.0035). For 222 turns in a layer and a height of the OH of 4.206 meter, the effective modulus would be $3250/(.008863*222/10/(4.206*39.37)) = 2.735e6$ psi = 18.8e9 Pa. Very low. This is for fully aligned conductors, but it still looks suspect compared with computed moduli. This could be backlash or fit-up issues with the platens, maybe lack of fill in the interlayers of the lapped Kapton, or the epoxy itself is softer than assumed in the analysis. The OH preload mechanism is instrumented and during early stages of the NSTX start-up, the change in OH height when energized, will be measured and this will give a direct indication of the OH winding pack modulus.

7.1.3 Measured Tensile Equivalent OH Modulus



8.0 Stresses Due to the Cooling Wave, Comparison with the original NSTX

At one of the reviews of the aquapour issue in which the cooling wave effect was raised, Mike Williams pointed out that this effect was not a problem with the original NSTX and should not be a problem with the upgrade. After the TF failure, the OH was removed and a post-mortem was done on the OH – Not actually a post-mortem because the TF failed and not the OH. The OH cross sections looked very good. All the insulation was intact. No formal testing was done, but despite the good appearance it was found that the insulators were not well bonded. It is not known if this was due to the cooling strains or other loading, or poor initial bonding. Figure 8.0-1 shows the NSTX OH section with one of the conductors slipped out of the array. This was done relatively easily with a pair of needle nose pliers.

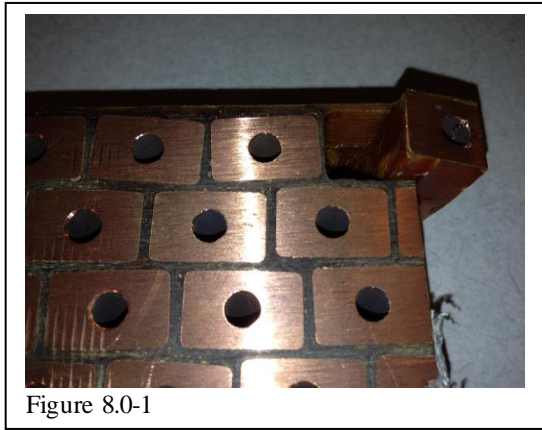


Figure 8.0-1

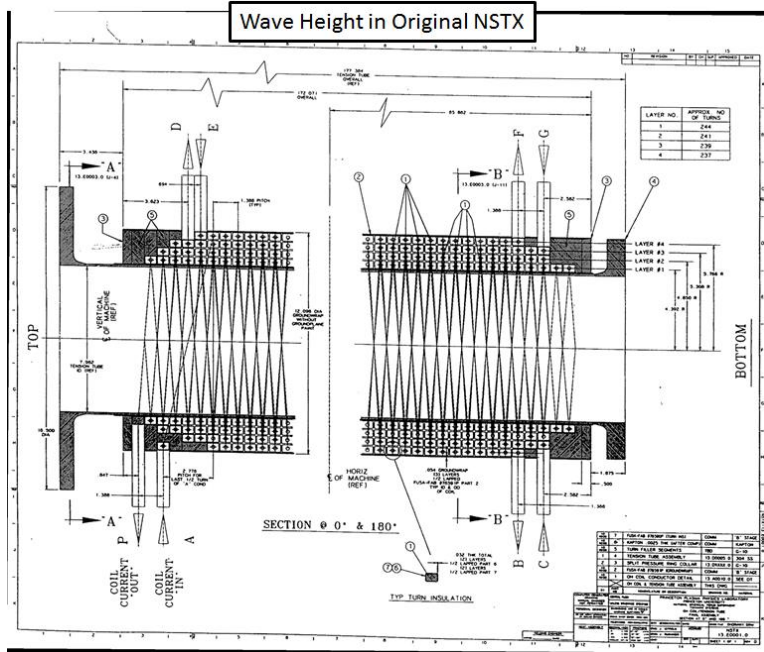


Figure 8.0-2

The success of NSTX is a reasonable benchmark for the cooling wave effect, but geometry differences cause higher stresses in the Upgrade. Figure 8.0-2 provides the dimensional data used in the comparison of NSXT and NSTX-U

Wave Height in Original NSTX

2inHand OH Layer 4, I=24KA, ESW=.5208s, V=2.75m/s

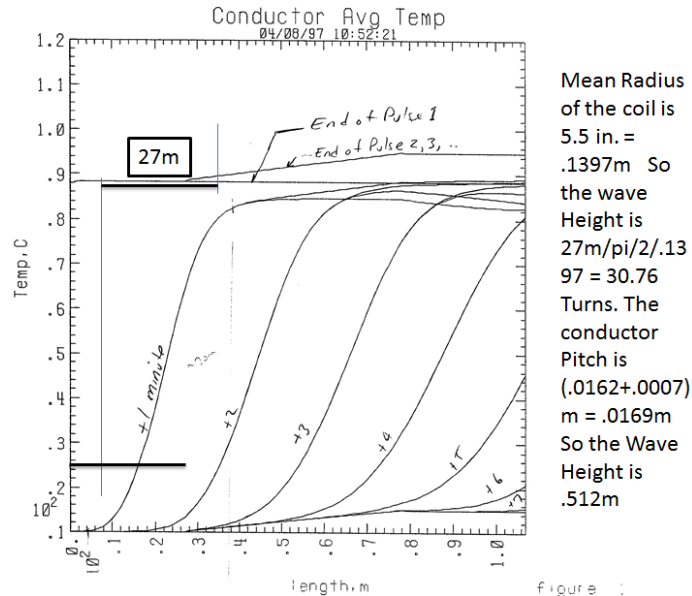


Figure 8.0-3 Estimate of NSTX Cooling Wave Height (ACOOL Plot from [3])

From Ali's NSTX-U calc and from Arts NSTX calc [3], the axial heights of the cooling wave were estimated in the two solenoids to be .27 m in the upgrade and .51m in NSTX - the main reason for this is that the cooling wave along the conductor is comparable for both, but in NSTX it is wrapped around a smaller diameter and thus goes a longer axial distance. For a given displacement the longer wave absorbs the radial strain with less bending stress. Based on a beam analogy the effect goes as L^2 . This makes NSTXU about 3.6 times worse.

The thermal radial growth of the coil is larger for the NSTX U than for NSTX, just because it is larger. The analogous beam stress is linear in displacement. - This is about a factor of 1.7 worse

The thickness of the coil is greater for NSTXU than NSTX - For a given bending displacement a thicker shell will have a bigger bending stress. This makes NSTXU about 1.5 times worse.

The total effect is $3.6*1.7*1.5 = 9.2$ times worse for NSTX-U than for NSTX. The effects were simulated in FEA models of the two solenoids. The effects are not as strong as the hand calculations, but are still large. These are shown in figure 8.0-3

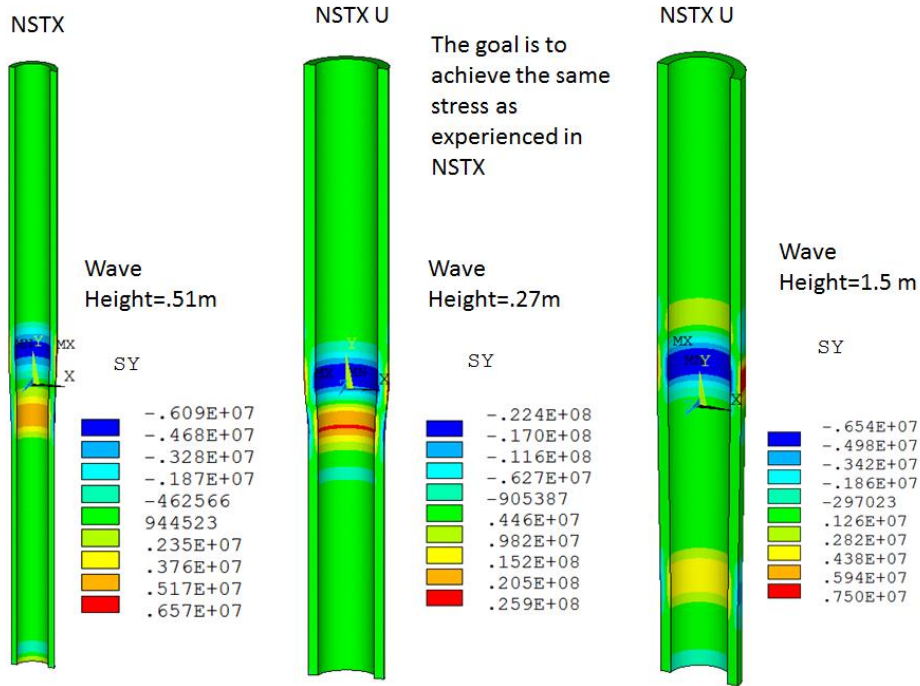


Figure 8.0-3 Comparison of NSTX Cooling Wave Height Stress for NSTX and NSTX-U

In the analyses shown above, the modulus was 100 GPa and the tensile strain imposed on the winding pack array is $25.9e6 / 100e9 = 2.59e-4$. With the wave height relief the tensile strain is $7.5e6 / 100e9 = 7.5e-5$

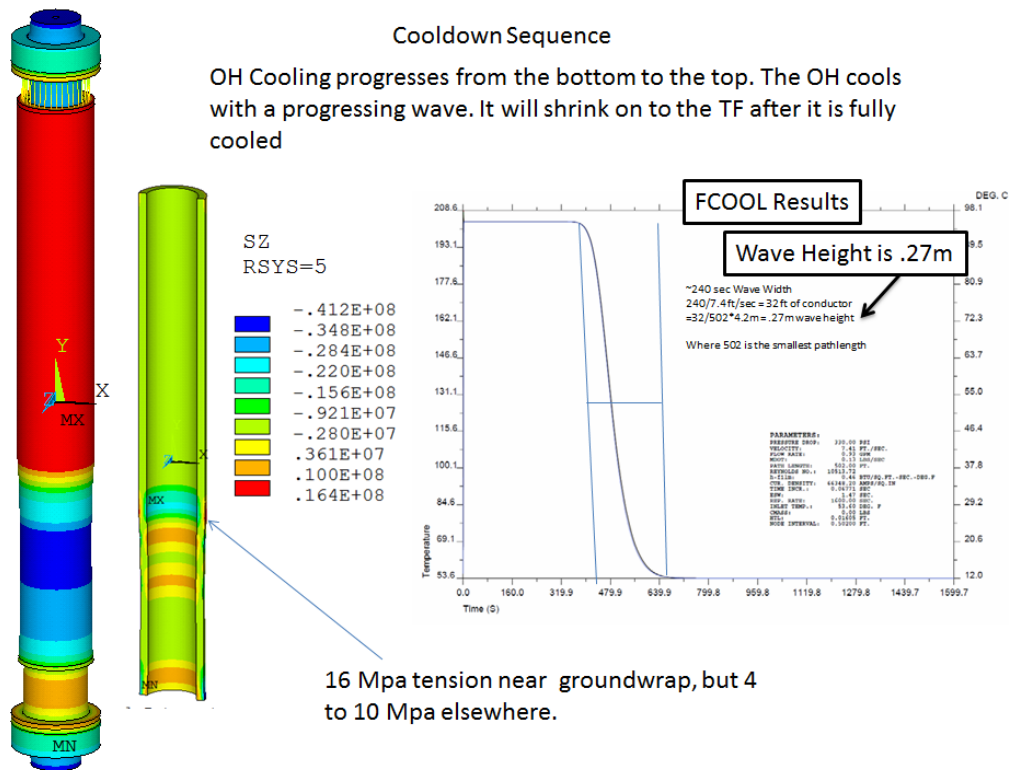


Figure 8.0-4 Cooling wave simulation with Frictional Interaction with the TF

9.0 FCOOL Runs, Wave Height Stress, Stepped Cooldown (Han Zhang)

The text output from FCOOL was used to create ADPL commands to apply the temperature to a model of the OH. The ADPL commands are included in attachment B at the end of this calculation. A normal cooldown was simulated and various initial temperatures, and pressures (and resulting flow rates) were simulated. The best solution was a three stage stepped decrease in initial temperature. In later analyses the three steps were replaced with a linear rampdown – See section 10.0

Han Zhang Results: OH cooling: tension stress from different cooling schemes

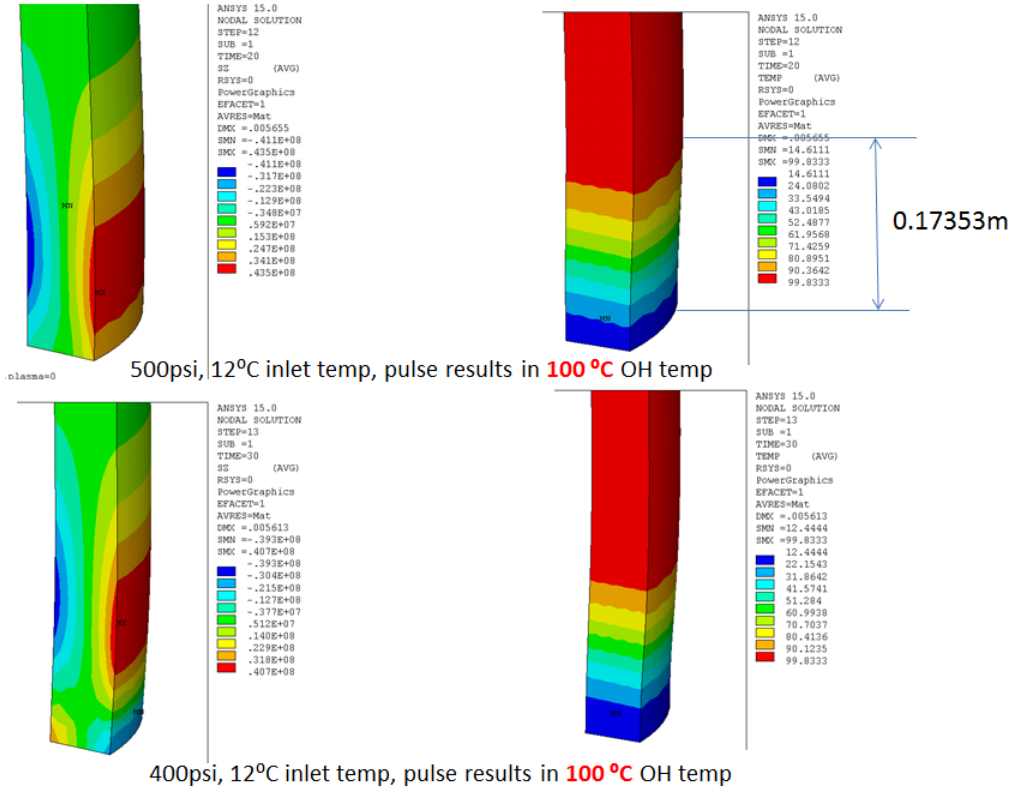


Figure 9.0-1

OH cooling: tension stress from different cooling scheme

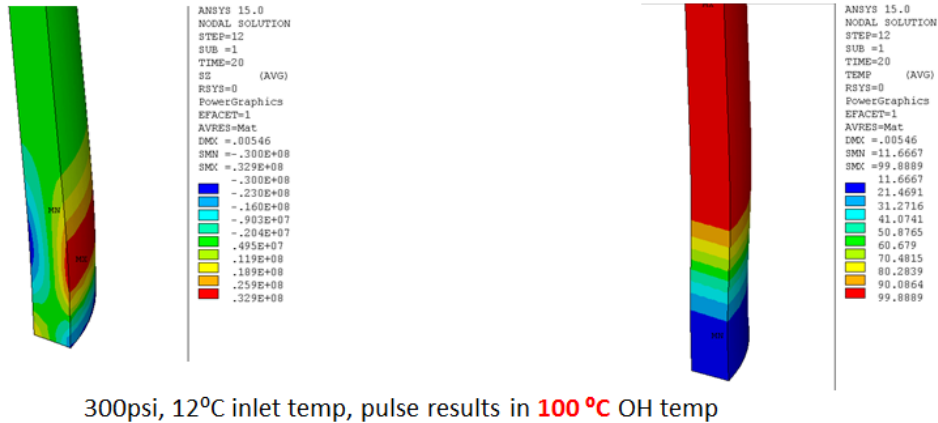


Figure 9.0-2

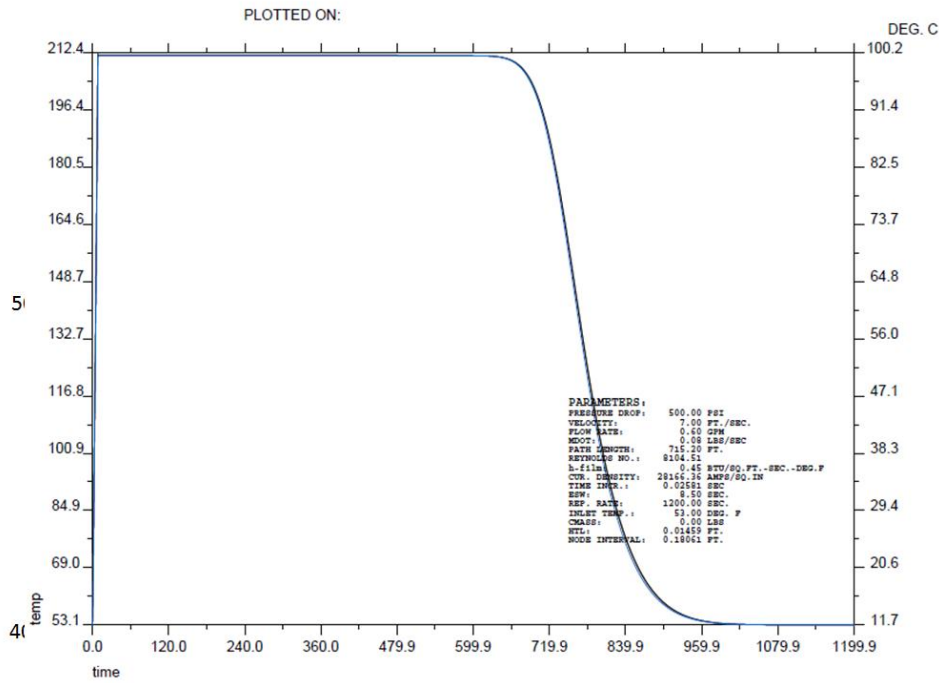
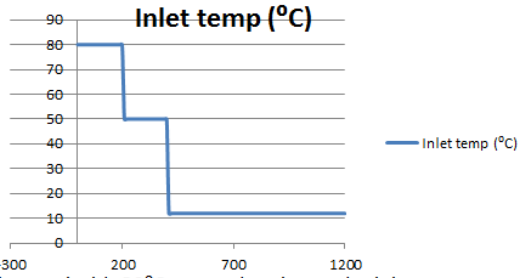


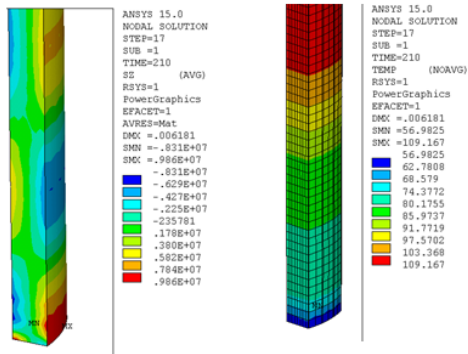
Figure 9.0-3 Han Zhang's

Han Suggests Stepped Temp Decrease:

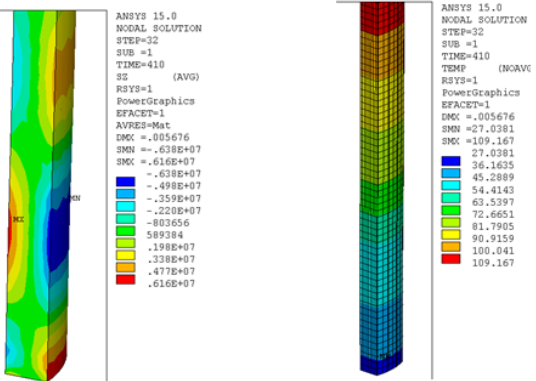
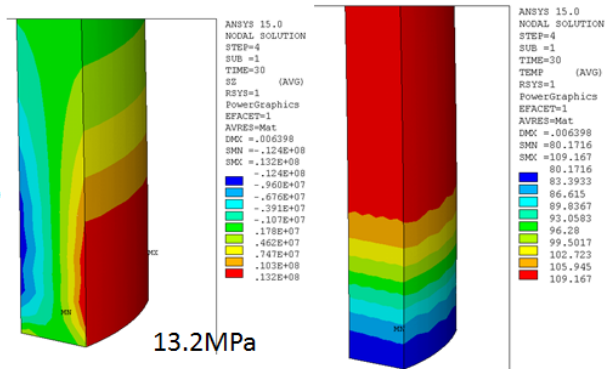
OH cooling: tension stress from different cooling scheme



First cool with 80°C water, then lower the inlet temp to 50°C@200s, then lower to 12°C@400s. pulse results in 110°C OH temp



After inlet temp changed to 45°C@200s



After inlet temp changed to 12°C@400s

Total time using this scheme to fully cool OH down hasn't been completed

Figure 9.0-4

10.0 ACOOL Runs, Ramped Cooldown (A. Brooks)

Han's results, with three steps in the cooling, suggested the idea that a linear rampdown would provide the necessary gradual thermal gradients needed to keep the axial tensile stresses low. Art Brooks provided the necessary coding in his version of FCOOL or ACOOL.

10.1 Linear Rampdown from 100C

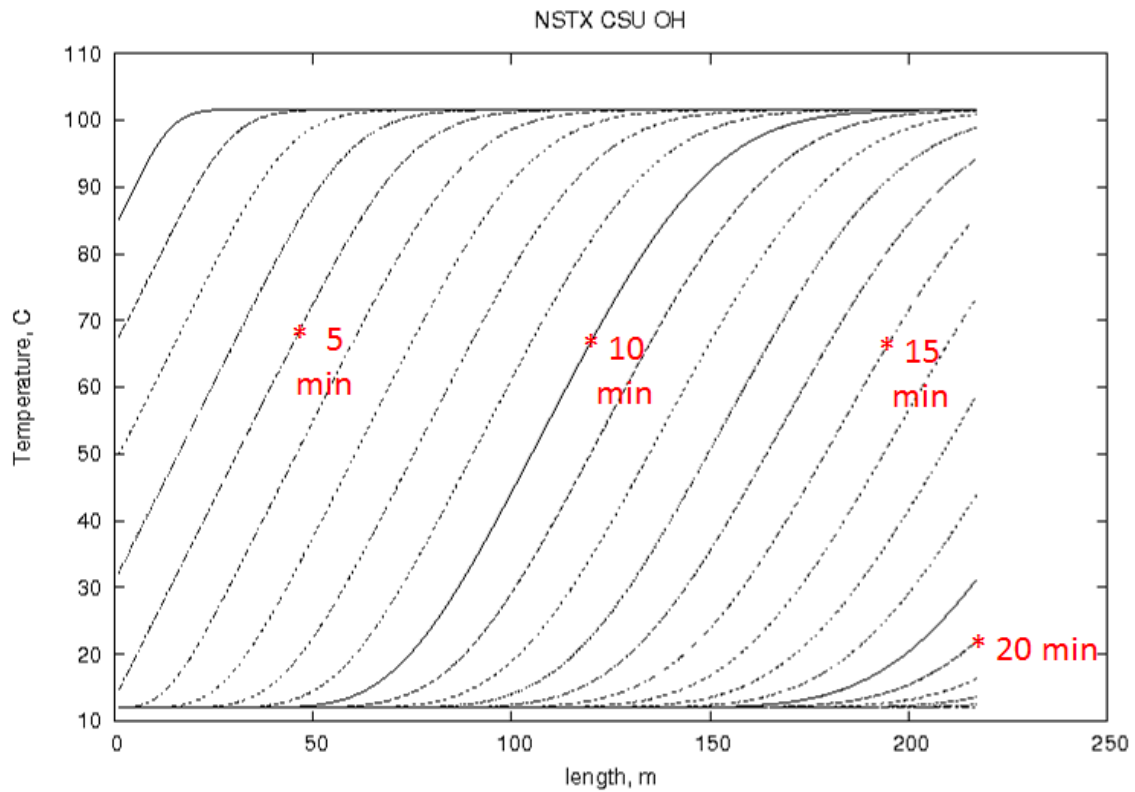


Figure 10.1-1 Ramping down Inlet Water from 100 C to 12 C in 300s This stretches out the wave height to >1.5m with cool down in 22 min

NSTX CSU OH			
217	xl,	length of conductor,	meters
.0155	wcu,	width or -dia of conductor,	meters
.0168	tcu,	thickness of conductor,	meters
-.0057	Aw,	area or -dia of coolant hole,	square meters
.00000	Fw,	wetted perimeter of coolant hole,	meters
12	Tc0,	inlet&initial temperature,	C
-12	Tw0,	inlet&initial temperature,	C - negative to read a table at end
2.13	v,	velocity of coolant,	m/s
1500	tend,	run time,	sec
60.	dtpr,	print out interval,	sec
217	n,	number of nodes along length,	-
10000	tmx,	max temperature before terminating,	C
1.724e-8	curho,	conductor resistivity at Tref,	ohm-m
0.00410	cualp,	temperature coefficient of resistance,	1/C
20.	Tref,	Reference temperature for curho,	C
8900.	cu dens,	conductor density	kg/m3
383.	cuspht,	conductor specific heat,	J/kg-C
400.	cucond,	conductor thermal conductivity,	w/m-C
1000.	wdens,	coolant density or -Pin,	kg/m3
4126.	wsphnt,	coolant specific heat,	J/kg-C
.994e-6	wkvisc,	coolant kinematic or -dynamic viscosity,	m2/s (1e-6 m2/s = 1 cs)
0.5984	wcond,	coolant thermal conductivity,	w/m-C
0000.	Rgas,	Ideal Gas Constant (use 0 for liquid),	J/kg-K
.0	emiss,	conductor surface emissivity	
0.6	vf,	view factor	
0.	Prad,	Perim of Rad Surf (replaced with pi*dia if wcu<0),	meters
100.	Trad,	Sink Temperature for Radiation,	C
-1	ncur,	number of values in time vs current table (use - for ESW)	
01 1.473 1500. 24000. 0.		! npulse, tpulse, trep, cur, qnuc	
3	ntw,	number of values in time vs water temperature table	
0. 100.			
300. 12.			
1500. 12.			

10.2 Linear Rampdown from 80C

10.3 Linear Rampdown with 10 seconds of initial 12C water

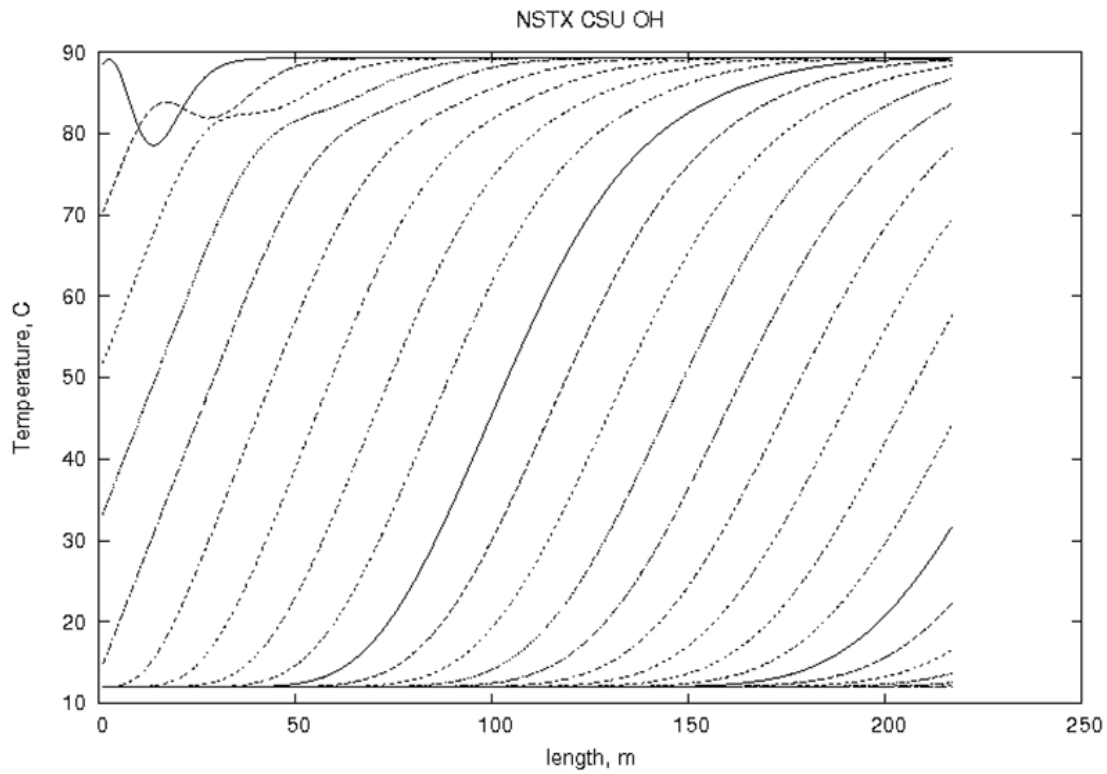


Figure 10.3-1

The control system (Section 12.5) and transit times (section 12.3) dictate a need for some tolerance on the times that the desired temperatures can be obtained. To set a limit, it is assumed that the coils will see 10 seconds of cold water prior to the availability of heated water.

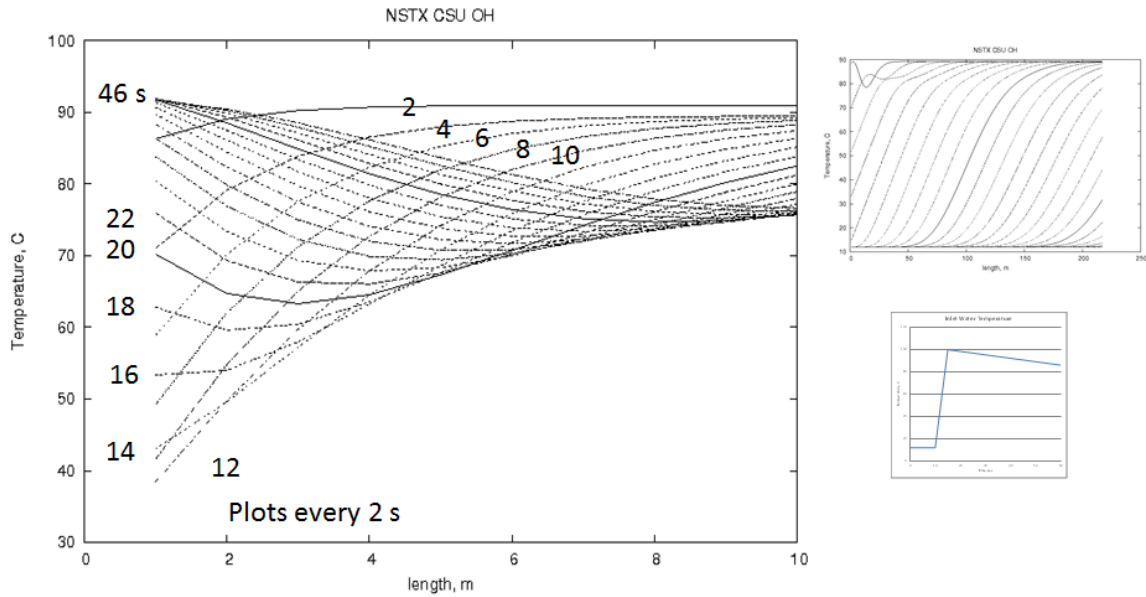


Figure 10.3-2

Figure 10.3-1 is a plot of the OH response to a water inlet temperature profile that is 12 C for the first 10 s, ramps to 100 C by 15 s and back down to 12 C by 300 s. As you can see it does take long to cool the inlet.

By 10 C the inlet has been cooled to ~40 C before being warmed back up as hot water begins to enter. That puts a gradient of 50 C over the first 10 m of coil (or 0.2 m of height)

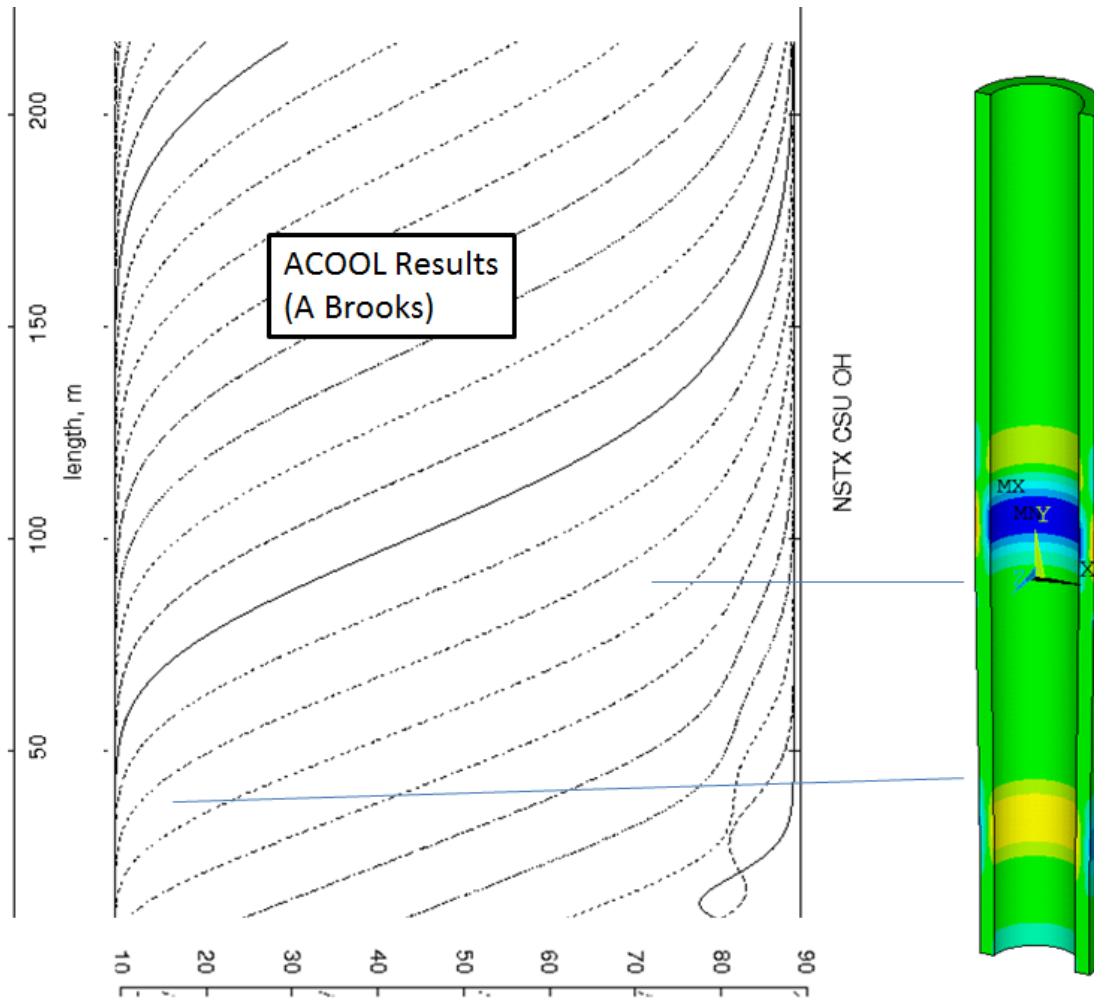


Figure 10.3-3

In this plot the calculation an attempt is made to connect the usual plot of the wave vs conductor length to the wave height in the coil geometry. The initial irregularity in the wave at the base of the coil evaluated in more detail in section 11.0.

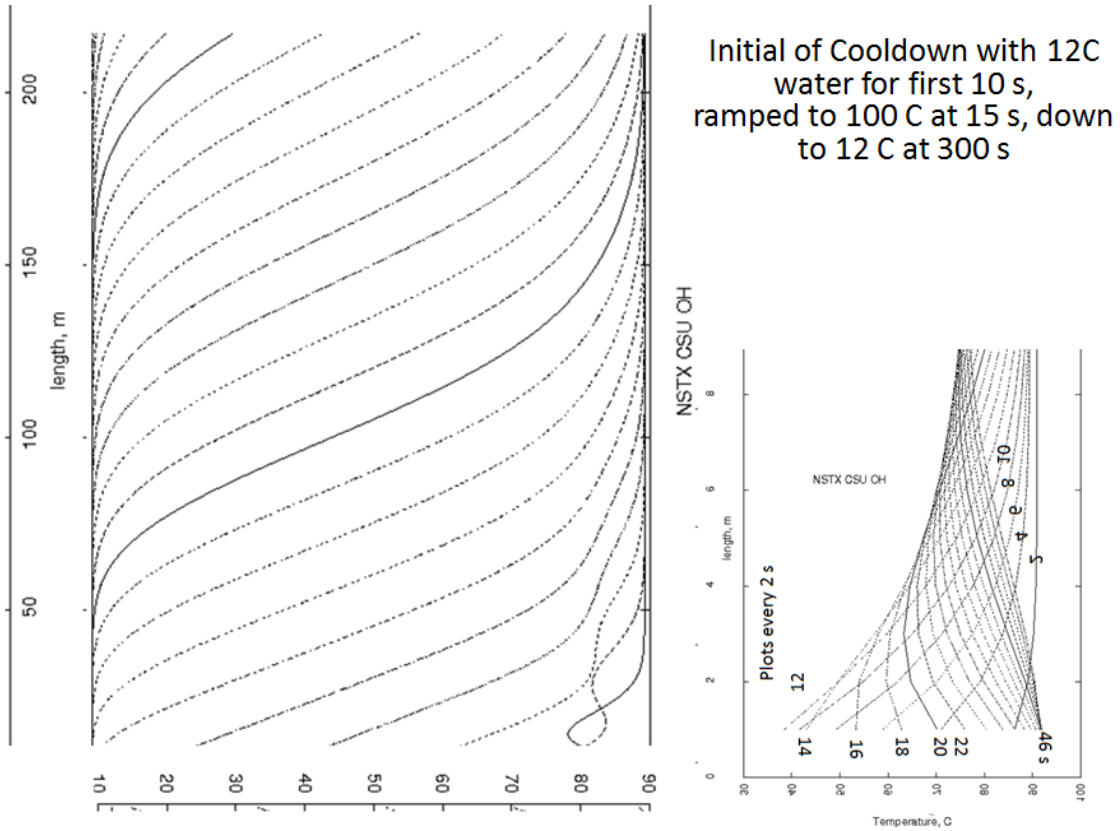


Figure 10.3-4 10 seconds of 12C water Prior to Inlet of Heated Water

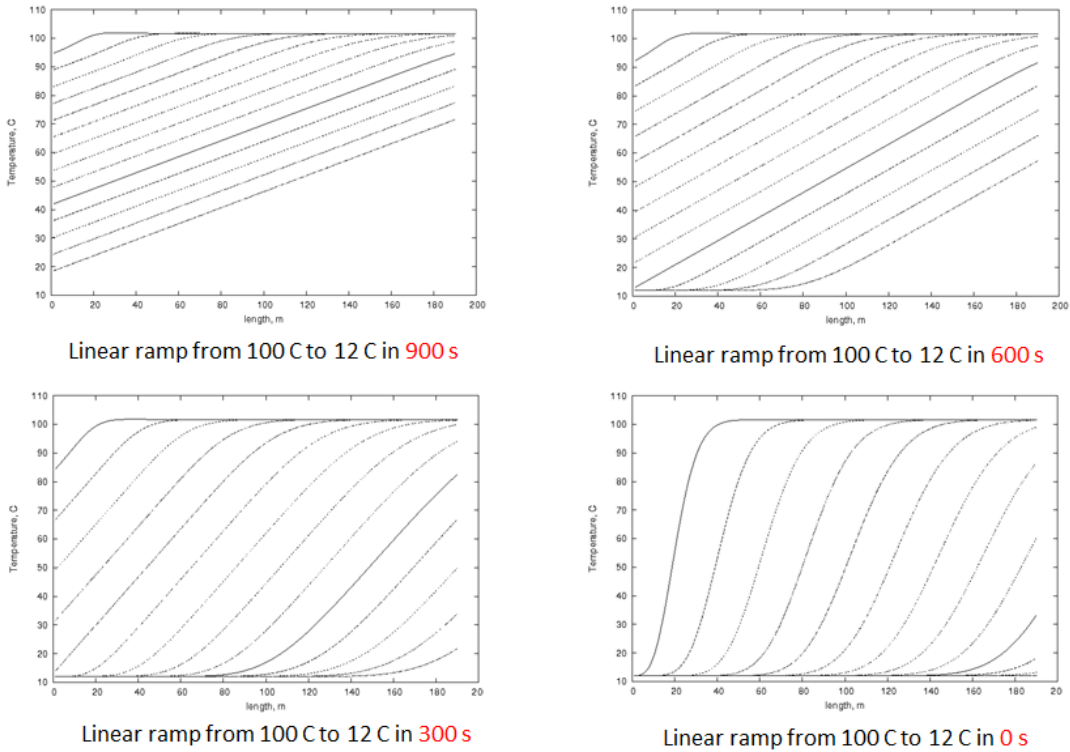
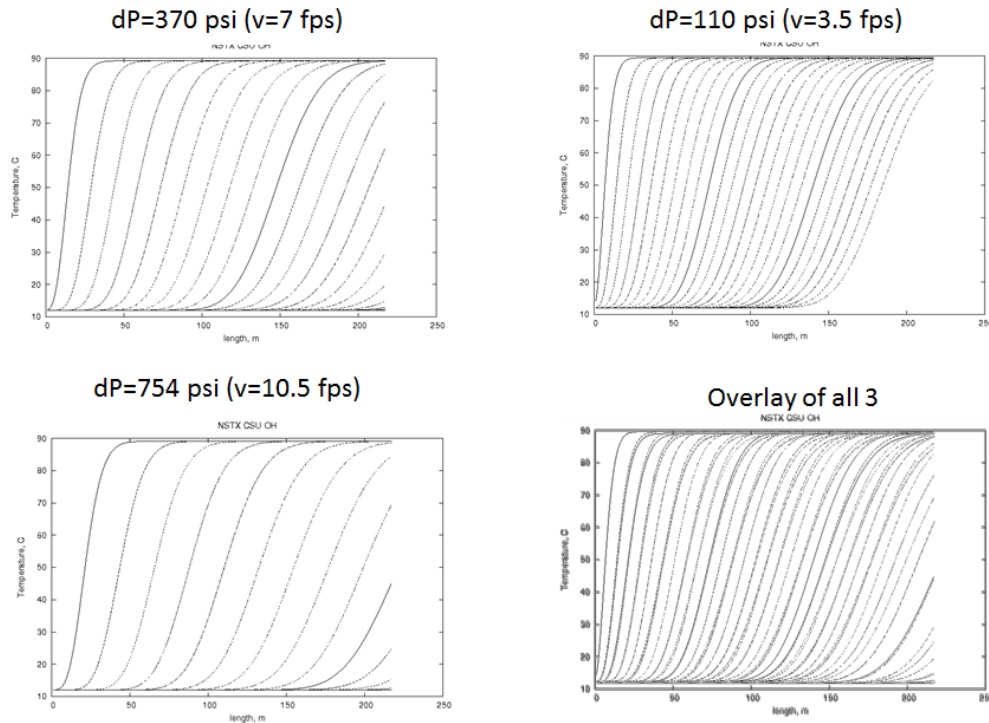


Figure 10.3-5 Cooldown of OH with Variable Inlet Water Temperature. Temperature is plotted vs. length every 60 seconds – Last curve is 900 seconds

10.4 Effect of Changing inlet Pressure (A.Brooks)

It was thought that slowing the water flow would lengthen the wave. Art investigated this. Lowering the water pressure lowers the flow velocity and the velocity of the propagation of the wave. It also increases the cooling time. Unfortunately the wave height does not change. So altering the pump pressure was not an option to improve the coil stress.

Changing Pressure Affects Cooling Wave Velocity But Not Height



11.0 Thermal Stress at the Restrained Base of the OH (A Khodak)

The analysis of record for the OH coaxial cable is: "NSTX Upgrade OH Coaxial Cable and Embedded Leads" NSTXU-CALC-133-07-00 10 October 2011 Prepared By M. Mardenfeld, and checked by Ali Zolfaghari [14]. Mike Mardenfeld made the analysis model available so that the increased operating temperature could be investigated. Temperatures of 100C and 120 C were simulated. At this writing 110C is the targeted allowed increase in peak operating temperature

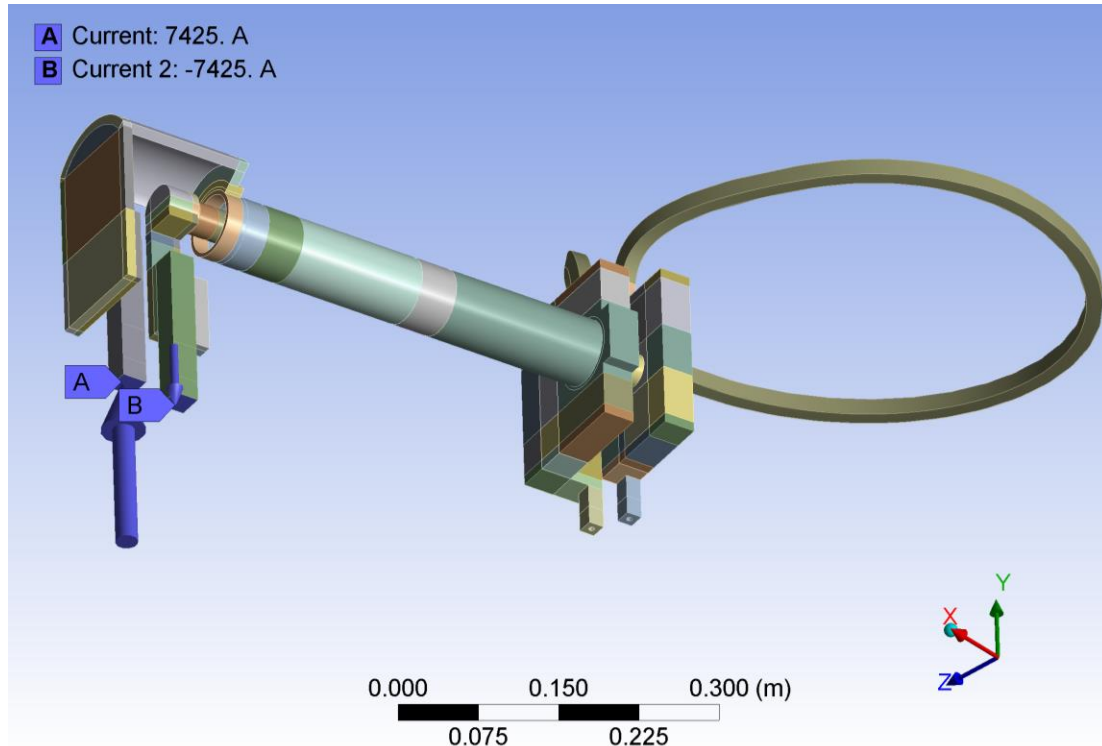
A three stage analysis was performed to simulate the OH restrained base under electric and thermal loads. The model included the OH coil represented by the solid copper cylinder, the OH coil leads represented by the copper loop buried in the G10 OH base, and parts of the OH bus bars in the vicinity of the OH coil.

At the first stage, the electrical analysis was performed on the copper loop enclosed within the base as shown on figs 11.1 and 11.2. This simulates behavior of the OH leads within the base. Boundary condition of the constant current was imposed at the ends of the loop as shown on figure 11.1. The values of the current are selected in way that Joule heat exported to the heat transfer problem produces predetermined maximum temperature level on the copper loop.

At the second stage transient thermal problem is solved for all copper parts and insulating OH base. The temperature is initially set to 12°C for all parts, and then heated for 20 seconds with volumetric heat source distribution representing the Joule heat source. Volumetric heat source in the OH base loop is imported directly from electrical problem. OH coil windings are represented by solid copper cylinder and constant

volumetric heat source density. The values of the volumetric heat source density for copper cylinder are presented on figure 11.3. These values are adjusted to achieve maximum temperatures of 100°C and 120°C. The values of loop current, which are used to obtain corresponding temperatures on the OH base loop, are also presented on figure 11.3.

The third stage is structural analysis of the OH base assembly. Temperature values imported from the thermal analysis at 20s were used as thermal load. Assembly was fixed in the areas shown on figure 11.4. Results for the deformation, axial stress and R-Z shear stress are presented on figures 11.5, 11.6, 11.7



11.1 Current condition for electrical problem in the base loop

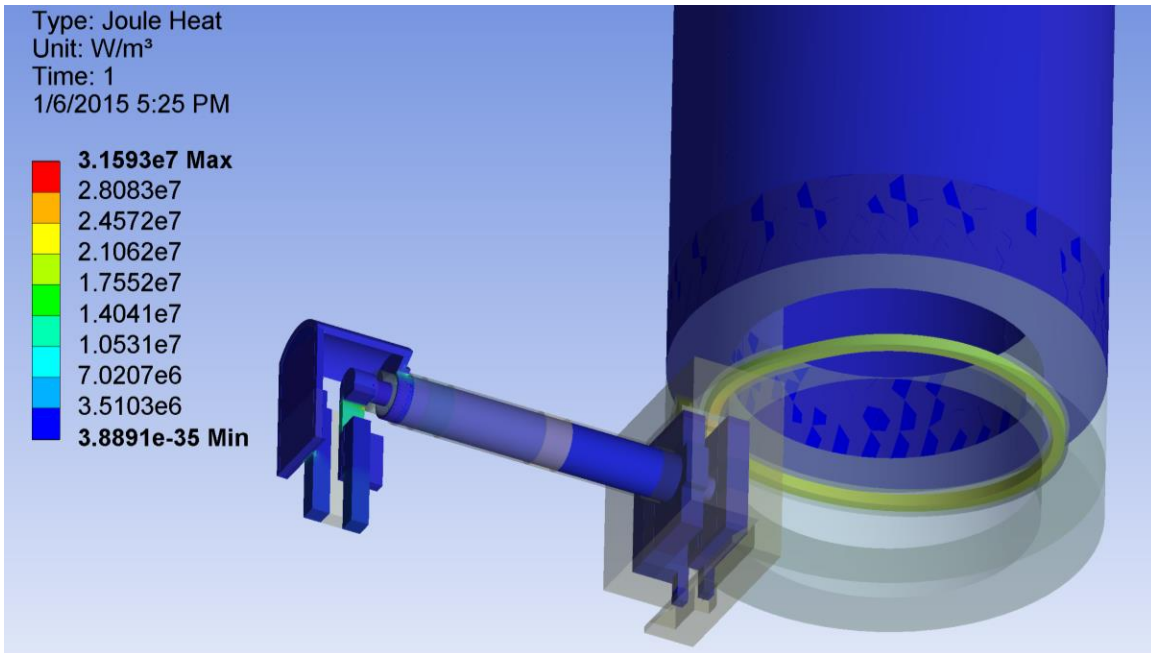
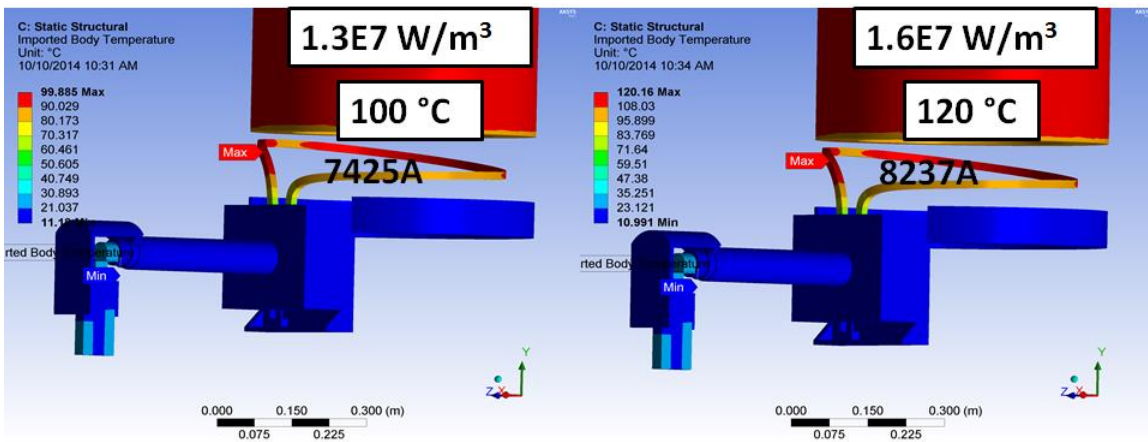
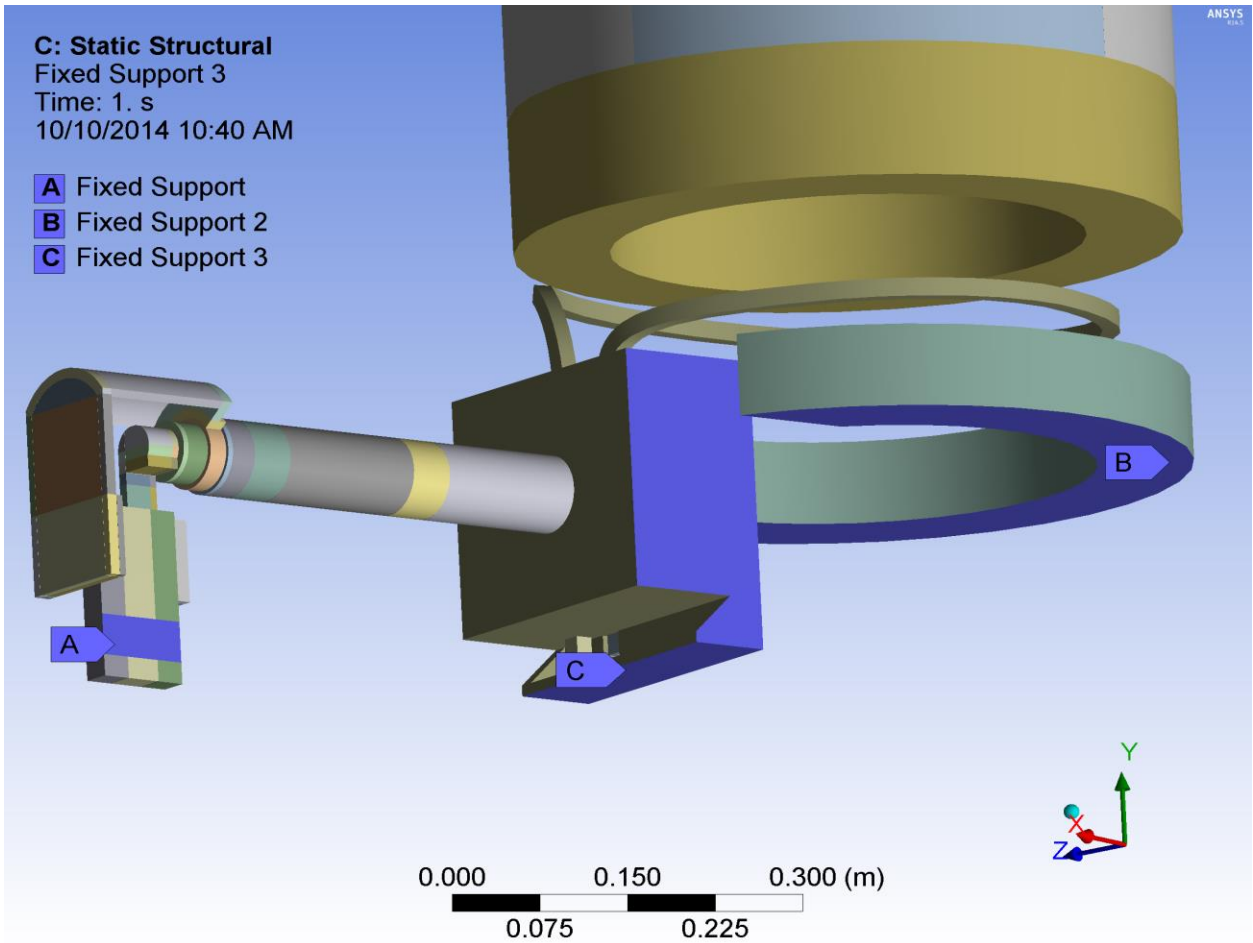


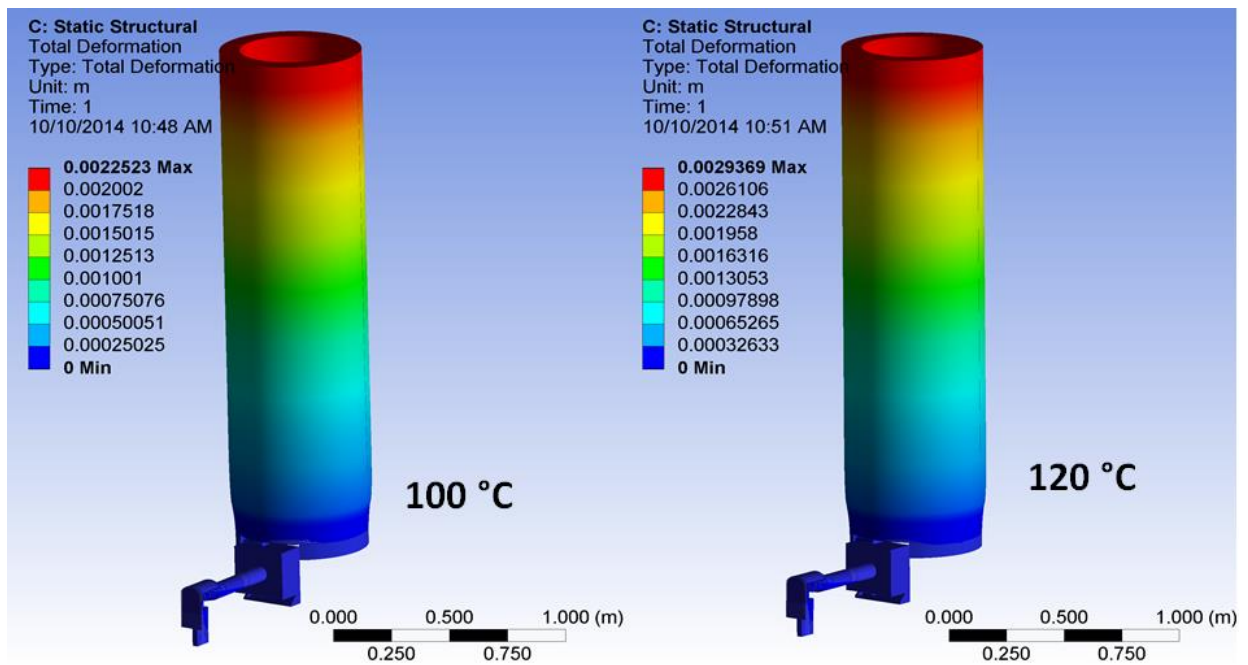
Figure 11.2 Joule heat generated in the base loop



11.3 Volumetric heat source density OH base loop current and temperature values on the copper parts for the cases of 100°C and 120°C



11.4 Boundary conditions for structural problem



11.5 Total deformation of the assembly

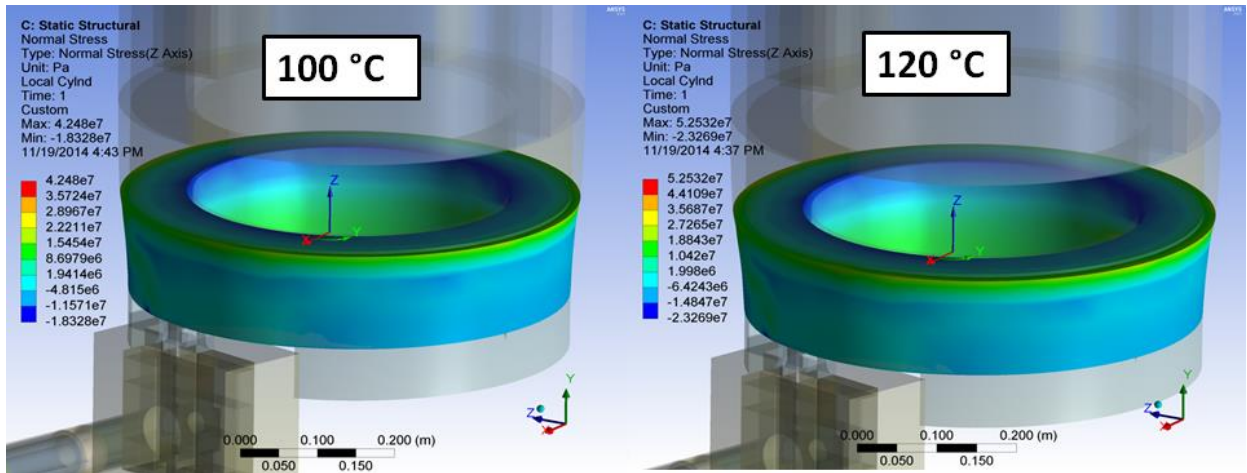


Figure 11.6 Axial stress

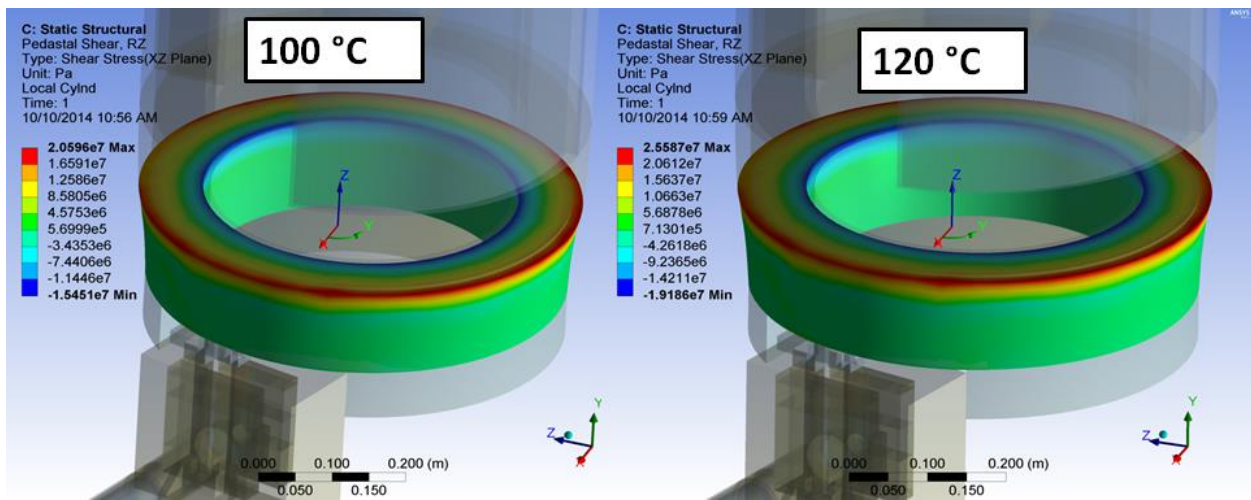
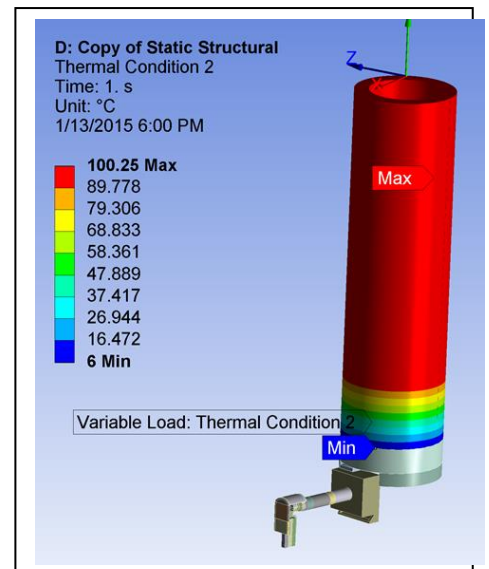


Figure 11.7 R-Z Shear Stress

Art simulated 10 sec of 12C flow. Andrei included it in his analysis of the base of the OH coil using Mike Mardenfelds OH coax model. 10 seconds of initial 12C cooling water was modeled. The base was qualified with the coil at 100C and the 12C cooling water with the G-10 and support structures remaining at 12C between shots. So the base structures and bottom of the coil take the thermal gradient - with a lot of extra Kapton tape for good measure. 5 seconds of 12 C flow is better and a better target to give us a margin.



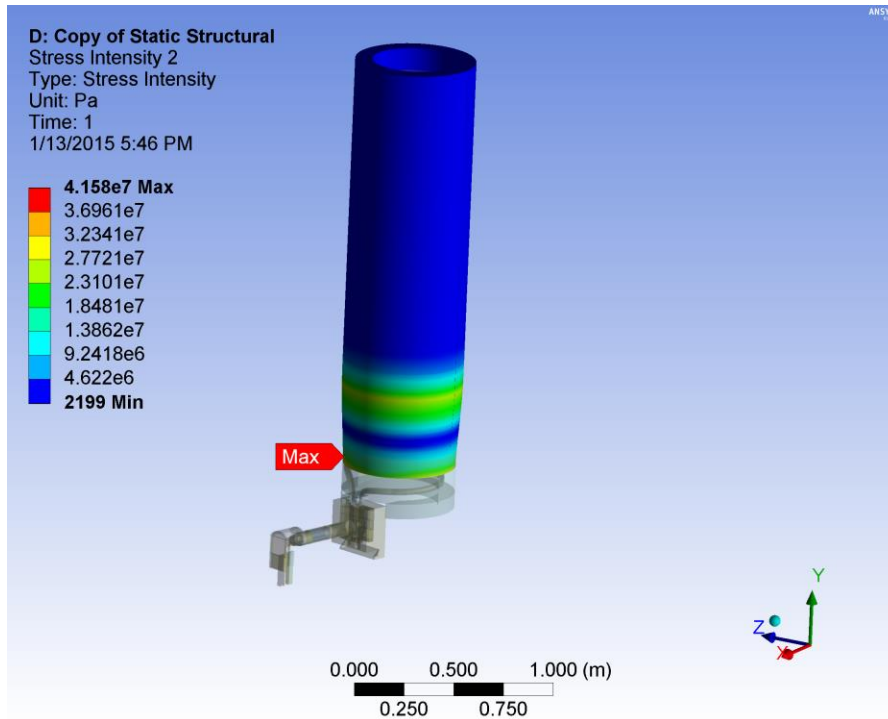


Figure 11.8 Stress Intensity With 111GPa Elastic modulus

The tensile strain is $41.58e6/111e9 = 3.75e-4$

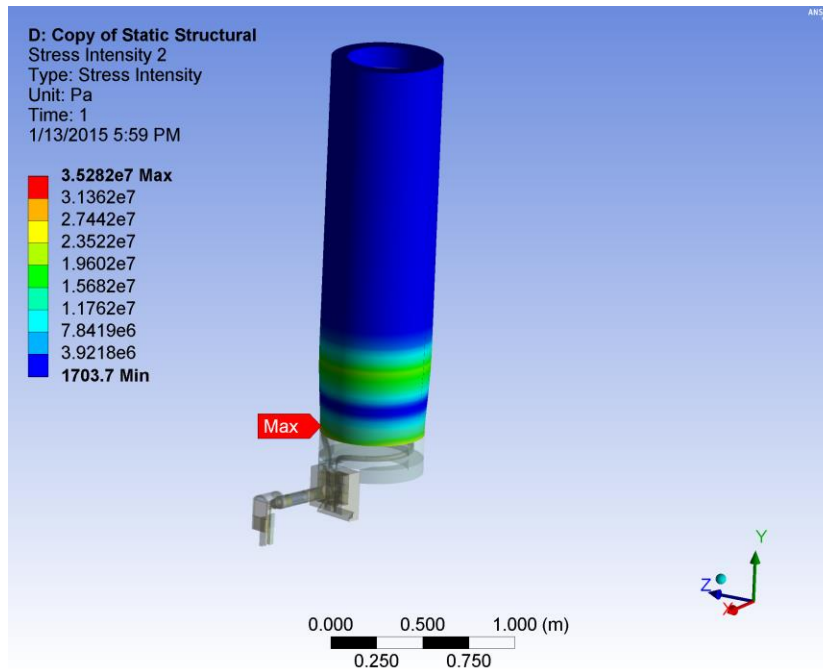


Figure 11.9 Stress Intensity With 85GPa Elastic modulus

The tensile strain is $35.28e6/85e9 = 4.1e-4$

11.2 10 second of initial 12C cooling water at the Base with Adjusted Moduli (P. Titus, A Brooks)

From Mike Mardenfeld's email, ref [20]:

“The original design calls for the “eyebrow” pieces as per 1EDC1483. The calculation tried to capture this in a simplified way, by modelling a solid G10 block which included representation of the “ridges and valleys” formed by the after-impregnated pieces. [I extracted this from the solid models, not the drawings].

In the field, cylindrical annuli were formed by wet lay up on mandrels per 1EDC1739. These blanks were precision turned to the correct IDs and ODs, but then cutting the annuli into pieces was done by hand with Sawzalls. In the end, due to the imperfections of the copper windings and the need to hand bend the leads, there ended up being many more smaller pieces than as shown in the eyebrow drawings, which were custom cut and filed, stuffed with glass, etc. to get everything to fit.”

Tests were performed on the wet layup done for the TF Flag collar [21] Attachment C. These produced the stress strain curve below:

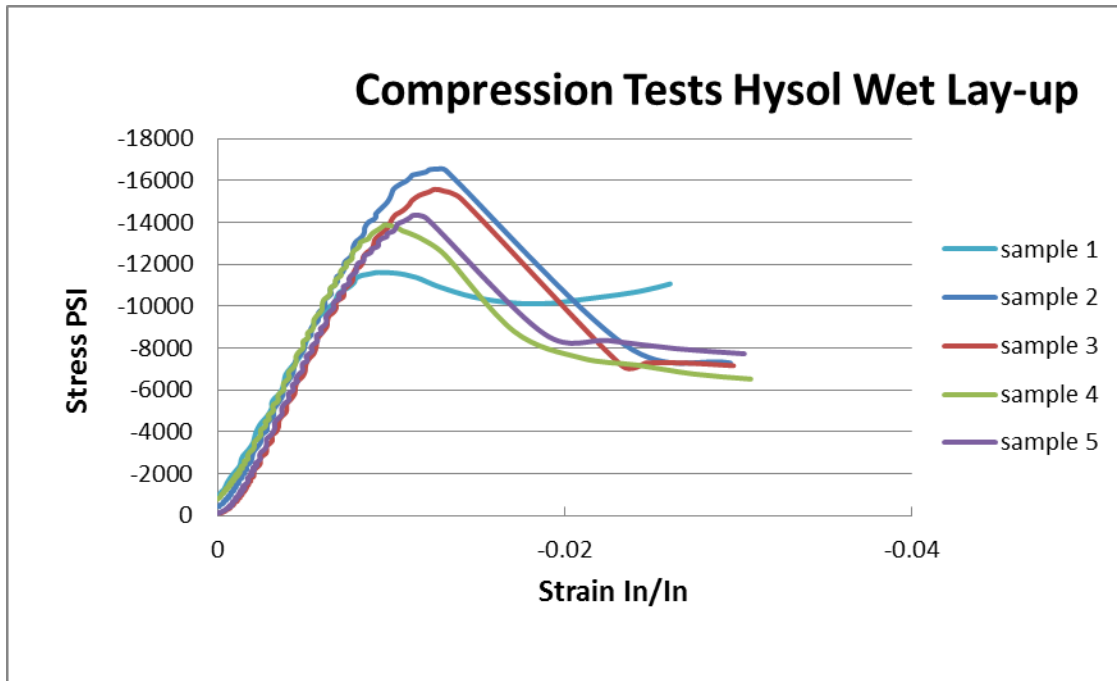
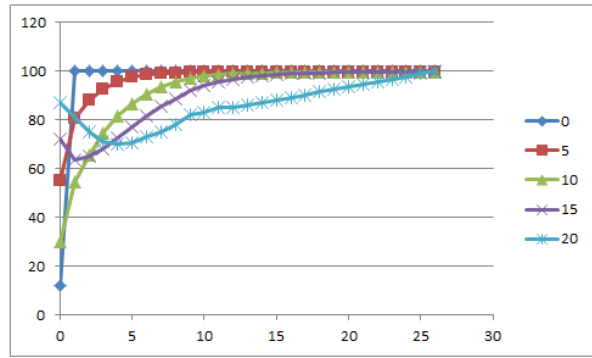
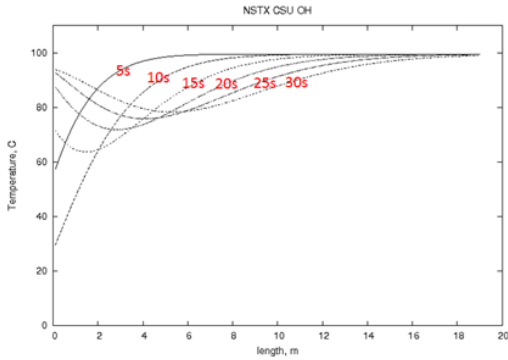


Figure 11.0-5 Wet Layup Stress Strain Curve

The compressive modulus from this test is $10000/.008 = 1.25e6 = 8.6 \text{ GPa}$

Cooling with 12C for 10 sec, stepped up to 100C,
ramped down in 300 s

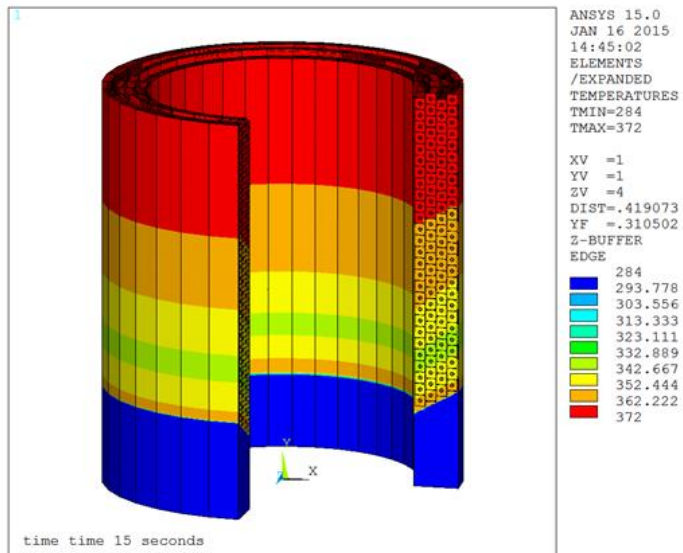


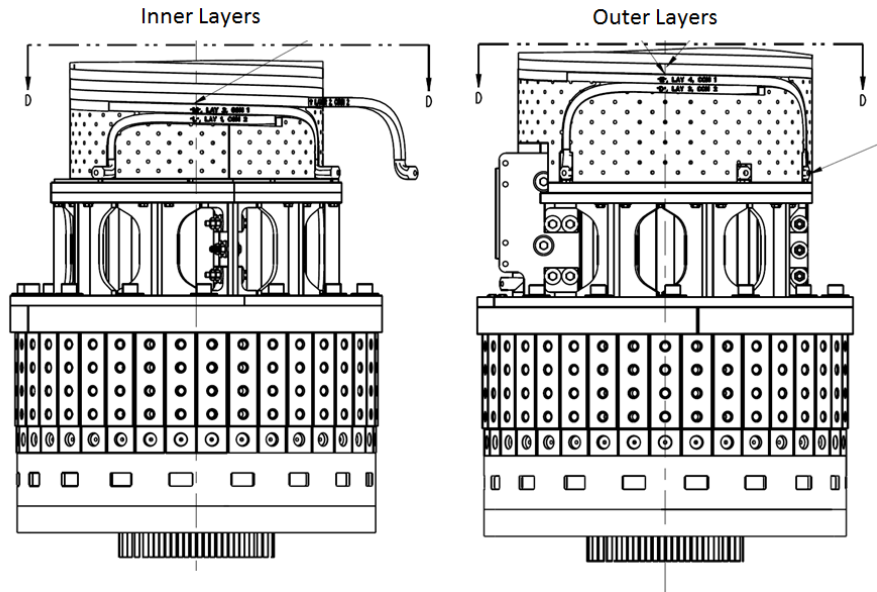
!time:	0	5	10	15	20
t100=	12	\$t105= 55	\$t1010= 30	\$t1015= 72	\$t1020= 87
t110=	100	\$t115= 80.731	\$t1110= 54.554	\$t1115= 63.739	\$t1120= 81
t120=	100	\$t125= 87.972	\$t1210= 65.541	\$t1215= 64.886	\$t1220= 75
t130=	100	\$t135= 92.676	\$t1310= 74.497	\$t1315= 68.135	\$t1320= 71
t140=	100	\$t145= 95.623	\$t1410= 81.526	\$t1415= 72.452	\$t1420= 70
t150=	100	\$t155= 97.403	\$t1510= 86.87	\$t1515= 77.079	\$t1520= 70.5
t160=	100	\$t165= 98.436	\$t1610= 90.817	\$t1615= 81.517	\$t1620= 73
t170=	100	\$t175= 99.011	\$t1710= 93.658	\$t1715= 85.482	\$t1720= 75
t180=	100	\$t185= 99.316	\$t1810= 95.655	\$t1815= 88.846	\$t1820= 78
t190=	100	\$t195= 99.482	\$t1910= 97.183	\$t1915= 91.929	\$t1920= 82
t200=	100	\$t205= 99.546	\$t2010= 98.054	\$t2015= 94.012	\$t2020= 83
t210=	100	\$t215= 99.573	\$t2110= 98.626	\$t2115= 95.602	\$t2120= 85
t220=	100	\$t225= 99.583	\$t2210= 98.994	\$t2215= 96.786	\$t2220= 85
t230=	100	\$t235= 99.586	\$t2310= 99.227	\$t2315= 97.649	\$t2320= 86.07142857
t240=	100	\$t245= 99.587	\$t2410= 99.371	\$t2415= 98.266	\$t2420= 87.14285714
t250=	100	\$t255= 99.588	\$t2510= 99.458	\$t2515= 98.699	\$t2520= 88.21428571
t260=	100	\$t265= 99.588	\$t2610= 99.51	\$t2615= 98.998	\$t2620= 89.28571429
t270=	100	\$t275= 99.588	\$t2710= 99.54	\$t2715= 99.2	\$t2720= 90.35714286
t280=	100	\$t285= 99.588	\$t2810= 99.557	\$t2815= 99.335	\$t2820= 91.42857143
t290=	100	\$t295= 99.588	\$t2910= 99.566	\$t2915= 99.423	\$t2920= 92.5
t300=	100	\$t305= 99.588	\$t3010= 99.571	\$t3015= 99.481	\$t3020= 93.57142857
t310=	100	\$t315= 99.588	\$t3110= 99.574	\$t3115= 99.517	\$t3120= 94.64285714
t320=	100	\$t325= 99.588	\$t3210= 99.576	\$t3215= 99.541	\$t3220= 95.71428571
t330=	100	\$t335= 99.588	\$t3310= 99.576	\$t3315= 99.555	\$t3320= 96.78571429
t340=	100	\$t345= 99.588	\$t3410= 99.577	\$t3415= 99.564	\$t3420= 97.85714286
t350=	100	\$t355= 99.588	\$t3510= 99.577	\$t3515= 99.569	\$t3520= 98.92857143
t360=	100	\$t365= 99.588	\$t3610= 99.577	\$t3615= 99.572	\$t3620= 100

```

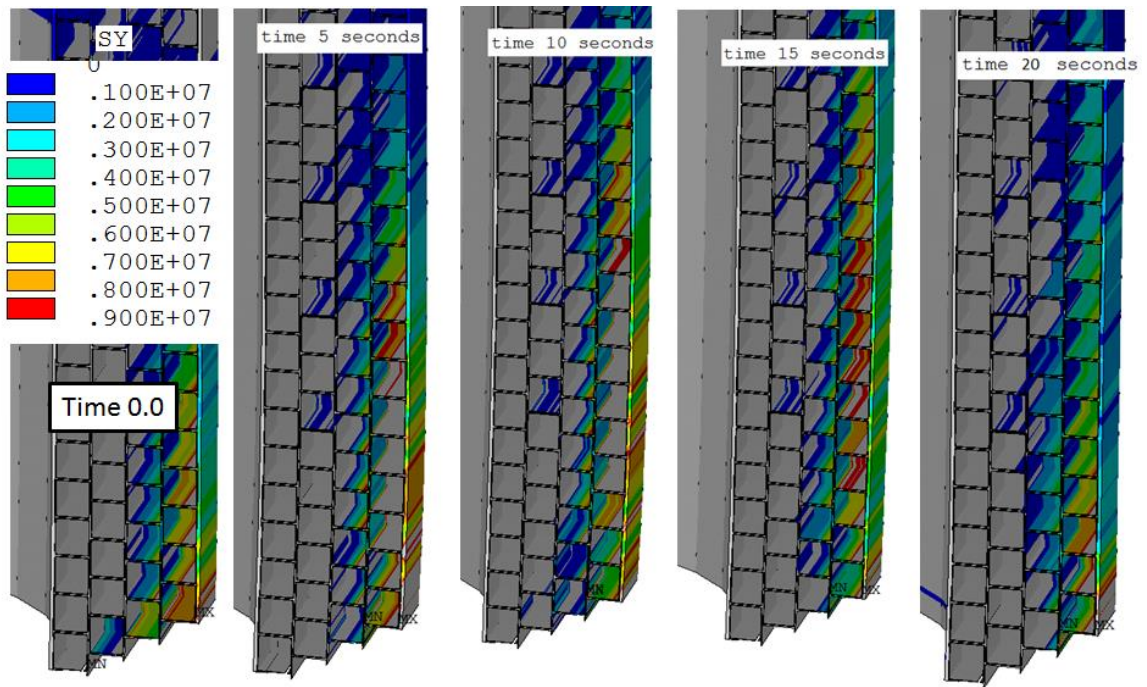
/title, time = 15 seconds
esel,mat,10
nelem
t,all,272+12
esel,mat,11
nelem
t,all,272+12
nselect,y,0,.25
t,all,272+12
nselect,y,.25,.35
t,all,(272+12+372)/2
nselect,y,.35,1
t,all,372
*do,r,11,36,1
esel,real,r
nelem
t,all,t%r%15 + 272
*enddo
nall
eall
save

```





The support pedestal is stepped



12.0 System Flow Diagram and Options

There were many ways to produce a system that would provide initial heated water at the beginning of the cooldown sequence. Figure 12.0-1 shows the desired inlet temperature profile.

Water Heater Temperature Setting

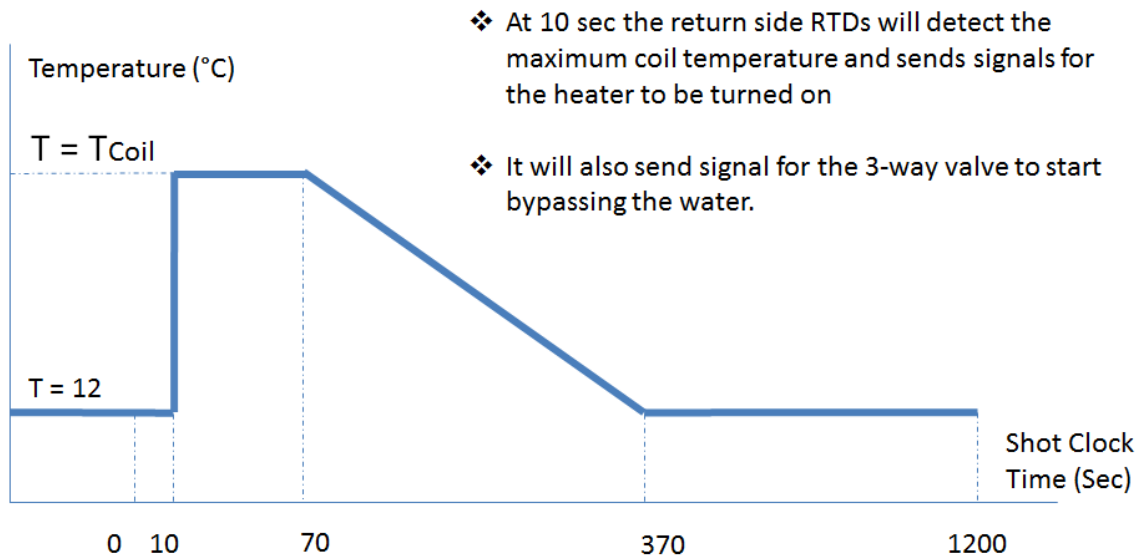


Figure 12.0-1

The energy needed to preheat the water entering the coil is modest. At .6 to .8 gallons per minute for 5 minutes, the energy need is equivalent to heating 2 gallons of water to the coil temp.

A small tank heater slowly heating the water in the latter part of the cooling process would be sufficient, but you would need knowledge of the required temperature

The instantaneous demand for water at the coil temperature could be met with supplying OH outlet water to the inlet. This would entail piping water from the top to the bottom with some temperature loss in the long pipes needed.

Inline heater – to raise the flow from 12C to 110 C in-line, takes 20kW per channel or 160 kW total. Heaters exist that are computer controlled and take the higher pressure (Wattco)–but they may be more expensive than other solutions. Mike Kalish found a unit from Grainger had the right heat capacity but is good only to 150 psi

There were options with mixing valves with hot water coming from a heat exchanger with OH exit water as the heating source,

The system chosen in the end is one that uses a high power in-line heater that can nearly instantaneously heat the water to 110.



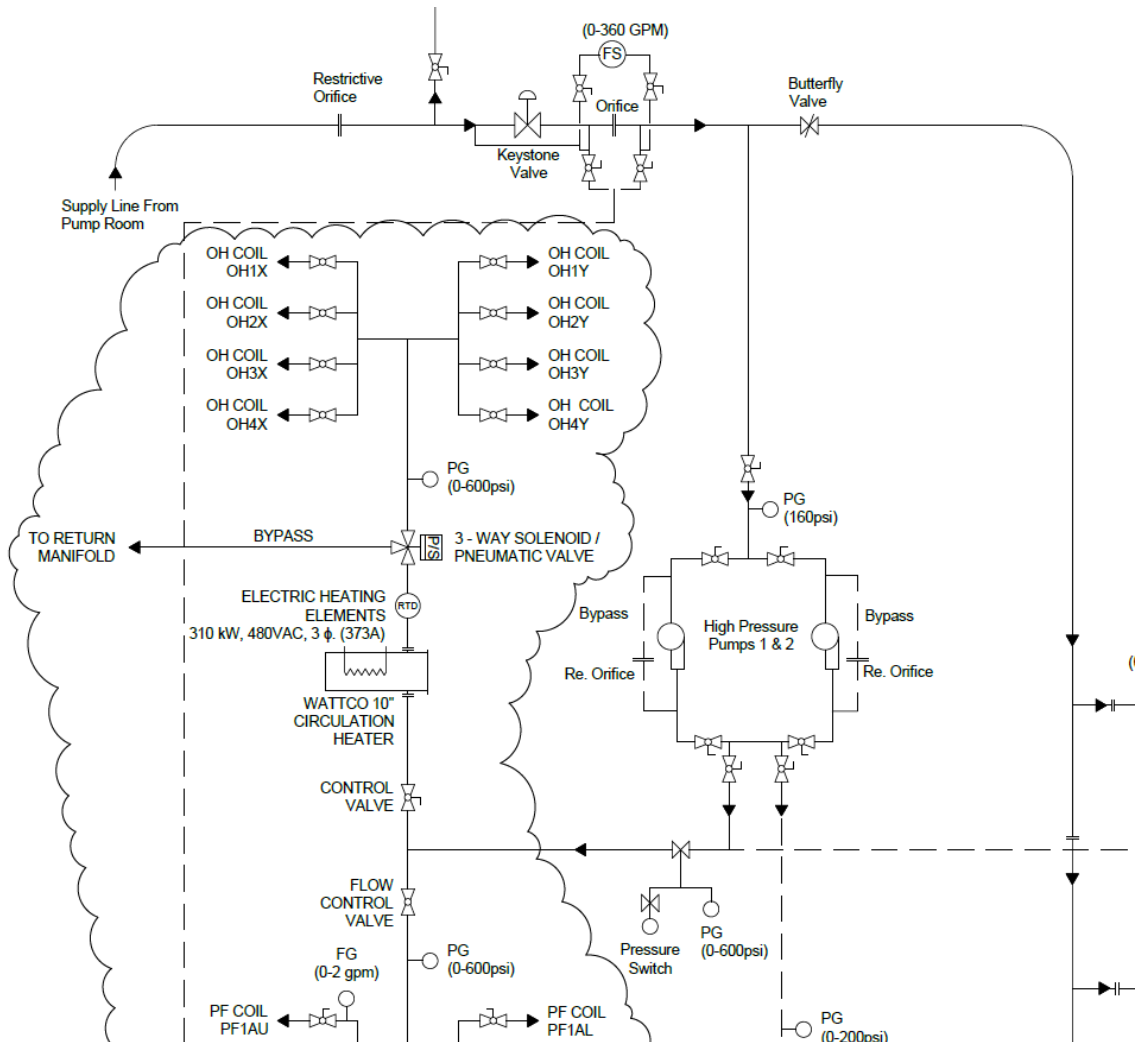


Figure 12.0-2

3-Way Valve Flow Direction Vs. Time

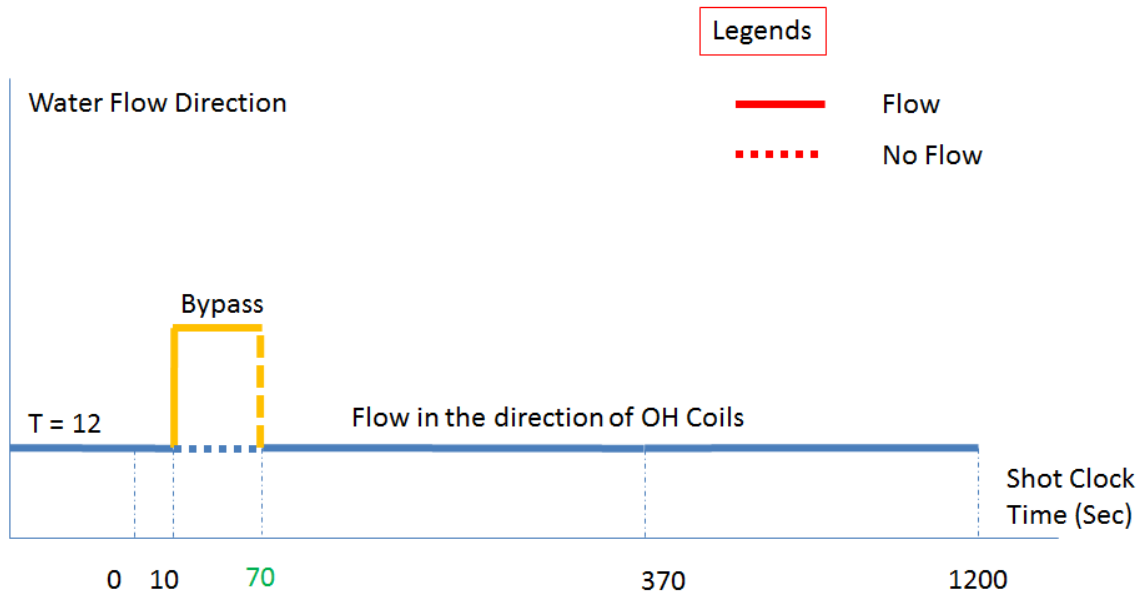


Figure 12.0-4

Key Features

- Flange sizes: up to 14" diameter
- Titanium, Carbon Steel or Stainless vessels fitted with 150# up to 2000#. psi flanges
- Insulated seamless vessels available
- Custom designed units
- American or European sizes, wattages, and materials are available upon request
- Vessels can be supplied with Steel, Stainless Steel parts and terminal boxes for heat protection and used in high temperature conditions.

Benefits

- Easy installations
- Skid mounted assembly available
- Durable and Clean
- Proven more energy efficient than alternative methods
- Provides even heat distribution
- Greater power available in a smaller heater bundle
- Provide maximum dielectric strength
- Reduced vessel heat loss
- Easy mounting support
- Suitable with general purpose terminal enclosures, NEMA 7, NEMA 4X NEMA 7, and unsafe or explosion proof locations
- Compatible with industrial piping and safety standards
- Digital Control Panels used with Thermocouples to regulate temperature and high limit protection control

Thermostatically controlled (0-255F), (55-550F)
Digitally Controlled, Thermocouple, RTD

Figure 12.0-5 Wattco Heater Picture and Description

12.2 PIPE FLOW Flow Calculations (Neway Atnafu)

Pipe Flow Expert is a software program for piping design and pipe system modeling. It calculates fluid flow in open or closed loop pipe networks with multiple supply & discharge tanks, multiple pumps in series or in parallel, and multiple pipe sizes & fittings. Pipe Flow Expert will calculate the flow rate in each pipe & it will calculate pipe pressure drop throughout your system.



Pipe Flow Design Results Data

PPPL - NSTXU High Pressure Water Supply - PF Expert Solution

11 December, 2014

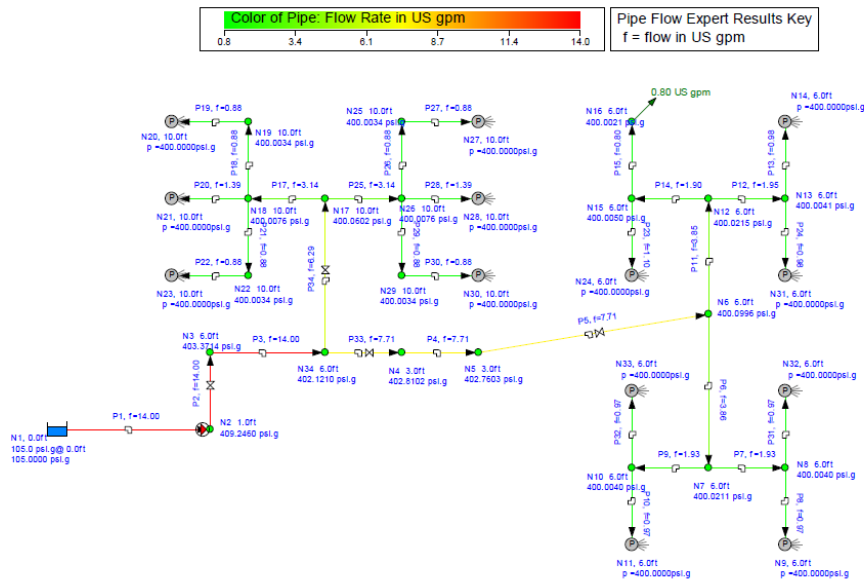


Figure 12.2-1 Pipe Flow Diagram

PPPL - NSTXU High Pressure Water Supply - PF Expert Solution

11 December, 2014

Fluid Data

Zone	Fluid Name	Chemical Formula	Temperature °F	Pressure psi-g	Density lb/ft³	Centistokes	Centipoise	Vapour Pressure psi-a	State
1	Water	H2O	68.000	0.0000	62.303	1.000	1.002	0.348091	Liquid

Figure 12.2-2 Pipe Flow Fluid Data

PPPL - NSTXU High Pressure Water Supply - PF Expert Solution

11 December, 2014

Pump Data

Pipe Id	Pipe Name	Pump Name	Speed rpm	Pref. Op From US gpm	Pref. Op To US gpm	Flow In/Out US gpm	Velocity ft/sec	Suction Pressure psi-g	Discharge Pressure psi-g	Pump Head ft.hd Fluid	Pump NPSH (absolute)	Pump NPSHa (absolute)	Pump Efficiency Percentage	Pump Power Horsepower
1	P1	Pump	Set Flow Rate			14.00	4.752	104.2205	409.2460	705.000	Not known	274.04	Not known	Not Known

Figure 12.2-3 Pipe Flow Pump Data

Pipe Data

Pipe Id	Pipe Name and Notes	Material	Inner Diameter inch	Roughness inch	Length inch	Total K	Mass Flow lb/sec	Flow US gpm	Velocity ft/sec	Entry Pressure psi.g	Exit Pressure psi.g
1	P1	1" Stainless Steel (ANSI) Sch. 10S	1.097	0.001811	36.000	1.4200	1.9434	14.00	4.752	105.0000	409.2460
2	P2	3/4" Stainless Steel (ANSI) Sch. 10S	0.884	0.001811	60.000	8.5000	1.9434	14.00	7.318	409.2460	403.3714
3	P3	3/4" Stainless Steel (ANSI) Sch. 10S	0.884	0.001811	24.000	2.7500	1.9434	14.00	7.318	403.3714	402.1210
4	P4	10" Stainless Steel (ANSI) Sch. 10S	10.420	0.001811	120.000	8817.2100	1.0705	7.71	0.029	402.8102	402.7603
5	P5	3/4" Stainless Steel (ANSI) Sch. 10S	0.884	0.001811	120.000	8.6000	1.0705	7.71	4.031	402.7603	400.0996
6	P6	3/4" Stainless Steel (ANSI) Sch. 10S	0.884	0.001811	24.000	2.0000	0.5361	3.86	2.019	400.0996	400.0211
7	P7	3/4" Stainless Steel (ANSI) Sch. 10S	0.884	0.001811	12.000	2.0000	0.2680	1.93	1.009	400.0211	400.0040
8	P8	1/2" Stainless Steel (ANSI) Sch. 10S	0.674	0.001811	12.000	0.0500	0.1340	0.97	0.868	400.0040	400.0000
9	P9	3/4" Stainless Steel (ANSI) Sch. 10S	0.884	0.001811	12.000	2.0000	0.2680	1.93	1.009	400.0211	400.0040
10	P10	1/2" Stainless Steel (ANSI) Sch. 10S	0.674	0.001811	12.000	0.0500	0.1340	0.97	0.868	400.0040	400.0000
11	P11	3/4" Stainless Steel (ANSI) Sch. 10S	0.884	0.001811	24.000	2.0000	0.5345	3.85	2.013	400.0996	400.0215
12	P12	3/4" Stainless Steel (ANSI) Sch. 10S	0.884	0.001811	12.000	2.0000	0.2710	1.95	1.021	400.0215	400.0041
13	P13	1/2" Stainless Steel (ANSI) Sch. 10S	0.674	0.001811	12.000	0.0500	0.1355	0.98	0.878	400.0041	400.0000

Pipe Id	Pipe Name and Notes	Material	Inner Diameter inch	Roughness inch	Length inch	Total K	Mass Flow lb/sec	Flow US gpm	Velocity ft/sec	Entry Pressure psi.g	Exit Pressure psi.g
14	P14	3/4" Stainless Steel (ANSI) Sch. 10S	0.884	0.001811	12.000	2.0000	0.2635	1.90	0.992	400.0215	400.0050
15	P15	1/2" Stainless Steel (ANSI) Sch. 10S	0.674	0.001811	12.000	0.0500	0.1110	0.80	0.719	400.0050	400.0021
17	P17	3/4" Stainless Steel (ANSI) Sch. 10S	0.884	0.001811	24.000	2.0000	0.4364	3.14	1.643	400.0602	400.0076
18	P18	3/4" Stainless Steel (ANSI) Sch. 10S	0.884	0.001811	36.000	0.7500	0.1220	0.88	0.459	400.0076	400.0034
19	P19	1/2" Stainless Steel (ANSI) Sch. 10S	0.674	0.001811	12.000	0.0500	0.1220	0.88	0.790	400.0034	400.0000
20	P20	1/2" Stainless Steel (ANSI) Sch. 10S	0.674	0.001811	12.000	0.0500	0.1924	1.39	1.246	400.0076	400.0000
21	P21	3/4" Stainless Steel (ANSI) Sch. 10S	0.884	0.001811	36.000	0.7500	0.1220	0.88	0.459	400.0076	400.0034
22	P22	1/2" Stainless Steel (ANSI) Sch. 10S	0.674	0.001811	12.000	0.0500	0.1220	0.88	0.790	400.0034	400.0000
23	P23	1/2" Stainless Steel (ANSI) Sch. 10S	0.674	0.001811	12.000	0.0500	0.1524	1.10	0.987	400.0050	400.0000
24	P24	1/2" Stainless Steel (ANSI) Sch. 10S	0.674	0.001811	12.000	0.0500	0.1355	0.98	0.878	400.0041	400.0000
25	P25	3/4" Stainless Steel (ANSI) Sch. 10S	0.884	0.001811	24.000	2.0000	0.4364	3.14	1.643	400.0602	400.0076
26	P26	3/4" Stainless Steel (ANSI) Sch. 10S	0.884	0.001811	36.000	0.7500	0.1220	0.88	0.459	400.0076	400.0034
27	P27	1/2" Stainless Steel (ANSI) Sch. 10S	0.674	0.001811	12.000	0.0500	0.1220	0.88	0.790	400.0034	400.0000
28	P28	1/2" Stainless Steel (ANSI) Sch. 10S	0.674	0.001811	12.000	0.0500	0.1924	1.39	1.246	400.0076	400.0000
29	P29	3/4" Stainless Steel (ANSI) Sch. 10S	0.884	0.001811	36.000	0.7500	0.1220	0.88	0.459	400.0076	400.0034

Pipe Id	Pipe Name and Notes	Material	Inner Diameter inch	Roughness inch	Length inch	Total K	Mass Flow lb/sec	Flow US gpm	Velocity ft/sec	Entry Pressure psi.g	Exit Pressure psi.g
30	P30	1/2" Stainless Steel (ANSI) Sch. 10S	0.674	0.001811	12.000	0.0500	0.1220	0.88	0.790	400.0034	400.0000
31	P31	1/2" Stainless Steel (ANSI) Sch. 10S	0.674	0.001811	12.000	0.0500	0.1340	0.97	0.868	400.0040	400.0000
32	P32	1/2" Stainless Steel (ANSI) Sch. 10S	0.674	0.001811	12.000	0.0500	0.1340	0.97	0.868	400.0040	400.0000
33	P33	3/4" Stainless Steel (ANSI) Sch. 10S	0.884	0.001811	120.000	1.7000	1.0705	7.71	4.031	402.1210	402.8102
34	P34	3/4" Stainless Steel (ANSI) Sch. 10S	0.884	0.001811	48.000	2.9500	0.8728	6.29	3.287	402.1210	400.0602

Figure 12.2-4 Pipe Flow Pipe Data

Node Data

Node Id	Node Type	Node	Elevation ft	Liquid Level ft	Surface Press. psi.g	Press. at Node psi.g	HGL at Node ft.hd Fluid	Demand In US gpm	Demand Out US gpm	Total Flow In US gpm	Total Flow Out US gpm
1	Tank	N1	0.000	0.000	105.0000	105.0000	242.68	N/A	N/A	0.00	14.00
2	Join Point	N2	1.000	N/A	N/A	409.2460	946.88	0.00	0.00	14.00	14.00
3	Join Point	N3	3.000	N/A	N/A	403.3714	938.30	0.00	0.00	14.00	14.00
4	Join Point	N4	3.000	N/A	N/A	402.8102	934.01	0.00	0.00	7.71	7.71
5	Join Point	N5	3.000	N/A	N/A	402.7603	933.89	0.00	0.00	7.71	7.71
6	Join Point	N6	5.000	N/A	N/A	400.0996	930.74	0.00	0.00	7.71	7.71
7	Join Point	N7	5.000	N/A	N/A	400.0211	930.56	0.00	0.00	3.86	3.86
8	Join Point	N8	5.000	N/A	N/A	400.0040	930.52	0.00	0.00	1.93	1.93
9	Demand Pressure	N9	5.000	N/A	400.0000	400.0000	930.51	N/A	N/A	0.97	0.00
10	Join Point	N10	5.000	N/A	N/A	400.0040	930.52	0.00	0.00	1.93	1.93
11	Demand Pressure	N11	5.000	N/A	400.0000	400.0000	930.51	N/A	N/A	0.97	0.00
12	Join Point	N12	5.000	N/A	N/A	400.0215	930.56	0.00	0.00	3.85	3.85
13	Join Point	N13	5.000	N/A	N/A	400.0041	930.52	0.00	0.00	1.95	1.95
14	Demand Pressure	N14	5.000	N/A	400.0000	400.0000	930.51	N/A	N/A	0.98	0.00
15	Join Point	N15	5.000	N/A	N/A	400.0050	930.52	0.00	0.00	1.90	1.90
16	Join Point	N16	5.000	N/A	N/A	400.0021	930.52	0.00	0.80	0.80	0.80
17	Join Point	N17	10.000	N/A	N/A	400.0602	934.65	0.00	0.00	6.29	6.29
18	Join Point	N18	10.000	N/A	N/A	400.0076	934.53	0.00	0.00	3.14	3.14
19	Join Point	N19	10.000	N/A	N/A	400.0034	934.52	0.00	0.00	0.88	0.88
20	Demand Pressure	N20	10.000	N/A	400.0000	400.0000	934.51	N/A	N/A	0.88	0.00
21	Demand Pressure	N21	10.000	N/A	400.0000	400.0000	934.51	N/A	N/A	1.39	0.00
22	Join Point	N22	10.000	N/A	N/A	400.0034	934.52	0.00	0.00	0.88	0.88
23	Demand Pressure	N23	10.000	N/A	400.0000	400.0000	934.51	N/A	N/A	0.88	0.00
24	Demand Pressure	N24	5.000	N/A	400.0000	400.0000	930.51	N/A	N/A	1.10	0.00
25	Join Point	N25	10.000	N/A	N/A	400.0034	934.52	0.00	0.00	0.88	0.88
26	Join Point	N26	10.000	N/A	N/A	400.0076	934.53	0.00	0.00	3.14	3.14
27	Demand Pressure	N27	10.000	N/A	400.0000	400.0000	934.51	N/A	N/A	0.88	0.00
28	Demand Pressure	N28	10.000	N/A	400.0000	400.0000	934.51	N/A	N/A	1.39	0.00
29	Join Point	N29	10.000	N/A	N/A	400.0034	934.52	0.00	0.00	0.88	0.88
30	Demand Pressure	N30	10.000	N/A	400.0000	400.0000	934.51	N/A	N/A	0.88	0.00
31	Demand Pressure	N31	5.000	N/A	400.0000	400.0000	930.51	N/A	N/A	0.98	0.00
32	Demand Pressure	N32	5.000	N/A	400.0000	400.0000	930.51	N/A	N/A	0.97	0.00
33	Demand Pressure	N33	5.000	N/A	400.0000	400.0000	930.51	N/A	N/A	0.97	0.00

Node Id	Node Type	Node	Elevation ft	Liquid Level ft	Surface Press. psi.g	Press. at Node psi.g	HGL at Node ft.hd Fluid	Demand In US gpm	Demand Out US gpm	Total Flow In US gpm	Total Flow Out US gpm
34	Join Point	N34	6.000	N/A	N/A	402.1210	935.41	0.00	0.00	14.00	14.00

Figure 12.2-5 Pipe Node Data

Energy Data

Pipe Id	Pipe Name	Energy Loss To Pipe Friction	Energy Loss To Pipe Fittings	Energy Loss To Pipe Components	Energy Loss To Pipe Control Valves	Energy Loss To Pump Inefficiency	SUBTOTAL Loss Pipe Items +Pump	Energy Loss To Discharge Pressure	Energy Loss To Change in Elevation	TOTAL USED Sum of All Items
		Horsepower	Horsepower	Horsepower	Horsepower	Horsepower	Horsepower	Horsepower	Horsepower	Horsepower
1	P1	0.001072	0.001761	0.000000	0.000000	0.000000	0.002833	0.000000	0.003533	0.006366
2	P2	0.005311	0.024998	0.000000	0.000000	N/A	0.030309	0.000000	0.017667	0.047976
3	P3	0.002125	0.008088	0.000000	0.000000	N/A	0.010212	0.000000	0.000000	0.010212
4	P4	0.000000	0.000225	0.000000	0.000000	N/A	0.000225	0.000000	0.000000	0.000225
5	P5	0.001903	0.004228	0.000000	0.000000	N/A	0.006131	0.000000	0.005839	0.011970
6	P6	0.000053	0.000123	0.000000	0.000000	N/A	0.000177	0.000000	0.000000	0.000177
7	P7	0.000004	0.000015	0.000000	0.000000	N/A	0.000019	0.000000	0.000000	0.000019
8	P8	0.000002	0.000000	0.000000	0.000000	N/A	0.000002	0.225271	0.000000	0.225274
9	P9	0.000004	0.000015	0.000000	0.000000	N/A	0.000019	0.000000	0.000000	0.000019
10	P10	0.000002	0.000000	0.000000	0.000000	N/A	0.000002	0.225271	0.000000	0.225274
11	P11	0.000053	0.000122	0.000000	0.000000	N/A	0.000175	0.000000	0.000000	0.000175
12	P12	0.000004	0.000016	0.000000	0.000000	N/A	0.000020	0.000000	0.000000	0.000020
13	P13	0.000002	0.000000	0.000000	0.000000	N/A	0.000002	0.227781	0.000000	0.227783
14	P14	0.000004	0.000015	0.000000	0.000000	N/A	0.000018	0.000000	0.000000	0.000018
15	P15	0.000001	0.000000	0.000000	0.000000	N/A	0.000001	0.000000	0.000000	0.000001
17	P17	0.000030	0.000067	0.000000	0.000000	N/A	0.000097	0.000000	0.000000	0.000097
18	P18	0.000002	0.000001	0.000000	0.000000	N/A	0.000002	0.000000	0.000000	0.000002
19	P19	0.000002	0.000000	0.000000	0.000000	N/A	0.000002	0.205073	0.000000	0.205075
20	P20	0.000006	0.000000	0.000000	0.000000	N/A	0.000006	0.323441	0.000000	0.323447
21	P21	0.000002	0.000001	0.000000	0.000000	N/A	0.000002	0.000000	0.000000	0.000002
22	P22	0.000002	0.000000	0.000000	0.000000	N/A	0.000002	0.205073	0.000000	0.205075
23	P23	0.000003	0.000000	0.000000	0.000000	N/A	0.000003	0.256178	0.000000	0.256181
24	P24	0.000002	0.000000	0.000000	0.000000	N/A	0.000002	0.227781	0.000000	0.227783
25	P25	0.000030	0.000067	0.000000	0.000000	N/A	0.000097	0.000000	0.000000	0.000097
26	P26	0.000002	0.000001	0.000000	0.000000	N/A	0.000002	0.000000	0.000000	0.000002
27	P27	0.000002	0.000000	0.000000	0.000000	N/A	0.000002	0.205073	0.000000	0.205075
28	P28	0.000006	0.000000	0.000000	0.000000	N/A	0.000006	0.323441	0.000000	0.323447
29	P29	0.000002	0.000001	0.000000	0.000000	N/A	0.000002	0.000000	0.000000	0.000002
30	P30	0.000002	0.000000	0.000000	0.000000	N/A	0.000002	0.205073	0.000000	0.205075
31	P31	0.000002	0.000000	0.000000	0.000000	N/A	0.000002	0.225271	0.000000	0.225274
32	P32	0.000002	0.000000	0.000000	0.000000	N/A	0.000002	0.225271	0.000000	0.225274

Pipe Id	Pipe Name	Energy Loss To Pipe Friction	Energy Loss To Pipe Fittings	Energy Loss To Pipe Components	Energy Loss To Pipe Control Valves	Energy Loss To Pump Inefficiency	SUBTOTAL Loss Pipe Items +Pump	Energy Loss To Discharge Pressure	Energy Loss To Change in Elevation	TOTAL USED Sum of All Items
33	P33	0.001903	0.000836	0.000000	0.000000	N/A	0.002738	0.000000	-0.005839	-0.003101
34	P34	0.000425	0.000786	0.000000	0.000000	N/A	0.001211	0.000000	0.006348	0.007559

12.3 Transit Time Calculations (Neway Atnafu)

Transit Time Calculation

Flow rate is adjusted for uniform time through Coils

Transit Time Calculation for the Flow of Water from High Pressure Pumps through the OH Coils								
Container	In. Dia. (in)	Length (in)	CS. Area (in ²)	Flow (gpm)	Velocity (ft/sec)	Transit Time (sec)	Flow Switch Setting for 1/2-251 (in. of water)	
OH-1X	0.225	6058	0.039740625	0.74	5.974130502	84.50323158	32.5	
OH-1Y	0.225	6058	0.039740625	0.74	5.974130502	84.50323158	32.5	
OH-2X	0.225	6494	0.039740625	0.79	6.377787969	84.85178079	39	
OH-2Y	0.225	6479	0.039740625	0.79	6.377787969	84.65578807	39	
OH-3X	0.225	6946	0.039740625	0.85	6.862176929	84.35126919	44	
OH-3Y	0.225	6942	0.039740625	0.85	6.862176929	84.30269374	44	
OH-4X	0.225	7365	0.039740625	0.9	7.265834395	84.47068384	50	
OH-4Y	0.225	7373	0.039740625	0.9	7.265834395	84.56243747	50	
Hose	0.25	600	0.0490625	0.74	4.839045707	10.33261577		
Pipe	0.75	240	0.4415625	6.7	4.868109045	4.108371406		
Heater	4.17 ft/sec @ 10 gpm & 0.2 psig pressure drop						53	
Transit Time from Pump to Coils					6.64	67.44098718		

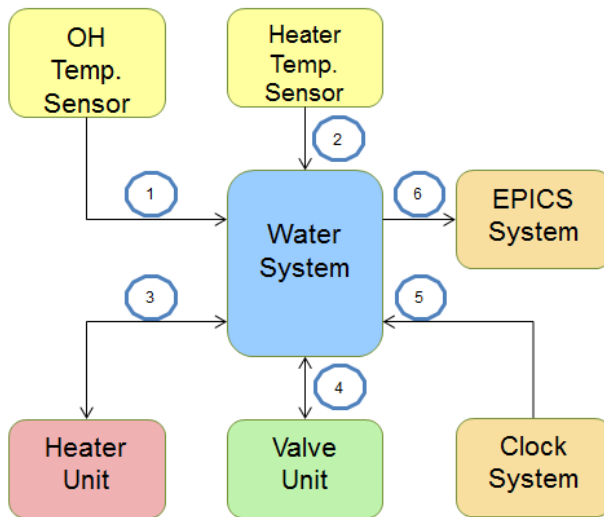
Figure 12.3-1

12.4 Pressure Relief Valve Venting Calculations

These calculations haven't been performed for components other than the heater, as of Feb 2015. It is assumed that the heater vendor is providing these calculations.

12.5 Control System Description (Xin Zhao)

CONTROL INTERFACE DIAGRAM



5. Clock system provides synchronized shot pulse to trigger control events.
6. The EPICS system monitors the OH and heated water temperature, heater unit status, and valve position.

1. The sensor reads OH water temperature at the end of shot (with some delay), and the temperature becomes the heating setpoint of the heater unit .
2. The sensor reads heated water temperature at the outbound of the heater.
3. At the end of shot, the heater is energized. The heater heats up the inlet cooling water to the measured OH water temperature while the water is bypassed. Then it controls temperature drop from OH setpoint to 12 degree C in 5 minutes while the water is flowing through OH coil.
4. The valve switches the inlet cooling water flow path from normal to bypass for heating process. At the end of shot, valve is switched to bypass. When the heated water temperature reaches the setpoint, the valve is switched to normal.

Figure 12.5-1

CONTROL INTERFACE SIGNALS



IND EX	LOCATIO N	TYPE	SIGNAL	DESCRIPTION
01	Test Cell	Analog Input	OH Outlet Temp 01	RTD temperature read 01 at top of structure
01	Test Cell	Analog Input	OH Outlet Temp 02	RTD temperature read 02 at top of structure
01	Test Cell	Analog Input	OH Outlet Temp 03	RTD temperature read 03 at top of structure
02	Test Cell	Analog Input	Heater Outlet Temp 01	RTD temperature read 01 at heater outlet
02	Test Cell	Analog Input	Heater Outlet Temp 02	RTD temperature read 02 at heater outlet
03	Test Cell	Digital Output	Remote Start/Stop	In-line heater controller should be able to be switched on by external 24Vdc signal.
03	Test Cell	Digital Input	Heater Alarm Status	In-line heater controller should be able to provide contact signal to external control.
03	Test Cell	Analog Output	Remote Setpoint	In-line heater controller should be able to receive external setpoint as 4-20mA signal.
03	Test Cell	Analog Input	Temperature Readout	In-line heater controller should be able to provide 4-20mA output for temperature retransmit.
04	Test Cell	Digital Output	Bypass Valve	3 Way Pneumatic valve only one path at one switching position.
04	Test Cell	Digital Input	Bypass On Status	Valve is in bypass position and no water flows through coil
04	Test Cell	Digital Input	Bypass Off Status	Valve is in normal position and water flows through coil
05	Pump Room	Digital Input	SOP Signal	Start of pulse clock signal, pulse width is 100mSec
05	Pump Room	Digital Input	EOP Signal	End of pulse clock signal, pulse width is 100mSec
05	Pump Room	Digital Input	Clock System OK	Clock signal hand shake every 5 sec
06	Control Room	Comm. Output	OH Outlet Temp 01	EPICS OH RTD temperature read 01
06	Control Room	Comm. Output	OH Outlet Temp 02	EPICS OH RTD temperature read 02
06	Control Room	Comm. Output	OH Outlet Temp 03	EPICS OH RTD temperature read 03
06	Control Room	Comm. Output	Heater Outlet Temp	EPICS Heated Water RTD temperature read
06	Control Room	Comm. Output	Heater Running Status	EPICS Heater is remotely started, running = green, not running = red
06	Control Room	Comm. Output	Heater Alarm Status	EPICS Heater unit is having alarm, normal = green, alarm = red
06	Control Room	Comm. Output	Bypass Valve Position	EPICS Valve is switched to either normal or bypass, normal = green, bypass = red

Figure 12.5-2 Control Interface Signals

CONTROL FAULT CONDITIONS



INDEX	DESCRIPTION	CAUSE	ACTION
01	OH Temperature Read Fault	<ol style="list-style-type: none"> Any 1 of the 3 RTD sensors does not read due to broken wire or faulty sensor. Any 2 of the 3 RTD sensors read 5 degree apart from each other for 10 seconds or more. 	Heater is de-energized. Valve is switched to bypass position. Power supply permissive is disabled.
02	Water Temperature Read Fault	<ol style="list-style-type: none"> Any 1 of the 2 RTD sensors does not read due to broken wire or faulty sensor. The 2 RTD sensors read 5 degree apart from each other for 10 seconds or more. 	Heater is de-energized. Valve is switched to bypass position. Power supply permissive is disabled.
03	Heater Fault	<ol style="list-style-type: none"> Heater controller is faulted. Heater temperature did not reach setpoint after 60 seconds. 	Heater is de-energized. Valve is switched to bypass position. Power supply permissive is disabled. Heater is de-energized.
04	Valve Position Fault	<ol style="list-style-type: none"> The position sensor does not show the same state as the commanded valve position within 5 seconds. 	Turnoff Pumps Valve is switched to bypass position. Power supply permissive is disabled.
05	Timing Fault	<ol style="list-style-type: none"> Clock signal is not received in 5 seconds. 	Heater is de-energized. Valve is switched to bypass position. Power supply permissive is disabled.
06	EPICS Comm Fault	<ol style="list-style-type: none"> Communication handshake signal is not received in 5 seconds. 	Heater is de-energized. Valve is switched to bypass position. Power supply permissive is disabled.

Figure 12.5-3 Control Fault Conditions

12.6 System FMEA (All Authors)

Input to the FMEA [21] for NSTX was developed in concert with the developing the system and evaluating the coil stresses during operation. The formal FMEA [document title page is shown at right. The input developed is shown below. This calculation can be considered a resource for developing and checking the FMEA content, but the calculation should not be considered the primary or sole source of content for the OH Preheater system FMEA.

NSTX Failure Modes & Effects Analysis / NSTX-FMEA-71-10 / p. 1 of 115
NSTX
FAILURE MODES AND EFFECTS ANALYSIS
(FMEA)
Revision 10
Dated: November 2014

Prepared By:

Name/WBS	Signature	Name/WBS	Signature
K. Tresener (WBS 11)		R. Kaita (WBS 4X)	
M. Smith (WBS 12)		R. Ramkrishnan (WBS 5X)	
S. Raftopoulos (WBS 13)		P. Sichts (WBS 6X)	
T. Stevenson (WBS 2X and DCPS)		C. Gentile (Operations)	
W. Blanchard (WBS 3X)			

Reviewed by:

Name	Signature	Name	Signature
P. Titus NSTX Project Engineer		L. Dudek NSTX Center Stack Upgrade	
T. Stevenson NSTX NBI Upgrade		J. Levine ES&H	

Approved by: _____
Rou Strykowski, NSTX Upgrade Project Manager

OH Coils Cooling Water System						
Failure Mode and Effects Analysis						
No.	Failure Mode	Effect	Detection	Recovery	Probability	Consequence
1	OH Heater not working	Unable to ramp up/down OH cooling water	The Heater Control Unit sends signal to PLC. Cooling Water will be bypassed. OH Coils cooldown at room temperature.	Heater is de-energized. Bypass Valve is switched to bypass position. Supply Valve is switched to off position. Power supply permissive is disabled.	UNLIKELY	MINIMAL
2	OH Heater Temp Control Fails	No Heating	The control unit sends signal to the PLC. Cooling Water will be bypassed. OH Coils cooldown at room temperature.	Shutdown and repair or replace	UNLIKELY	MINIMAL
3	3-way Valve unable to Open Bypass Port	Cold water enters hot OH Coils	The valve position sensor sends signal to PLC. PLC shuts off 2-way valve. OH Coils cooldown at room temperature.	Shutdown and repair or replace	UNLIKELY	MAJOR Improbable but possible insulation damage. Perform electrical tests on OH
4	OH Supply RTD not working	Unable to detect the supply water temperature	Any 1 of the 2 RTD sensors does not read due to broken wire or faulty sensor. The 2 RTD sensors read 5 degree apart from each other for 5 seconds or more.	Heater is de-energized. Bypass Valve is switched to bypass position. Supply Valve is switched to off position. Power supply permissive is disabled. Troubleshoot and repair or shutdown and replace	UNLIKELY	MINIMAL
5	OH Return RTD not working	Sends wrong temperature signal to PLC, Heater, 3-Way Valve and Supply	Any 1 of the 2 RTD sensors does not read due to broken wire or faulty sensor. The 2 RTD sensors read 5 degree apart from each other for 5 seconds or more.	Heater is de-energized. Bypass Valve is switched to bypass position. Supply Valve is switched to off position. Power supply permissive is disabled. Troubleshoot and repair or shutdown and replace	UNLIKELY	MINIMAL
6	Flow Balance at Flow Control Valves is Lost	Layer to Layer Temperatures Vary near exit	PLC compares temperature readings from the three RTDs. If the readings vary by 5 C or more, it will shut down operation	Troubleshoot and repair or shutdown and replace	UNLIKELY	MAJOR Improbable but possible insulation damage. Perform electrical tests on OH
7	Valve Position Fault	not knowing valve position	The position sensor does not show the same state as the commanded valve position within 5 seconds.	Heater is de-energized. Bypass Valve is switched to bypass position. Supply Valve is switched to off position. Power supply permissive is disabled.	UNLIKELY	MINIMAL
8	Shot Clock Timing Fault	Heating can not be started	Clock signal is not received in 5 seconds.	Heater is de-energized. Bypass Valve is switched to bypass position. Supply Valve is switched to off position. Power supply permissive is disabled.	UNLIKELY	MINIMAL
9	EPICS Comm Fault	EPICS not updating	Communication handshake signal is not received in 5 seconds.	Heater is de-energized. Bypass Valve is switched to bypass position. Supply Valve is switched to off position. Power supply permissive is disabled.	UNLIKELY	MINIMAL

Figure 12.6-1 Excerpt from FMEA Spreadsheet

The consequence of a cold slug of water entering the coil once or a few times has been shown to be acceptable. Based on the CTD tests[25]. The flow balance for cooling the four layers would have similar risks to the insulation.

13.0 Testing, Creep, and Displacement Controlled Tensile Strain

Composite Technology Development Corporation (CTD) performed tests on stack compression samples and array tensile strain samples. The stack test is intended to address the retention of preload due to creep of the insulation system at the higher temperatures planned for operation. The nominal temperature of 100C and slightly elevated temperatures desired for less restrictive aquapour operation are being tested. Figure 13.1 shows the compressive creep stack sample. The array tests are strain controlled tests intended to simulate strains imposed from the cooldown wave effect and potentially non-optimum coil interactions resulting from the failure to remove the aquapour.



Figure 13.0-1 Compressive Creep Stack Sample

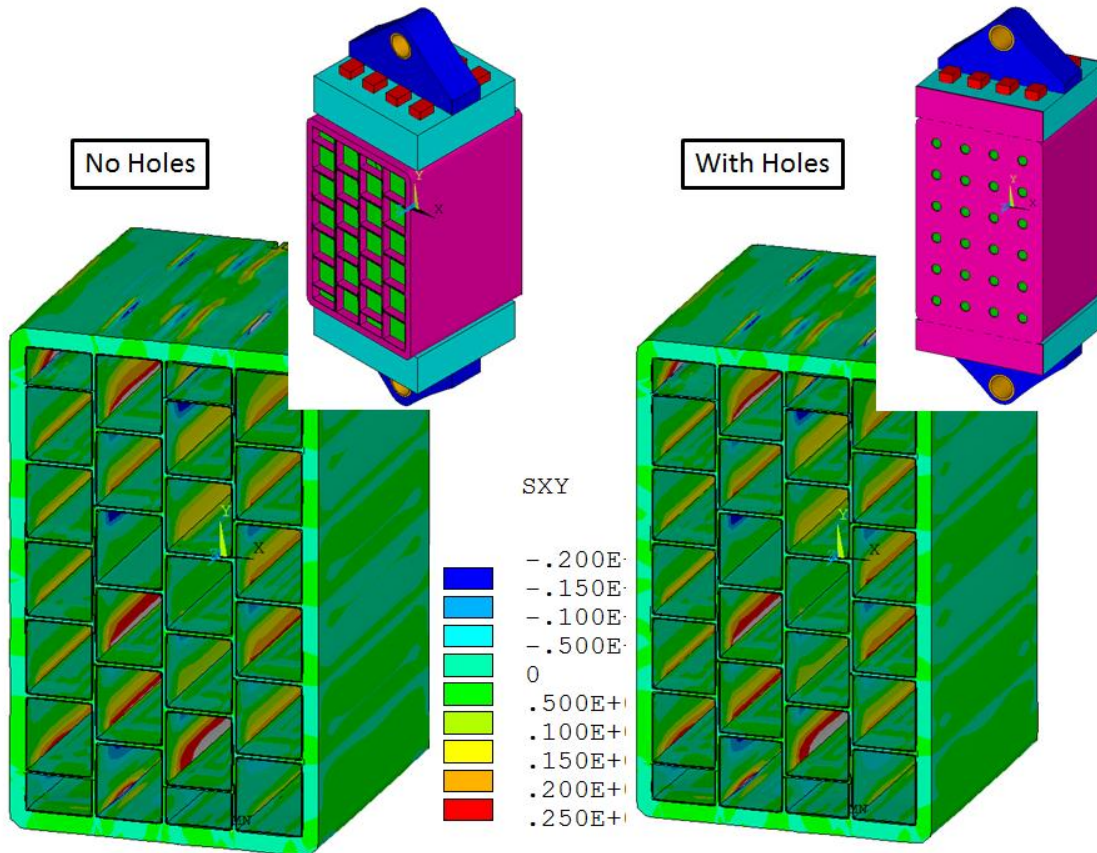


Figure 13.0-2 Tensile Strain Test with Coolant Holes or without?

The proposed tests were expected to be expensive and the simplest samples were desired. The tensile strain test specimen was analyzed with the coolant holes and without. The “without” case allowed use of off the shelf copper bars. The “with holes” case would require either machining of the bars or use of spare OH conductor from PPPL. The analysis showed indiscernible differences in the insulation stress. Consequently the no hole option was specified. The array samples shown in figure 13.0-2 were 4 by 6 (the misaligned sample is shown) adequate results were expected from a smaller the smaller sample shown in figure 13.1-1

13.1 Aligned Array Tensile Strain Test and Simulations

Strain controlled tests are in process (as of Feb 3,2015) [23]. These will determine the ability of NST-U’s Kapton-glass interleaved system to survive the tensile strains imposed on the OH coil during cooldown. For the ITER central solenoid coil, as well as other superconducting magnets, it is important for the cables to be electrically insulated from each other. Due to the large forces in the magnets, the insulation systems must be designed so that the insulation will break benignly, if at all. The tensile strain, normal to the surface of the insulation layers, comes from flexure of the conductor jacket as well as from quenches. Under tension, the insulation is expected to break along the Kapton planes, which is considered a benign break since the insulation would still be electrically insulating. However, if the insulation breaks through the insulation exposing a path from one conductor to another, arcing or tracking can occur. Investigating the consequences of cracking and debonding will help in the evaluation of the NSTX-U insulation system when exposed to the tensile strains caused by the cooldown process and potentially due to frictional interactions with the TF

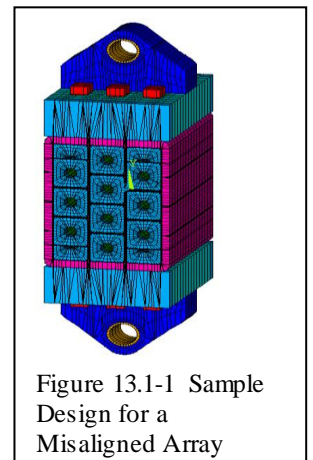
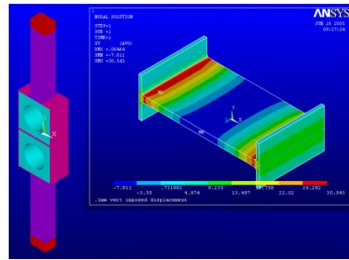
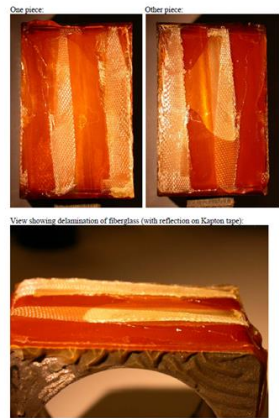


Figure 13.1-1 Sample Design for a Misaligned Array



PSFCRR-06-1
Desktop Vacuum Pressure Impregnation Experiment for ITER Insulation Testing
 Mahar S., Titus P., Gang C., Hooker M., Minervini J., Schütz J., Stable P., Takayasu M.
 April 2006



- Broke at only 100 lbs
- Broke at Kapton Bonds
- Withstood 21kV after air gap tracking fixed.



Figure 13.1-2 Results from the MIT Tensile Strain Test

The tests done on the NSTX-U CTD 425 system are similar to tests attempted at MIT to understand the performance of interleaved Kapton and glass insulation system used for the ITER CS coil. The purpose of the MIT experiment was to develop a test method and sample to qualify through thickness tensile strains expected in the ITER CS conductor. Once the sample had been created, it was broken in tension. After the sample was broken, the electrical barrier of the cracked insulation between the two samples were be tested.

TPX [21]
Kapton Wrap

MAST Cyanate Ester, CTD 403/450 Primer Test Coil

ITER CS Coil

Four by Four array of 55 mm square conductors with 39 mm round hole
Tested to 60,000 cycles

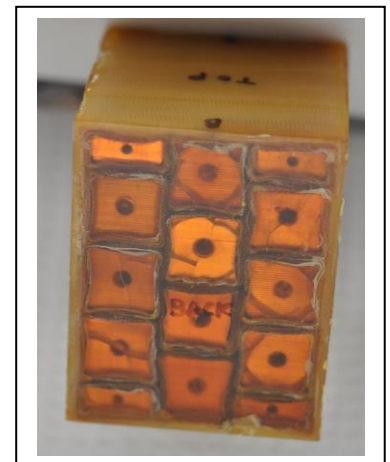
ITER TF Coil CTD 425 77K

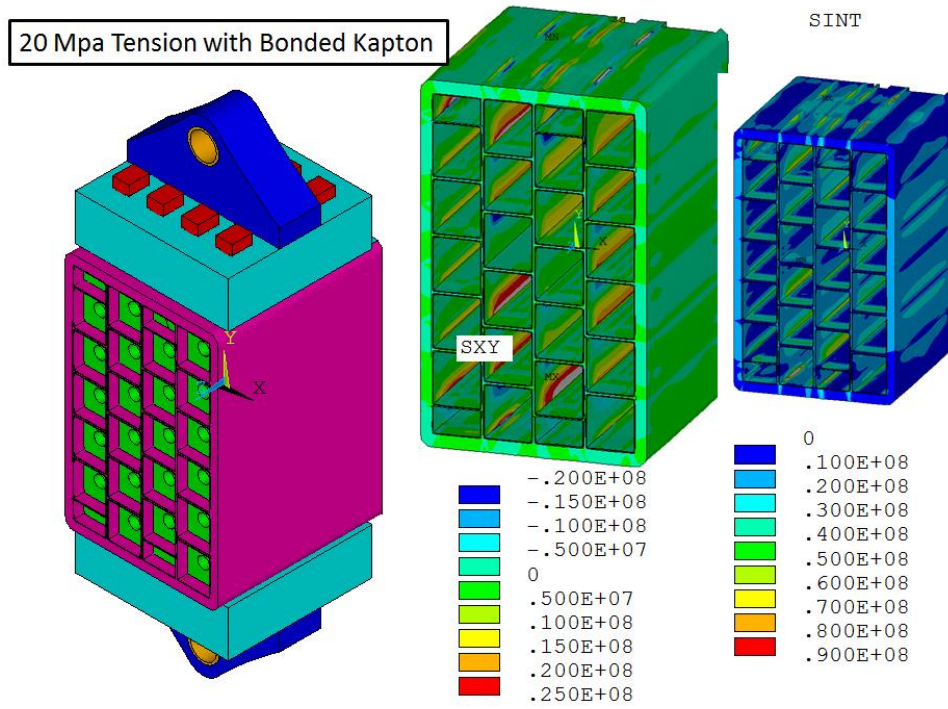
Four 1 cm X 1 cm Cu Conductor Sample

Piston
Sample
Fixture

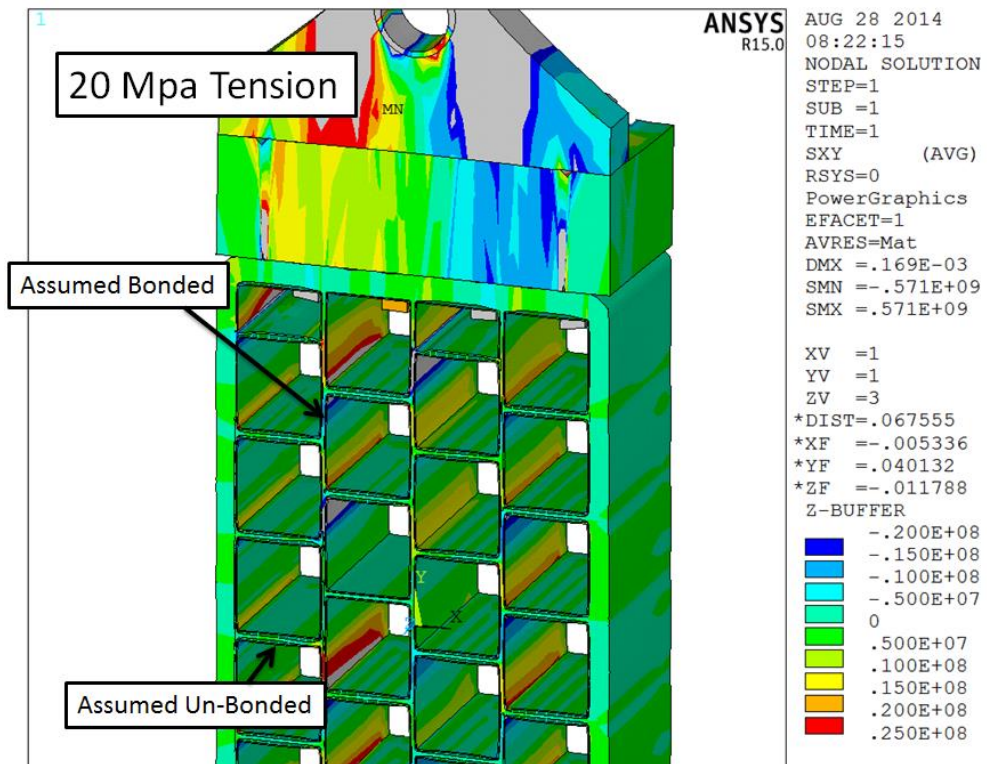
13.1.1, Bonded Simulation of the Misaligned Array Tensile Strain Test

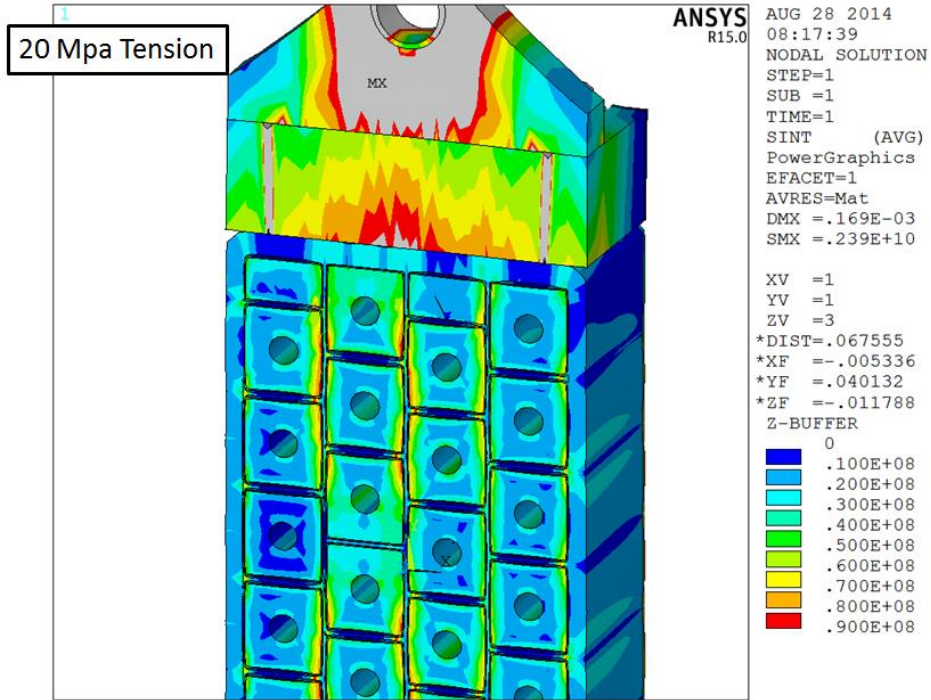
OH Cooldown System



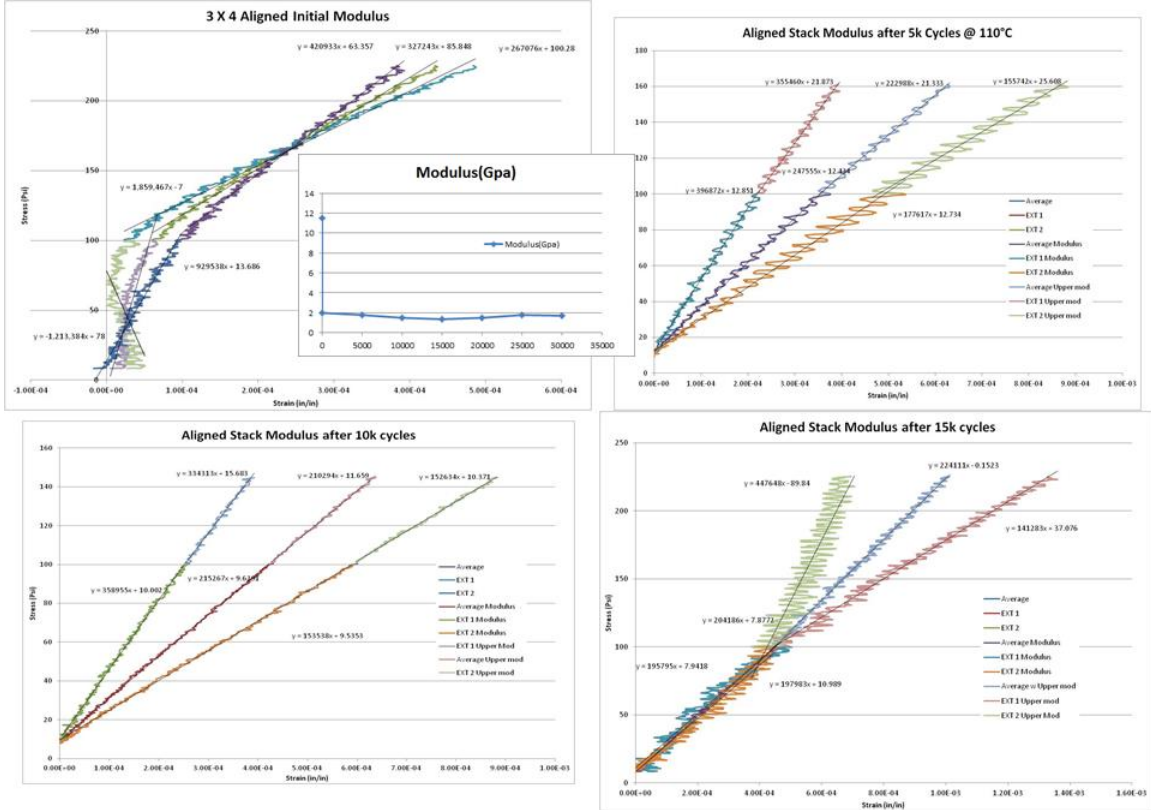


13.1.3 Partially Bonded Simulation of the Array Tensile Strain Test

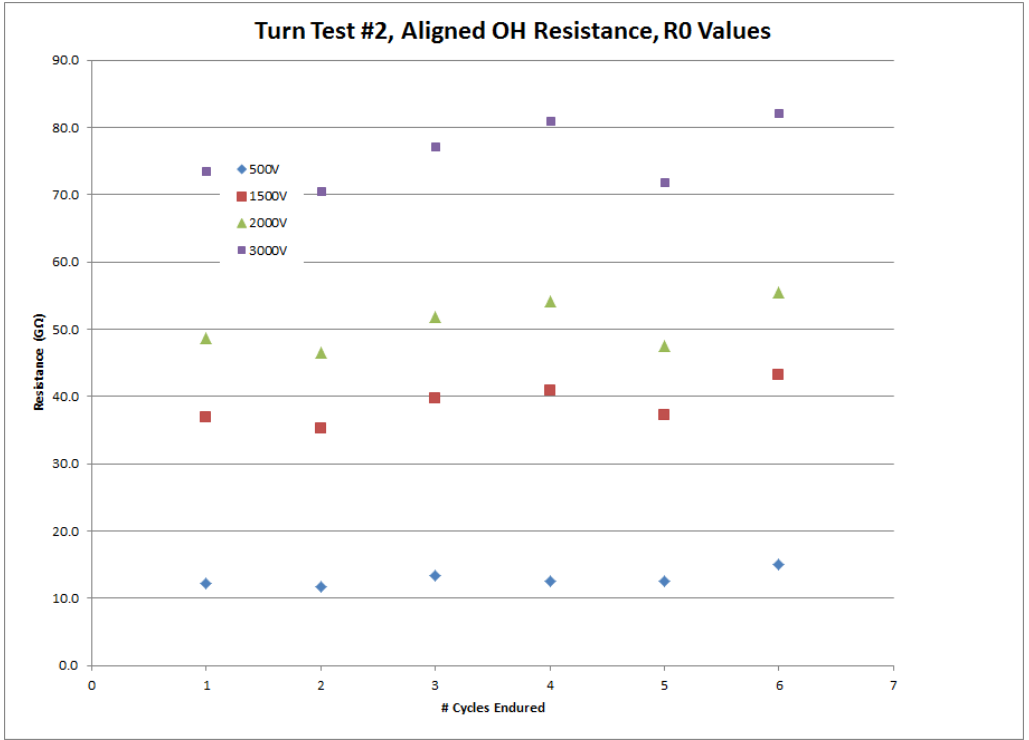




13.2 Aligned Conductor Tests and Simulations



The calculated modulus for the un-bonded configuration was 40 GPa.



13.2.1 Bonded Simulation of the Array Tensile Strain Test

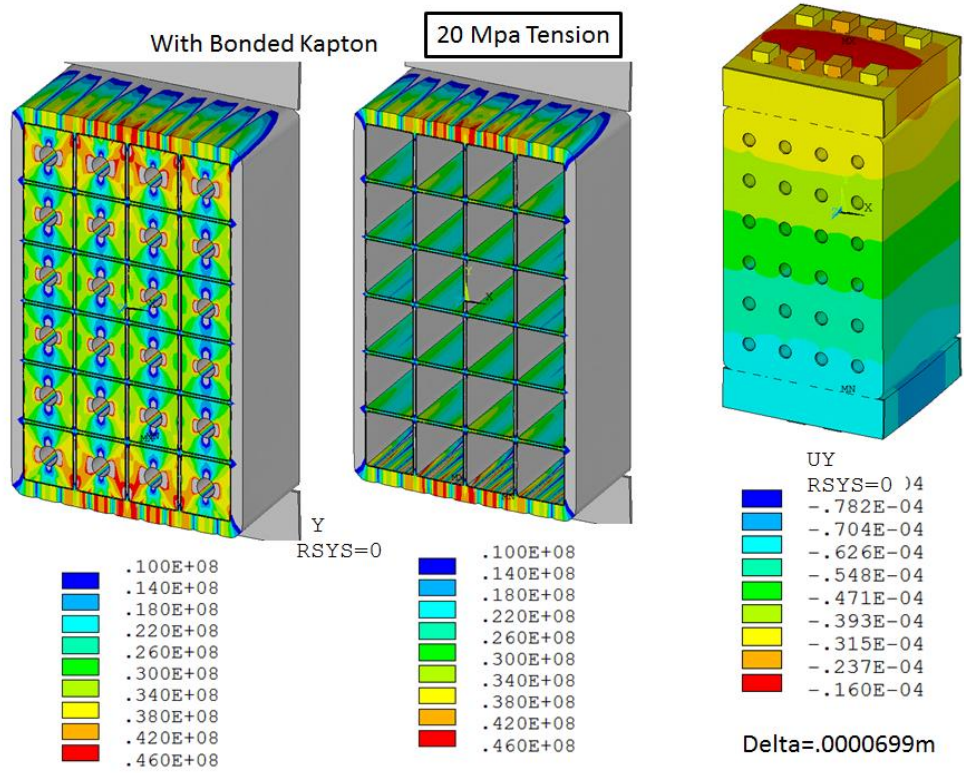


Figure 13.2-1

13.2.2 Un-Bonded Simulation of the Array Tensile Strain Test

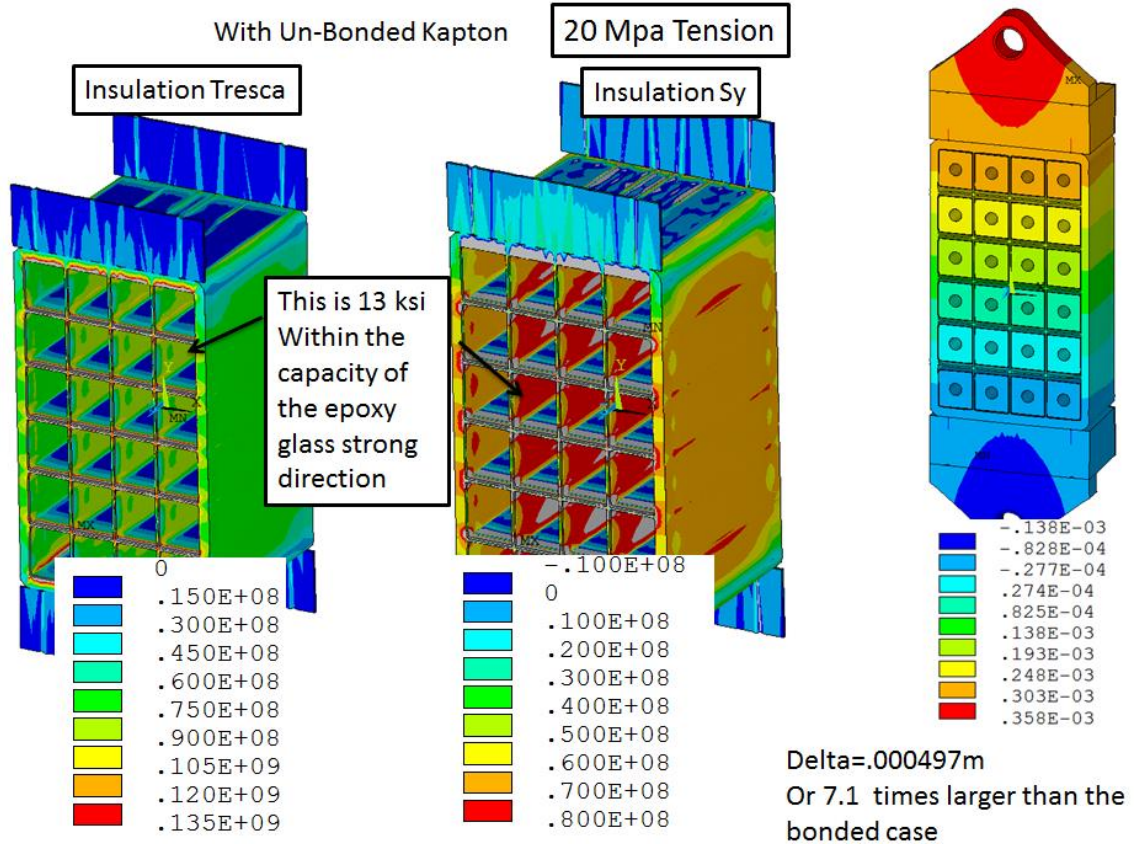


Figure 13.2.2 Un-bonded Array Simulation

13.3 Creep Stack Test

Creep needs stress, time, and temperature to develop. While a portion of the coil is at 110+C for 700 seconds during cooldown, it is not loaded by the preload mechanism very much - only 1.5 MPa vs. 30 MPa during a pulse. So I specified 24 hrs for the CTD creep tests.

Load a stack of 10 insulation layers, with copper sheet between each layer, with the whole stack VPI'd together. The width and depth of the column of layers should be large enough to avoid buckling and at least 20 times the layer thickness. The load would be 30 MPa compression normal to the layers. Insulation would be the same half lapped Kapton/glass system using the CTD 425 system including primer. The stack should be VPI'd with steel platens top and bottom, so there is no platen-to-insulation irregular contact.

The sample would first be held at 120C and 30 MPa compression for 24 hrs with the stack height measured five minutes after the first application of temperature and compression. and at 6 hrs, 12 hrs and 24 hrs. If the change in stack height after 24 hrs is more than .05%, then repeat the test at 110C with a new sample. (.05% is 2mm on the 4m coil height and translates into about a 10% loss in preload at the Bellevilles)

Attachment A

Email Communications

From Mike Mardenfeld Jan 16 2015 [20]:

Pete,

The original design calls for the “eyebrow” pieces as per 1EDC1483. The calculation tried to capture this in a simplified way, by modelling a solid G10 block which included representation of the “ridges and valleys” formed by the after-impregnated pieces. [I extracted this from the solid models, not the drawings].

In the field, cylindrical annuli were formed by wet lay up on mandrels per 1EDC1739. These blanks were precision turned to the correct IDs and ODs, but then cutting the annuli into pieces was done by hand with sawzalls. In the end, due to the imperfections of the copper windings and the need to hand bend the leads, there ended up being many more smaller pieces than as shown in the eyebrow drawings, which were custom cut and filed, stuffed with glass, etc. to get everything to fit.

Michael Mardenfeld

Tel: 609-243-2082

On February 6, 2015 at 6:54:28 PM EST, John Desandro <desandro@pppl.gov> wrote:

Using the black compression ring we tested the hose to 700 psi at room temperature and 500 psi at 120 C. The hose has passed both tests.

Attachment B

ADPL For Inputing FCOOL Output Files to Han's OH FEA

```
/clear,start
```

```
/config,nres,2000  
/PLOPTS,WP,0  
/PLOPTS,DATE,0  
/TRIAD,ORIG  
/REPLOT
```

```
resume,OH_base,db
```

```
FileNam='OH_cool'  
FileNamTYPE='_500psi_12c'
```

```
/filename,%FileNam%%FileNamTYPE%
```

```
/prep7  
save  
finish
```

```
/solu  
allsel,all  
csys,0  
ANTYPE,STATIC ! STATIC MAGNETIC FIELD ANALYSIS  
EQLV,SPARSE
```

```
tunif,100
```

```
tref,20
time,0
```

```
! read temperature from fcool results.
```

```
*dim,pt_time,STRING ,12
*DIM,temp_temp,array,198,20,
*do,rrr,1,198,1
*VREAD,temp_temp(rrr,1), fcouta%FileNamTYPE% ,,,ijk,1,20,,1+rrr
(F7.1,19F6.1)
*enddo
```

```
csys,1
```

```
*DIM,oh_temp,array,110,3,
jjj=0
kkk=1
*do,rrr,1,198,1
  *do,ccc,1,20,1
    jjj=jjj+1
    *if, jjj,le,3,then
      oh_temp(kkk,jjj)=temp_temp(rrr,ccc)
    *elseif, jjj,eq,36
      jjj=0
      kkk=kkk+1
    *endif
  *enddo
*enddo
```

```
*do,kkk,1,110,1
  d,node(0.2680855,-10,-2.1208+3.856e-2*(kkk-1)),temp,(oh_temp(kkk,1)-32)/1.8
  d,node(0.2680855,-10,-2.10152+3.856e-2*(kkk-1)),temp,(oh_temp(kkk,1)-32)/1.8
  d,node(0.2680855,0,-2.1208+3.856e-2*(kkk-1)),temp,(oh_temp(kkk,2)-32)/1.8
  d,node(0.2680855,0,-2.10152+3.856e-2*(kkk-1)),temp,(oh_temp(kkk,2)-32)/1.8
  d,node(0.2680855,10,-2.1208+3.856e-2*(kkk-1)),temp,(oh_temp(kkk,3)-32)/1.8
  d,node(0.2680855,10,-2.10152+3.856e-2*(kkk-1)),temp,(oh_temp(kkk,3)-32)/1.8
  *do,i,1,3,1
    d,node(0.2680855-i* 1.7335e-2,-10,-2.1208+3.856e-2*(kkk-1)),temp,(oh_temp(kkk,1)-32)/1.8
    d,node(0.2680855-i* 1.7335e-2,-10,-2.10152+3.856e-2*(kkk-1)),temp,(oh_temp(kkk,1)-32)/1.8
    d,node(0.2680855-i* 1.7335e-2,0,-2.1208+3.856e-2*(kkk-1)),temp,(oh_temp(kkk,2)-32)/1.8
    d,node(0.2680855-i* 1.7335e-2,0,-2.10152+3.856e-2*(kkk-1)),temp,(oh_temp(kkk,2)-32)/1.8
    d,node(0.2680855-i* 1.7335e-2,10,-2.1208+3.856e-2*(kkk-1)),temp,(oh_temp(kkk,3)-32)/1.8
    d,node(0.2680855-i* 1.7335e-2,10,-2.10152+3.856e-2*(kkk-1)),temp,(oh_temp(kkk,3)-32)/1.8
  *enddo
*enddo
csys,0
allsel,all
solve
```

```
str_rrr=1
```

```
*do,ls,1,9,1
  time,ls
```

```
!!=====
num_rrr=str_rrr
kkk=1
```

```

*dowhile,kkk
*SREAD,pt_time, fcouta_500psi_50c,,12,num_rrr*601,1
*if,pt_time(1),eq,' TIME= %ls%.',then
  kkk=0
  !/output,fff,txt
  !*vwrite,%ijk%'
  !('find time ',A1,',')
  !/output
*else
  num_rrr=num_rrr+1
*endif
*enddo
str_rrr=num_rrr+1
!!=====
*do,rrr,1,198,1
*VREAD,temp_temp(rrr,1), fcouta%FileNamETYPE%,,,ijk,1,20,,1+rrr+num_rrr*601
(F7.1,19F6.1)
*enddo

csys,1
jjj=0
kkk=1
*do,rrr,1,198,1
  *do,ccc,1,20,1
    jjj=jjj+1
    *if, jjj,le,3,then
      oh_temp(kkk,jjj)=temp_temp(rrr,ccc)
    *elseif, jjj,eq,36
      jjj=0
      kkk=kkk+1
    *endif
  *enddo
*enddo

*do,kkk,1,110,1
  d,node(0.2680855,-10,-2.1208+3.856e-2*(kkk-1)),temp,(oh_temp(kkk,1)-32)/1.8
  d,node(0.2680855,-10,-2.10152+3.856e-2*(kkk-1)),temp,(oh_temp(kkk,1)-32)/1.8
  d,node(0.2680855,0,-2.1208+3.856e-2*(kkk-1)),temp,(oh_temp(kkk,2)-32)/1.8
  d,node(0.2680855,0,-2.10152+3.856e-2*(kkk-1)),temp,(oh_temp(kkk,2)-32)/1.8
  d,node(0.2680855,10,-2.1208+3.856e-2*(kkk-1)),temp,(oh_temp(kkk,3)-32)/1.8
  d,node(0.2680855,10,-2.10152+3.856e-2*(kkk-1)),temp,(oh_temp(kkk,3)-32)/1.8
*do,i,1,3,1
  d,node(0.2680855-i*1.7335e-2,-10,-2.1208+3.856e-2*(kkk-1)),temp,(oh_temp(kkk,1)-32)/1.8
  d,node(0.2680855-i*1.7335e-2,-10,-2.10152+3.856e-2*(kkk-1)),temp,(oh_temp(kkk,1)-32)/1.8
  d,node(0.2680855-i*1.7335e-2,0,-2.1208+3.856e-2*(kkk-1)),temp,(oh_temp(kkk,2)-32)/1.8
  d,node(0.2680855-i*1.7335e-2,0,-2.10152+3.856e-2*(kkk-1)),temp,(oh_temp(kkk,2)-32)/1.8
  d,node(0.2680855-i*1.7335e-2,10,-2.1208+3.856e-2*(kkk-1)),temp,(oh_temp(kkk,3)-32)/1.8
  d,node(0.2680855-i*1.7335e-2,10,-2.10152+3.856e-2*(kkk-1)),temp,(oh_temp(kkk,3)-32)/1.8
*enddo
*enddo

csys,0
allsel,all
solve
*enddo

```



```

*do,ls,1,9,1
  time,ls*10

!!=====
num_rrr=str_rrr
kkk=1
*dowhile,kkk
*SREAD,pt_time, fcouta_500psi_50c,,,12,num_rrr*601,1
*if,pt_time(1),eq,' TIME= %ls*10%.',then
  kkk=0
*else
  num_rrr=num_rrr+1
*endif
*enddo
str_rrr=num_rrr+1
!!=====
*do,rrr,1,198,1
*SREAD,temp_temp(rrr,1), fcouta%FileNamETYPE%,,,ijk,1,20,,1+rrr+num_rrr*601
(F7.1,19F6.1)
*enddo

csys,1
jjj=0
kkk=1
*do,rrr,1,198,1
  *do,ccc,1,20,1
    jjj=jjj+1
    *if,jjj,le,3,then
      oh_temp(kkk,jjj)=temp_temp(rrr,ccc)
    *elseif,jjj,eq,36
      jjj=0
      kkk=kkk+1
    *endif
  *enddo
*enddo

*do,kkk,1,110,1
  d,node(0.2680855,-10,-2.1208+3.856e-2*(kkk-1)),temp,(oh_temp(kkk,1)-32)/1.8
  d,node(0.2680855,-10,-2.10152+3.856e-2*(kkk-1)),temp,(oh_temp(kkk,1)-32)/1.8
  d,node(0.2680855,0,-2.1208+3.856e-2*(kkk-1)),temp,(oh_temp(kkk,2)-32)/1.8
  d,node(0.2680855,0,-2.10152+3.856e-2*(kkk-1)),temp,(oh_temp(kkk,2)-32)/1.8
  d,node(0.2680855,10,-2.1208+3.856e-2*(kkk-1)),temp,(oh_temp(kkk,3)-32)/1.8
  d,node(0.2680855,10,-2.10152+3.856e-2*(kkk-1)),temp,(oh_temp(kkk,3)-32)/1.8
*do,i,1,3,1
  d,node(0.2680855-i*1.7335e-2,-10,-2.1208+3.856e-2*(kkk-1)),temp,(oh_temp(kkk,1)-32)/1.8
  d,node(0.2680855-i*1.7335e-2,-10,-2.10152+3.856e-2*(kkk-1)),temp,(oh_temp(kkk,1)-32)/1.8
  d,node(0.2680855-i*1.7335e-2,0,-2.1208+3.856e-2*(kkk-1)),temp,(oh_temp(kkk,2)-32)/1.8
  d,node(0.2680855-i*1.7335e-2,0,-2.10152+3.856e-2*(kkk-1)),temp,(oh_temp(kkk,2)-32)/1.8
  d,node(0.2680855-i*1.7335e-2,10,-2.1208+3.856e-2*(kkk-1)),temp,(oh_temp(kkk,3)-32)/1.8
  d,node(0.2680855-i*1.7335e-2,10,-2.10152+3.856e-2*(kkk-1)),temp,(oh_temp(kkk,3)-32)/1.8
*enddo
*enddo

csys,0
allsel,all
solve

```

```

*enddo

*do,ls,3,6,1
  time,ls*50

!!=====
num_rrr=str_rrr
kkk=1
*dowhile,kkk
*SREAD,pt_time, fcouta_500psi_50c,,12,num_rrr*601,1
*if,pt_time(1),eq,' TIME= %ls*50%.',then
  kkk=0
*else
  num_rrr=num_rrr+1
*endif
*enddo
str_rrr=num_rrr+1
!!=====
*do,rrr,1,198,1
*VREAD,temp_temp(rrr,1), fcouta%FileNameTYPE%,,,ijk,1,20,,1+rrr+num_rrr*601
(F7.1,19F6.1)
*enddo

csys,1
jjj=0
kkk=1
*do,rrr,1,198,1
  *do,ccc,1,20,1
    jjj=jjj+1
    *if,jjj,le,3,then
      oh_temp(kkk,jjj)=temp_temp(rrr,ccc)
    *elseif,jjj,eq,36
      jjj=0
      kkk=kkk+1
    *endif
  *enddo
*enddo

*do,kkk,1,110,1
  d,node(0.2680855,-10,-2.1208+3.856e-2*(kkk-1)),temp,(oh_temp(kkk,1)-32)/1.8
  d,node(0.2680855,-10,-2.10152+3.856e-2*(kkk-1)),temp,(oh_temp(kkk,1)-32)/1.8
  d,node(0.2680855,0,-2.1208+3.856e-2*(kkk-1)),temp,(oh_temp(kkk,2)-32)/1.8
  d,node(0.2680855,0,-2.10152+3.856e-2*(kkk-1)),temp,(oh_temp(kkk,2)-32)/1.8
  d,node(0.2680855,10,-2.1208+3.856e-2*(kkk-1)),temp,(oh_temp(kkk,3)-32)/1.8
  d,node(0.2680855,10,-2.10152+3.856e-2*(kkk-1)),temp,(oh_temp(kkk,3)-32)/1.8
  *do,i,1,3,1
    d,node(0.2680855-i*1.7335e-2,-10,-2.1208+3.856e-2*(kkk-1)),temp,(oh_temp(kkk,1)-32)/1.8
    d,node(0.2680855-i*1.7335e-2,-10,-2.10152+3.856e-2*(kkk-1)),temp,(oh_temp(kkk,1)-32)/1.8
    d,node(0.2680855-i*1.7335e-2,0,-2.1208+3.856e-2*(kkk-1)),temp,(oh_temp(kkk,2)-32)/1.8
    d,node(0.2680855-i*1.7335e-2,0,-2.10152+3.856e-2*(kkk-1)),temp,(oh_temp(kkk,2)-32)/1.8
    d,node(0.2680855-i*1.7335e-2,10,-2.1208+3.856e-2*(kkk-1)),temp,(oh_temp(kkk,3)-32)/1.8
    d,node(0.2680855-i*1.7335e-2,10,-2.10152+3.856e-2*(kkk-1)),temp,(oh_temp(kkk,3)-32)/1.8
  *enddo
*enddo

csys,0

```

```
allse1,all  
solve  
*enddo
```

```
finish
```

Attachment C Hysol Wet Lay-up

Compression Test (By Stephan Jurczynski)

2014-02-27

WR#20141474

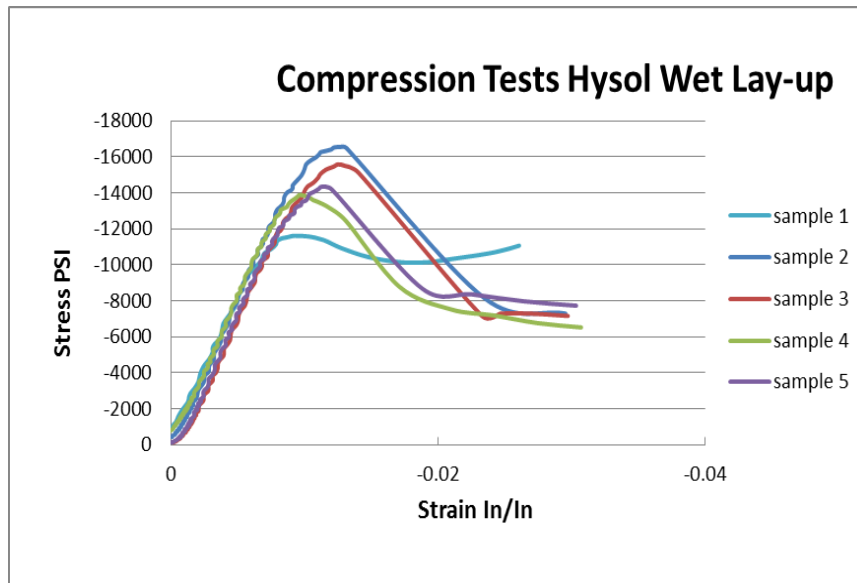
MTL#398

Testing comprised of 5 samples cut from a TF Connecting Ring Wet Lay-up ("Crown") exposing samples with the fibers running axially in the longitudinal direction.

Sample:	Rupture Load	Rupture Stress
#1: 0.440" x 0.440" x 0.760"	-2250lbs	-11.6ksi
#2: 0.440" x 0.440" x 0.755"	-3200lbs	-16.5ksi
#3: 0.440" x 0.440" x 0.755"	-3020lbs	-15.6ksi
#4: 0.440" x 0.440" x 0.752"	-2690lbs	-13.9ksi
#5: 0.440" x 0.440" x 0.755"	-2780lbs	-14.3ksi

Cross sectional area used for test calculation: $0.440" \times 0.440" = 0.1936 \text{sqin}$

Load and strain data readings were taken directly in real time using a MTS 10kip servo-hydraulic tensile and compression test machine.



Attachment D

Megger.

S1 Series

5-kV and 10-kV Insulation Resistance Testers

S1 Series

5-kV and 10-kV Insulation Resistance Testers



- CAT IV 600 V safety rating
- Line supply or battery operated
- Noise rejection (2mA or 4mA rms@200v and above) for use in high voltage substations or switchyards
- 5mA output current provides fast charging and testing of capacitive loads
- Measurement range to 15 TΩ (5-kV models) and 35 TΩ (10-kV models)
- Automatic insulation resistance (IR), dielectric absorption ratio (DAR), polarization index (PI), step voltage (SV), and dielectric discharge (DD) tests
- RS232 or USB download of results
- On board memory for results storage

DESCRIPTION

The new Megger S1 Series of 5 kV and 10 kV insulation resistance testers are designed specifically to assist the user with the testing and maintenance of high voltage equipment. This series of testers includes the following models and distinct capabilities including voltage, test current and noise rejection:

Model #	Output Voltage	Test Current	Noise Rejection
S1-552/2	5 kV	5 mA	2 mA
S1-1052/2	10 kV	5 mA	2 mA
S1-554/2	5 kV	5 mA	4 mA
S1-1054/2	10 kV	5 mA	4 mA

All four models are heavy duty and reliable with features that meet the most demanding testing applications in existence today.

First, the user has a choice of 5 or 10 kV voltage output capability. The 10 kV option is particularly suitable for testing to the IEEE standards required for testing motors rated greater than 12 kV.

Second, all four models provide 5 mA output current to provide fast charging and testing of high capacity loads such as long cables.

Third, all four models feature extra noise rejection capability. The Models S1-554/2 and S1-1054/2 incorporate a hardware filter designed to tolerate a industry best 4 mA rms of noise current at 50Hz and above. This filter is enabled by default, but may be switched off in order to speed up the settling time when there is little noise current. The Insulation Resistance mode offers additional firmware filtering to average out slow variations during

testing. This virtually eliminates the possibility of poor, unreliable or unstable readings being made in noisy 345-kV and above substations or switchyards.

These instruments have been designed with expanded measurement ranges, up to 15TΩ for the 5kV models and up to 35TΩ for the 10kV models, in order to provide trending values for testing high quality insulating materials.

A large, easy-to-read backlit LCD is provided on all models making them suitable for use in both bright sunlight and poorly lit environments. Information displayed includes resistance, voltage, leakage current, capacitance, battery status and time constant. In addition, the elapsed time is continuously displayed, removing the need for separate timers. Adjustable timers and limit alarms are included.

A built-in, integral timer starts automatically at the beginning of a test, and displays minutes and seconds. At the end of any test, the load is automatically discharged and the decay voltage is displayed. The timer enables the performance of an automatic IR test, plus the capability of preprogrammed DAR, PI, SV and DD. They each include an alarm mode, which allows the operator to preset a specific resistance level. The unit will beep until the limit is exceeded.

In addition to the preprogrammed automated testing routines, the units are equally suited for simple insulation testing. The controls of the instruments are clear and unambiguous, and a "quick start" guide is included in the lid as a permanent refresher for the operator.

A guard terminal is provided with each model to allow greater accuracy when testing complex insulation systems with multiple terminals. A guard test lead is included as standard with each instrument.